

ΠΑΝΕΠΙΣΤΗΜΙΟ ΘΕΣΣΑΛΙΑΣ-ΠΟΛΥΤΕΧΝΙΚΗ ΣΧΟΛΗ

ΤΜΗΜΑ ΜΗΧΑΝΟΛΟΓΩΝ ΜΗΧΑΝΙΚΩΝ



# PERMEABILITY OF FLUID ABSORBING MEDIA

**ΠΟΥΡΝΑΡΑΣ ΓΕΩΡΓΙΟΣ**  
**ΧΑΤΖΟΠΟΥΛΟΣ ΑΡΙΣΤΕΙΔΗΣ**

Επιβλέπων Καθηγητής

**Δρ ΠΑΠΑΘΑΝΑΣΙΟΥ ΑΘΑΝΑΣΙΟΣ**

**ΒΟΛΟΣ 2018**



© 2018 Χατζόπουλος Αριστείδης, Πουρνάρας Γεώργιος

Η έγκριση της Διπλωματικής Εργασίας από το Τμήμα Μηχανολόγων Μηχανικών της Πολυτεχνικής Σχολής του Πανεπιστημίου Θεσσαλίας δεν υποδηλώνει αποδοχή των απόψεων των συγγραφέων (Ν. 5343/32 αρ. 202 παρ. 2).



## Εξεταστική Επιτροπή

Πρώτος εξεταστής  
(Επιβλέπων)

Δρ. Τσιακάρης Παναγιώτης,  
Καθηγητής,  
Τμήμα Μηχανολόγων Μηχανικών,  
Πανεπιστήμιο Θεσσαλίας

Δεύτερος εξεταστής

Δρ. Ανδρίτσος Νικόλαος,  
Καθηγητής,  
Τμήμα Μηχανολόγων Μηχανικών,  
Πανεπιστήμιο Θεσσαλίας

Τρίτος εξεταστής

Δρ. Αγγελική Μπούζγου,  
Επιστημονικός Συνεργάτης,  
Τμήμα Μηχανολόγων Μηχανικών,  
Πανεπιστήμιο Θεσσαλίας

## Ευχαριστίες

Αρχικά, θα θέλαμε να ευχαριστήσουμε τον επιβλέποντα καθηγητή της εργασίας κ. Αθανάσιο Παπαθανασίου, καθηγητή του τμήματος Μηχανολόγων Μηχανικών του Πανεπιστημίου Θεσσαλίας, για τη βοήθεια, τις γνώσεις, την παρότρυνση αλλά και για τις πολύτιμες συμβουλές του κατά την εκπόνηση της συγκεκριμένης διπλωματικής εργασίας.

Επιπλέον, για τη βοήθεια σε κρίσιμα σημεία, την υποστήριξη και την παροχή πολύτιμων πληροφοριών θα θέλαμε να ευχαριστήσουμε τον Φώτη Φωτιάδη, διπλωματούχο πάνω στο ίδιο αντικείμενο, καθώς και τον Ανδρέα Τσιαντή, ερευνητικό μέλος του τμήματος.

Τέλος, θα θέλαμε να ευχαριστήσουμε τις οικογένειές μας για όλα τα εφόδια που μας έχουν προσφέρει και για τη συνεχή και αμέριστη υποστήριξη τους.

# Table of Contents

Table of figures.....	x
Abstract.....	xiii
Aim.....	xv
Chapter 1 Theoretical background.....	1
1.1 Porosity and Volume fraction.....	1
1.2 Permeability.....	2
1.3 Swelling.....	3
1.4 Case Studies.....	5
1.4.1 Flow across bundles of non-absorbing filaments.....	6
1.4.2 Flow across bundles of absorbing (and swelling) filaments.....	7
1.5 Darcy's law.....	7
Chapter 2 Computational tool.....	12
2.1 Introduction to OpenFoam.....	12
2.2 Familiarity with the environment.....	13
2.2.1 SimpleFoam.....	14
2.2.2 Pre-Processing.....	16
2.2.3 Running application.....	21
2.2.4 Post-processing.....	21

Chapter 3 Non-linear behavior of absorption rate .....	25
3.1 Geometry generation.....	25
3.2 Mesh.....	28
3.3 Boundary conditions.....	29
3.4 Absorption.....	30
3.5 Computational results.....	36
3.5.1 Post-processing of the results.....	41
Chapter 4 Linear behavior of absorption rate .....	51
4.1 Absorption at a constant flow rate.....	51
4.2 Computational results.....	54
4.3 Comparison and conclusions.....	61
4.4 Proposals for further study.....	62
Appendix.....	64
Appendix A.....	64
Appendix B.....	67
Appendix C.....	69
Appendix D.....	71
Appendix E.....	74
Appendix F.....	79



Appendix G.....	84
References.....	88

## Table of Figures

Figure 1: Examples of various media, ranging from impermeable to porous and permeable.....	2
Figure 2: Structure of muscle.....	3
Figure 3: Tows of hexagonal arranged filaments, of infinite length, arranged in square packing. The square of two dimensions formed is a unit cell.....	5
Figure 4: A unit cell with hexagonal arranged filaments and the direction of the flow.....	6
Figure 5: Diagram showing the definition of Darcy's law.....	8
Figure 6: Overview of OpenFOAM structure.....	12
Figure 7: Filaments placed in the center of a cell in a periodic arrangement.....	14
Figure 8: Flow rate for the left side of the unit cell ( $Q_{in}$ ).....	22
Figure 9: Flow rate for the right side of the unit cell ( $Q_{out}$ ).....	22
Figure 10: Minimum and maximum pressure for an exact location.....	22
Figure 11: paraView environment - velocity profile of a unit cell.....	23
Figure 12: paraView environment - pressure profile of a unit cell.....	23
Figure 13: paraView environment - velocity vectors in the unit cell.....	24
Figure 14: 1D structure for hexagonal arrays of filaments.....	26
Figure 15: Visual result of the program that creates the unit cell.....	27
Figure 16: Mesh of a unit cell.....	28

Figure 17: Vertical flow of liquid into the porous medium due to absorption.....	31
Figure 18: Velocity vectors of a single impermeable filament, used for the calculation of $Q_{base}$ .....	31
Figure 19: Appears where flow rate is present.....	32
Figure 20: Mathematica code used for solving Eq. 3.12.....	34
Figure 21: Graphs of the radius of the filaments versus time for various values of the absorption coefficient (a).....	35
Figure 22: Graphs of the fluid absorbed versus time for various values of the absorption coefficient (a).....	36
Figure 23: Graph of the permeability versus time for various values of absorption coefficient (a), compared with Gebart's model.....	38
Figure 24: Zoom in a certain area of Figure 23.....	39
Figure 25: Graph of minimum pressure versus time for various values of absorption coefficient (a).....	40
Figure 26: A log-log graph of minimum pressure versus time for various values of absorption coefficient (a).....	41
Figure 27: Contour pressure maps through time for all the five values of the absorption coefficient (a).....	44
Figure 28: Contour velocity maps through time for all the five values of the absorption coefficient (a).....	47

Figure 29: Velocity vectors of the swelling porous media through time for all the five values of the absorption coefficient (a).....50

Figure 30: Mathematica code for calculating the values of the radius of the filaments at each time step, for  $Q_{ab}$  that decreases at a constant rate.....52

Figure 31: Graph of the radius of the filaments versus time for  $Q_{ab}$  that decreases at a constant rate.....53

Figure 32: Graph of the fluid absorbed that decreases at a constant rate versus time, for  $a=1\%$ .....53

Figure 33: Graph of the permeability versus time for various values of absorption coefficient (a), at a constantly decreasing amount of fluid absorbed.....54

Figure 34: A log-log graph of the permeability versus time for various values of absorption coefficient (a), at a constantly decreasing amount of fluid absorbed.....55

Figure 35: Graph of the minimum pressure versus time for various values of absorption coefficient (a), at a constantly decreasing amount of fluid absorbed.....56

Figure 36: A log-log graph of the minimum pressure versus time for various values of absorption coefficient (a), at a constantly decreasing amount of fluid absorbed.....56

Figure 37: Contour pressure maps through time for all the five values of the absorption coefficient (a) for  $Q_{ab}$  that decreases at a constant rate.....60

Figure 38: Comparison between Figures 23 and 33.....61

Figure 39: Comparison between Figures 25 and 35.....62

## Περίληψη

Η διπλωματική εργασία που ακολουθεί, με τίτλο “Υδραυλική διαπερατότητα ινωδών συστημάτων με παράλληλη απορρόφηση ρευστού”, αναφέρεται στην διερεύνηση του προβλήματος ροής ρευστού διαμέσου ενός σύνθετου υλικού. Το υλικό αποτελείται από πορώδεις κυκλικές δέσμες ινών τοποθετημένων σε τετραγωνική διάταξη. Κάθε δέσμη απαρτίζεται από ίνες απείρου μήκους παρατεταγμένες σε εξαγωνική διάταξη. Ανάμεσα στις ίνες υπάρχει κενό, το οποίο κατά την διαδικασία του πειράματος καλύπτεται από ρευστό. Οι ίνες μπορεί να είναι είτε αδιαπέρατες από το ρευστό, είτε να απορροφούν ρευστό με κάποιον συγκεκριμένο ρυθμό. Κατά την διάρκεια αυτής της απορρόφησης, η ακτίνα των ινών αυξάνεται έτσι ώστε να εξασφαλίζεται η εξίσωση συνέχειας. Προκείμενου να αποφευχθεί υπολογιστικό φορτίο, εκμεταλλευόμενοι την συμμετρία του προβλήματος, απλοποιούμε τη γεωμετρία και περιοριζόμαστε στην μελέτη ενός μοναδιαίου κελιού δύο διαστάσεων. Το χαρακτηριστικό της ροής που ερευνάται σε όλη την έκταση της εργασίας είναι η υδραυλική διαπερατότητα καθώς και η υποπίεση που αναπτύσσεται μέσα στην δέσμη ινών όταν οι ίνες απορροφούν ρευστό. Πιο συγκεκριμένα, εξετάζεται υπολογιστικά η περίπτωση που το υγρό ρέει ανάμεσα από τις ίνες, χωρίς να απορροφάται, καθώς και δύο περιπτώσεις ροής με παράλληλη απορρόφηση των ινών τις οποίες και θα συγκρίνουμε. Στην πρώτη περίπτωση, έχουμε μία μη γραμμική συνάρτηση μεταβολής της ακτίνας των ινών όπου μεταβάλλεται η απορρόφηση της ίνας στο πέρας του χρόνου, ενώ στην δεύτερη περίπτωση η απορρόφηση των ινών μειώνεται με σταθερό ρυθμό καθ’ όλη την διάρκεια έως ότου οι ίνες έρθουν σε επαφή μεταξύ τους και η ροή ρευστού σταματήσει ολοκληρωτικά. Και στα δύο ενδεχόμενα παρατηρείται διόγκωση των ινών με αποτέλεσμα την αύξηση του στερεού κλάσματος όγκου μέσα στην δέσμη. Επίσης, με την συνεχή απορρόφηση το πορώδες της δέσμης μειώνεται, γεγονός που οδηγεί σε μεταβολή της διαπερατότητας. Η ανάλυση των διαδικασιών γίνεται μέσω της χρήσης του υπολογιστικού εργαλείου OpenFOAM και των υπόλοιπων προγραμμάτων με τα οποία ο χρήστης θα πρέπει να έχει εξοικειωθεί για να φέρει εις πέρας τις απαραίτητες προσομοιώσεις. Τελικά, μέσα από γραφήματα και διαγράμματα, θα προσπαθήσουμε να χαρακτηρίσουμε και να προσδιορίσουμε την συμπεριφορά της ροής και της διαπερατότητας σε σχέση με τον χρόνο απορρόφησης για τα ενδεχόμενα που προαναφέραμε.

## Abstract

The following thesis is related to a computational analysis of viscous flow through a fibrous medium. The material under consideration, consists of porous circular bundles of filaments arranged in a square arrangement. Each bundle consists of filaments of infinite length packed in hexagonal arrangement. There are gaps between the bundles as well as between filaments within each bundle, which are covered by fluid during the experiment. The filaments may be either liquid-impervious or absorb fluid at a certain rate. During this absorption, the filament radius is increased so that the equation of continuity can be ensured. In order to avoid unnecessary computational load, we take advantage of the symmetry of the problem and we simplify the geometry by confining ourselves to the study of a two-dimensional unit cell. Implicit in this is the assumption that the filament bundles are arranged in uniform (square in our case) packing. Flow analysis through a unit cell provides the ability to compute the hydraulic permeability as well as underpressure which develops within the filament bundle while the filaments absorb fluid. More specifically, we will examine computationally in which cases the liquid flows between the filaments without being absorbed, as well as two cases of flow with parallel absorption by the filaments. In the first case, we have a non-linear variation of the filament radius with time, when the filament absorption of fluid changes over time, while in the second case the fiber absorption of fluid decreases on a constant rate throughout the duration until the filaments come in contact with each other and the fluid flow through the filament bundle stops completely. In both cases there is a swelling of the filaments resulting in an increase in the solid volume fraction within the bundle. As a result, the porosity of the bundle decreases, resulting in a change in its permeability. The analysis of the processes is made through the use of the computing tool OpenFoam and other programs (such as for the geometry generation) with which the user should be familiar to carry out the necessary simulations. Finally, through a number of simulations and graphs, we will try to determine behaviors of flow and permeability with respect to the above-mentioned scenarios.

## Aim

The aim of the work described in this thesis is to assist in the characterization of the permeability of a certain class of fibrous porous media in which the fibers absorb the fluid used in the permeability measurement. There are several examples of such materials, as swelling polymers, woven glass composite and polymer materials. Study of flow in fibrous porous media is important in many industrial processes such as: filtration, composite fabrication, compact heat exchangers, paper production and fuel cell technology.





# Chapter 1 Theoretical background

## 1.1 Porosity and Volume fraction

These measures are used to describe the geometry of a fibrous porous medium, a material that consists of numerous alternating filaments and void spaces.

### Definitions

Porosity is a measure of the void (i.e. empty) spaces in a material, and is a fraction of the volume of voids over the total volume, between 0 and 1, or as a percentage between 0% and 100%. The mathematical symbol of porosity is  $\varphi$  and defined as [3]:

$$\varphi = \frac{V_{void}}{V_{total}} \quad (1.1)$$

Where:

$\varphi$  : porosity

$V_{void}$  : Volume of void-space within the material [m<sup>3</sup>]

$V_{total}$  : Volume of material [m<sup>3</sup>]

In order to calculate the percentage of filament volume in the entire volume of a filament-reinforced composite material, we introduce the measure of filament volume fraction symbolized with  $\Phi$ , and described by the equation

$$\Phi = \frac{V_s}{V_{total}} \quad (1.2)$$

$\Phi$  : Volume fraction, [percentage]

$V_s$  : Volume of filaments [m<sup>3</sup>]

The total volume of the composite material constitutes the aggregate of the void and solid space of the material:

$$V_{\text{total}} = V_{\text{void}} + V_s \quad (1.3)$$

By dividing the above equation (1.3) with  $V_{\text{total}}$ , we derive a relationship between porosity and volume fraction:

$$\Phi = 1 - \varphi \quad (1.4)$$

## 1.2 Permeability

The way these filaments are arranged determines the ease with which a fluid can pass through the porous medium. This is quantified through the property called hydraulic permeability. Permeability, in general depends on the internal geometry of the porous space, the degree of saturation and on the viscosity of the fluid. In this study we consider fully saturated fibrous porous materials that have the ability to absorb some of the fluid passing through. As a result the material starts to swell and its porosity changes over time. Such swelling porous media will be studied, in order to observe how permeability changes during the absorption process. Permeability is symbolically represented as  $K$  [11].

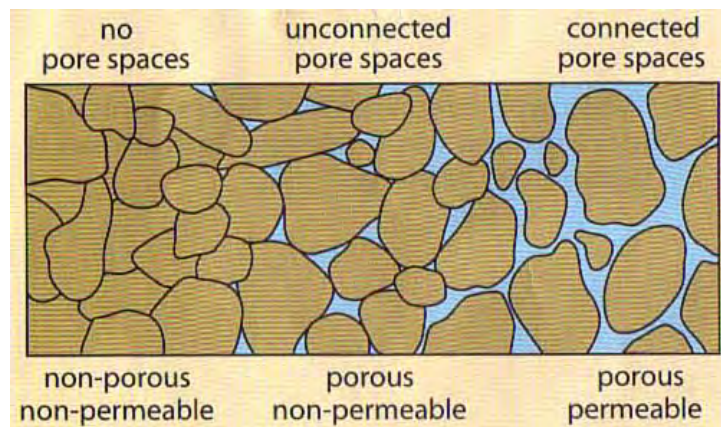


Figure 1: Examples of various media, ranging from impermeable to porous and permeable [12]

### 1.3 Swelling

The capacity to swell is a characteristic property of some materials comprised of macromolecular compounds (polymers). There are many examples where we encounter the phenomenon of swelling. For instance in medicine, where the medical term of swelling is 'edema', body parts swell from injury or inflammation. This can affect a small area or the entire body. Medications, pregnancy, infections and many other medical problems can cause edema. Edema happens when small blood vessels leak fluid into nearby tissues. That extra fluid builds up, which makes the tissue swell and it can happen almost anywhere in the body [14]. Another example is the human muscles, which consist of bundles of muscle fibers which also swell. When a muscle lifts loads that it is unaccustomed to, the stress causes tiny tears in its fibers. These tears are a natural part of building stronger muscles because when the damage is repaired, the muscle fibers are rebuilt stronger than before. Almost immediately after exercise, white blood cells rush into the muscle to clear up the debris from the muscle damage. Along with white blood cells, fluids carrying other nutrients and enzymes rush into the muscle to support the rebuilding process. The extra fluids packed into the muscle also contribute to swelling.

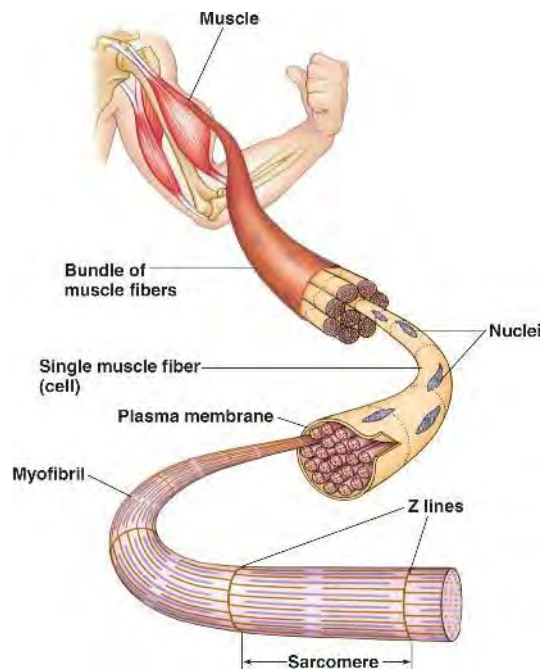


Figure 2: Structure of muscle [1]

Swelling is caused by diffusion and convection processes, which are usually accompanied by solvation (the binding of a low molecular weight substance by a polymer). It is important to mention that in our case we are not studying the phenomenon of swelling between a particular fluid and a particular material at the molecular level, but we treat it phenomenologically by assuming a Newtonian fluid and a rate of absorption. In other words, we describe swelling as a macroscopic process which results in change of the interior porosity of filament bundles, the pore radius (the geometry changes) and therefore the permeability [9].

Swelling has wide use in industry and in everyday life. It frequently accompanies bonding of polymer materials, processing of polymers to produce various articles, production of rubber adhesives and other processes such as preparation of many foods and many natural processes (germination of seeds and spores).

- Swelling polymers

The phenomenon of swelling is broadly observed and applied in certain classes of polymers. These materials are very high molecular mass, cross-linked polyelectrolytes that can absorb or imbibe more than 10 times their mass of water or aqueous solutions [16]. In order to absorb this large quantity of aqueous fluid, the polymers must be only slightly cross-linked so that the polymer chains can adopt widely spaced configurations. And in order to remain largely insoluble, while at the same time being highly expanded, the polymer chains must have very high molecular mass so that the small number of cross-links connect together all the chains. The principal use of swelling polymers is as a liquid absorbent in disposable hygiene products, which include baby diapers, feminine hygiene and adult incontinence products. Smaller volume uses include liquid absorbent pads for packaged meats and water-blocking tapes and coatings for electrical and telecommunication cables. Other notable applications are in construction materials and concrete walls in order to block water leaking, in the agricultural sector where the swelling polymers are mixed with the soil in order to help it to retain the moisture and in sensor systems (for changes in water content, pH and ionic strength) where due to their swelling ability and rubbery nature a signal is generated, because of the difference of mechanical stress between the stressed and unstressed parts, that can be measured.

## 1.4 Case Studies

The cases we study are devoted to a computational analysis of viscous flow of Newtonian liquid across unidirectional (one way) arrays of infinite filament bundles. In the analysis of flow through fibrous media, the latter are usually idealized as made up of cylinders arranged in space in a defined periodic order. We consider systems made of infinitely long cylindrical bundles arranged in a square packing and with their axes perpendicular to the direction of flow. Each bundle consists of a number  $N$  of solid individual cylindrical filaments of radius  $R_f$ . It is these filaments that are assumed to absorb the surrounding fluid in our study. Permeability is independent of the number of filaments when this number is large ( $N > 300$ ) and depends exclusively on the porosity and the packing order. In our study, these filaments are arranged in hexagonal packing within the bundle. Therefore such systems are characterized by an inter-tow (gaps between bundles) and intra-tow (void space within a bundle) porosity. Inter-tow and intra-tow porosities are symbolized with  $\varphi_i$  and  $\varphi_t$  respectively. At low values of  $\varphi_t$  practically no fluid passes through the bundle. In all the above described arrangements, a two dimensional unit cell [8] can be identified as shown in Figure (4).

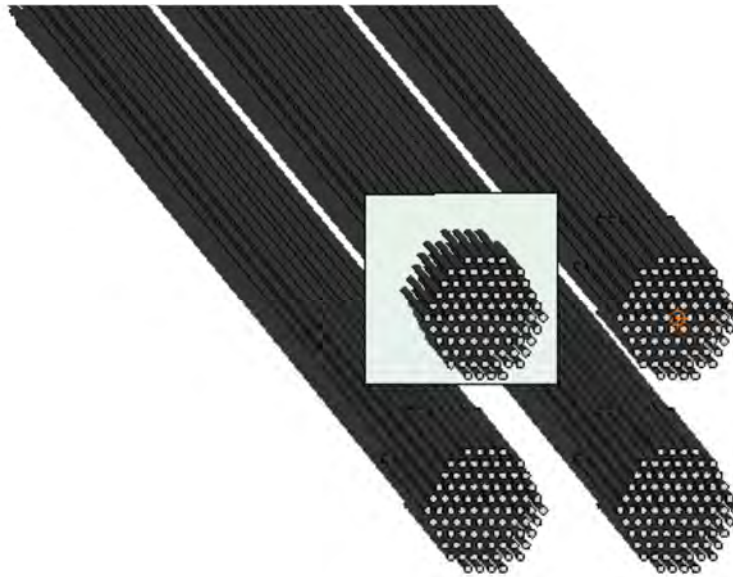


*Figure 3: Tows of hexagonal arranged filaments, of infinite length, arranged in square packing. The square of two dimensions formed is a unit cell. (Visualized using Salome software)*

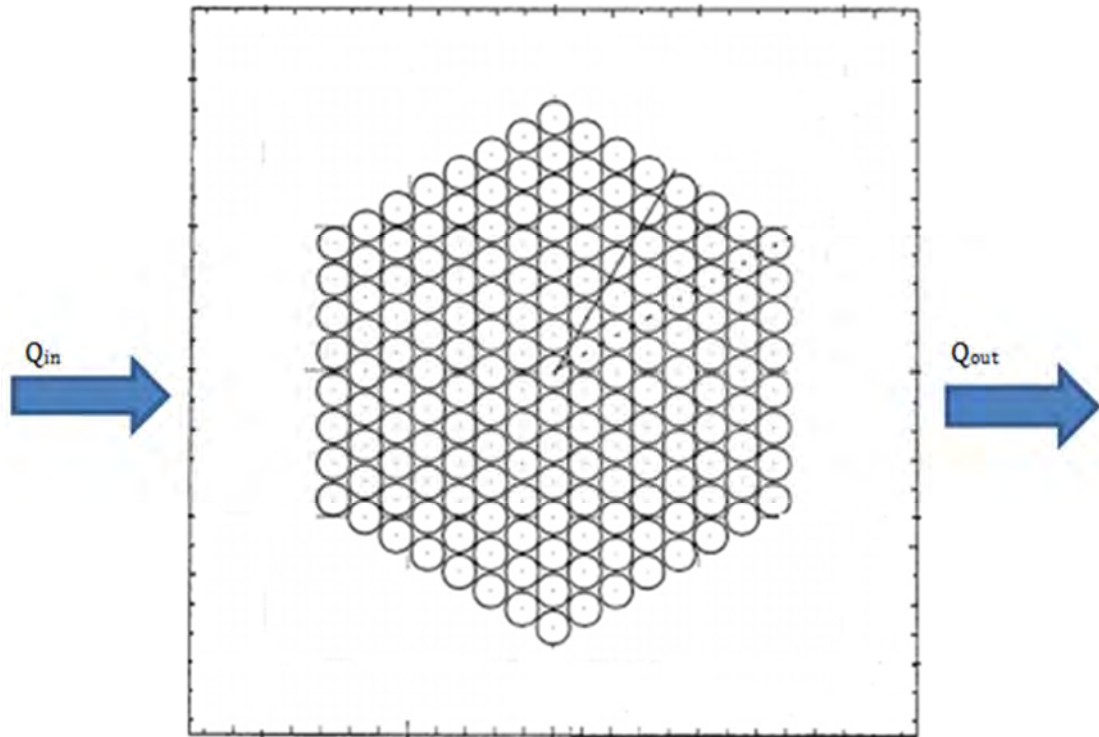


Figure 4: A unit cell with hexagonal arranged filaments and the direction of the flow

#### 1.4.1 Flow across bundles of non-absorbing filaments

In the first instance, we only consider arrays of filaments in which there is no absorption of fluid. Therefore the following flow balance equation applies:

$$Q_{inlet} = Q_{outlet} \quad (1.5)$$

Where

$Q_{inlet}$ : Volume flowrate of liquid at input [ $m^3/s$ ]

$Q_{outlet}$ : Volume flowrate of liquid at output [ $m^3/s$ ]

## 1.4.2 Flow across bundles of absorbing (and swelling) filaments

In swelling media, we apply the same approach with the exception that the filaments absorb the flowing liquid. The absorption leads to swelling of the filaments comprising the fibrous medium and as a result a continuous increase of the filament diameters in time. The following flow balance equation applies:

$$Q_{\text{inlet}} = Q_{\text{ab}} + Q_{\text{outlet}} \quad (1.6)$$

Where

$Q_{\text{ab}}$ : Volume flowrate of liquid that the porous medium absorbs [ $\text{m}^3/\text{s}$ ]

## 1.5 Darcy's law

Darcy's law is an equation that relates the flowrate through a porous medium to the applied pressure drop. It postulates that the amount of flow between two points is directly related to the difference in pressure between the points, the distance between the points, the viscosity of the fluid and the interconnectivity of flow pathways between the points. Permeability is the physical property which expresses that interconnectivity.

In its one-dimensional form, Darcy's law is expressed as [13]:

$$U = -\frac{K}{\mu} \frac{dP}{dx} \quad (1.7)$$

Where:

$U$  = velocity of liquid through the porous medium in the x-direction [ $\text{m}/\text{s}$ ]

$$U = \frac{Q}{A}$$

$Q$  = flowrate through the porous medium [ $\text{m}^3/\text{s}$ ]

$A$  = cross-sectional area of sample perpendicular to the direction of flow [ $\text{m}^2$ ]

$K$  = permeability [ $\text{m}^2$ ]

$\mu$  = viscosity of the fluid [Pa · s]

$\frac{dP}{dx}$  = Pressure drop in the x direction

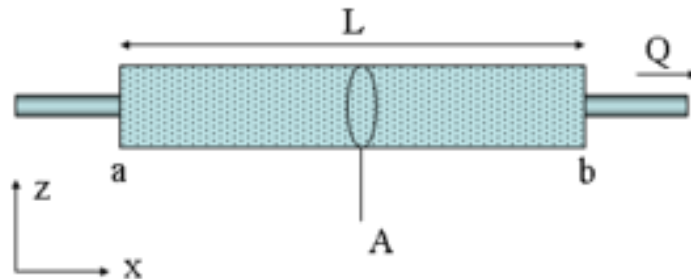


Figure 5: Diagram showing the definition of Darcy's law [5]

In order for flow to occur in the x direction, we apply a pressure drop ( $\Delta P$ ) at the ends of the geometry. This is succeeded by setting the following boundary conditions:

$$P=P_1 @ x=0$$

and

$$P=P_2 @ x=L$$

Darcy's equation can be now written as:

$$\frac{U\mu}{K} dx = dP \quad (1.8)$$

We integrate the above equation and we get:

$$\int_0^L \frac{U\mu}{K} dx = \int_{P_1}^{P_2} dP \quad (1.9)$$



At this point we need to make use of the equation of continuity in order to be able to solve and simplify the above equation.

$$\nabla \cdot (\mathbf{u}\rho) = 0 \quad (1.10)$$

Where

$\rho$  = liquid density [kg/m<sup>3</sup>]

$\mathbf{u}$  = vector velocity [m/s]

The density is considered constant because we assume an incompressible fluid so the form of the equation that we get is:

$$\nabla \cdot (\mathbf{u}) = 0 \quad (1.11)$$

We see that the divergence of the velocity equals to zero, so we reach to the conclusion that the amount of fluid going into a region equals to the amount going out. So it is obvious that the volumetric flowrate is a constant value. The definition of the volumetric flowrate is:

$$Q = \int_A \mathbf{u}dA \quad (1.12)$$

So by integrating the velocity in the inlet or outlet of the geometry we can calculate the flowrate. For a given area A and uniform velocity over that area, the above equation can be written as:

$$Q = U \cdot A \quad (1.13)$$

As a result the Darcy's law equation for a porous medium can be written on the following forms:

$$Q = -A \frac{K \Delta P}{\mu L} \quad (1.14)$$

Or

$$U = -\frac{K \Delta P}{\mu L} \quad (1.15)$$

There is a minus in these equations because the fluid flows from high pressure towards lower pressure ( $P_1 > P_2 \rightarrow \Delta P < 0$ )

In the case of a geometry of an infinite width compared with the length and height, the flowrate per unit width must be entered in the formula:

$$q = \frac{Q}{W} \left[ \frac{m^2}{s} \right] \quad (1.16)$$

W = width of the medium [m]

Thus, by combining the equations we end up to the following form of Darcy's law (Eq. 1.17) that can be applied to a two-dimensional unit cell of an infinite width and which allows us to calculate the permeability of the unit cell when we know the flowrate and the corresponding pressure drop:

$$K = -q \frac{\mu L}{H \Delta P} \quad (1.17)$$

It must be mentioned that Darcy's law is valid only for a laminar and Newtonian flow, which occurs for Reynold's numbers less than 1. Reynold's number (Re) is a dimensionless quantity which quantifies the effect of fluid inertia and is defined as [15]:

$$Re = \frac{\rho UL}{\mu} = \frac{UL}{\nu} \quad (1.18)$$

Where:

$\rho$  = fluid density [kg/m<sup>3</sup>]

$\nu$  = kinematic viscosity [m<sup>2</sup>/s]

$U$  = characteristic velocity [m/s]

$L$  = characteristic length [m]

At the following chapters we are going to describe how the effective permeability of the fibrous medium (Figures 3 and 4) can be calculated from the velocity profile at unit cell's boundary and the corresponding pressure drop, using Darcy's law and so we will be able to investigate its dependence upon fluid absorption (and swelling) by the filaments, as the radius of the latter changes through time due to the absorption process (Chapter 3,4). The velocity profile and the calculations of the flow rate are obtained by the computer-aided design model OpenFOAM which is explained on Chapter 2.

## Chapter 2 Computational tool

### 2.1 Introduction to OpenFoam

OpenFOAM is first and foremost a *C++* library, used primarily to create executables, known as applications. The applications fall into two categories: *solvers*, that are each designed to solve a specific problem in continuum mechanics and utilities that are designed to perform tasks that involve data manipulation. New solvers and utilities can be created by its users with some pre-requisite knowledge of the underlying method, physics and programming techniques involved.

OpenFOAM is supplied with pre- and post-processing environments. The interface to the pre- and post-processing are themselves OpenFOAM utilities, thereby ensuring consistent data handling across all environments. The overall structure of OpenFOAM is shown in Figure 6.

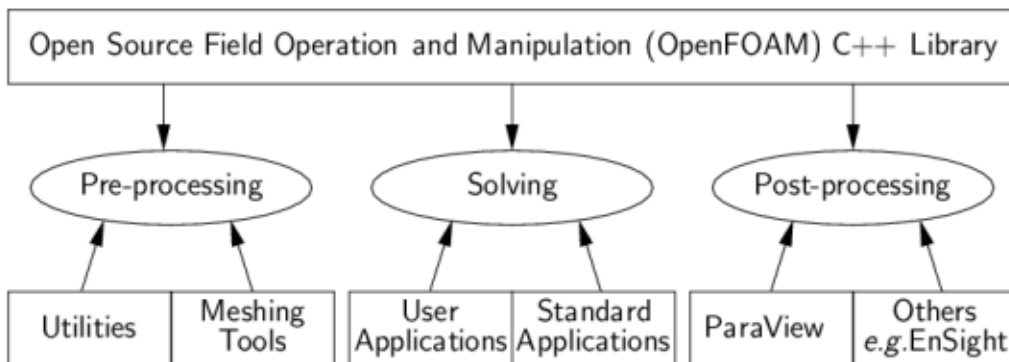


Figure 6: Overview of OpenFOAM structure [10].

OpenFOAM has tutorials and instructions that contain many cases that demonstrate the use of all the solvers and supplied many utilities. The tutorial cases describe the use of the *blockMesh* pre-processing tool, case setup and running OpenFOAM solvers and post-processing using ParaFoam

Before attempting to run the tutorials, the users must first make sure that they have installed OpenFOAM correctly and afterwards, they can have access to third-party post-processing tools (supported in OpenFOAM). Then they have the option of following the tutorials using *paraFoam*; or refer to the User Guide for details on post-processing with external applications.

OpenFOAM does not have a generic solver applicable to all cases. Instead, users must choose a specific solver for a class of problems to solve. The current list of solvers distributed with OpenFOAM is given below [4]:

- 'Basic' CFD codes
- Incompressible flow
- Compressible flow
- Multiphase flow
- Direct numerical simulation (DNS)
- Combustion
- Heat transfer and buoyancy-driven flows
- Particle-tracking flows
- Molecular dynamics methods
- Direct simulation Monte Carlo methods
- Electromagnetics
- Stress analysis of solids
- Finance

## 2.2 Familiarity with the environment

This part describes how to pre-process, run and post-process a case involving incompressible flow in a two-dimensional unit cell that in its center are located a number of solid cylindrical filaments arranged in periodic order (Figure 7). A pressure value is set at the left edge while at the right this value is zero. This pressure difference created between the two borders causes the flow of fluid to start. The flow is supposed laminar and will be worked out on a mesh using the simpleFoam solver for laminar, incompressible liquid movement. SimpleFoam is a steady state solver that is using the SIMPLE (Semi-Implicit Method for Pressure-Linked Equations) algorithm. Finally the fluid that flows across the unit cell is set to be Newtonian fluid, this results in a low and fixed Reynolds number.

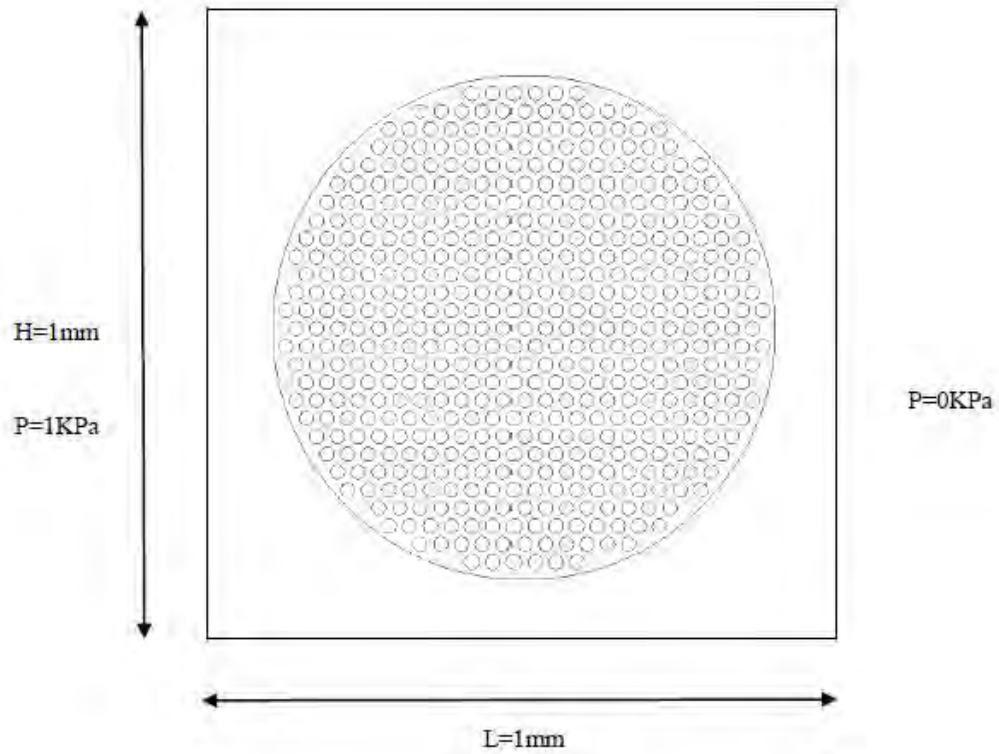


Figure 7: Filaments placed in the center of a cell in a periodic arrangement

### 2.2.1 SimpleFoam

The computational model solves system of Navier-stokes equations for incompressible fluid flow (implemented in OpenFOAM).

Generally the flow of fluids is a phenomenon described by means of conservation of mass, momentum and energy. Because we have assumed incompressible fluid flow the density is constant so the continuity equation of mass limits to

$$\nabla \cdot \mathbf{u} = 0 \quad (2.1)$$

$\mathbf{u}$ =velocity vector [m/s]

Also, we have the Momentum conservation equation (velocity equation) for a single-phase flow where density and viscosity are constant [2],

$$\frac{\partial \mathbf{u}}{\partial t} + (\mathbf{u} \cdot \nabla) \mathbf{u} = \nu \nabla^2 \mathbf{u} - \nabla p + g \quad (2.2)$$

Where

$\rho$ = density [kg/m<sup>3</sup>]

$\mathbf{u}$ = velocity vector [m/s]

t= time [s]

p= static pressure [Pa]

$\nu$ = kinematic viscosity [m<sup>2</sup>/s]

$\mu$ = dynamic viscosity [Pa·s=kg/(s·m)]

And we can also consider:

$\bar{\tau} = \mu(\nabla \mathbf{u} + \nabla \mathbf{u}^T)$  = Stoke's stress constitutive equation for incompressible viscous fluid

So, we have the following equation consists of Stoke's stress equation and ignoring the effects of gravity,

$$\rho \mathbf{u} \nabla \mathbf{u} = -\nabla p + \nabla \cdot \bar{\tau} \quad (2.3)$$

The solution of these partial differential equations is not straightforward because an explicit equation for the pressure is not available. One of the most common approaches is to derive an equation for the pressure by taking the divergence of the momentum equation and by substituting it in the continuity equation until convergence is achieved.

The SimpleFoam (Semi-Implicit Method for Pressure-Linked Equations) allows to couple the Navier-Stokes equations with an iterative procedure, which can be summed up as follows:

1. Set the boundary conditions.
2. Solve the discretized momentum equation to compute the intermediate velocity field.
3. Compute the mass fluxes at the cells faces.
4. Solve the pressure equation and apply under-relaxation.
5. Correct the mass fluxes at the cell faces.
6. Correct the velocities on the basis of the new pressure field.
7. Update the boundary conditions.
8. Repeat till convergence.

It should be pointed out that the steps 4 and 5 can be repeated for a prescribed number of steps (iterations) until convergence is achieved.

### 2.2.2 Pre-Processing

Data for mesh, physical properties, fields, control parameters etc. are involved in a case simulation.

#### Mesh generation:

OpenFOAM always operates in a 3 dimensional Cartesian coordinate system and all geometries are generated in 3 dimensions. OpenFOAM solves the case in 3 dimensions by default but can be instructed to solve in 2 dimensions by specifying a 'special' *empty* boundary condition on boundaries normal to the (3rd) dimension for which no solution is required. OpenFOAM provides a mesh generator, *blockMesh*, which generates meshes from a description located in system folder, *blockMeshDict* file. Mesh generates by running on this file. Also, the running status of *blockMesh* is reported in the terminal window.

```
frontAndBack
{
    type empty;
    faces
    (
        (22 28 29 23)
        (23 29 30 24)
        (24 30 31 25)
        (26 32 33 27)
        (27 33 34 28)
        (28 34 35 29)
        (29 35 36 30)
        (30 36 37 31)
    )
}
```



```

(32 38 39 33)
(33 39 40 34)
(34 40 41 35)
(35 41 42 36)
(36 42 43 37)
(0 1 7 6)
(1 2 8 7)
(2 3 9 8)
(4 5 11 10)
(5 6 12 11)
(6 7 13 12)
(7 8 14 13)
(8 9 15 14)
(10 11 17 16)
(11 12 18 17)
(12 13 19 18)
(13 14 20 19)
(14 15 21 20)
);
}

```

### Boundary and initial conditions

Once the mesh generation is complete, the user can look at this initial fields set up for this case. The case is set up to start at time  $t=0s$ , so the initial field data is stored in a  $0$  sub-directory.

The  $0$  sub-directory contains 2 files,  $p$  and  $U$ , one for each of the pressure and velocity fields whose initial values and boundary conditions must be set.

Let us first examine the file  $U$ :

```

dimensions      [0 1 -1 0 0 0 0];
internalField   uniform (0 0 0);
boundaryField
{
    left
    {
        type          zeroGradient;
    }
    right
    {
        type          zeroGradient;
    }

    top
    {
        type          cyclicAMI;
    }

    bottom
    {
        type          cyclicAMI;
    }

    internal
    {

```

```

        type flowRateInletVelocity;
        volumetricFlowRate -0.000043;
value      uniform (0 0 0); // placeholder
    }

    front
    {
        type          empty;
    }

    back
    {
        type          empty;
    }
}

```

As well as the file p:

```

dimensions      [0 2 -2 0 0 0 0];
internalField   uniform 0;
boundaryField
{
    left
    {
        type          fixedValue;
        value         uniform 1;
    }

    right
    {
        type          fixedValue;
        value         uniform 0;
    }

    top
    {
        type          cyclicAMI;
    }

    bottom
    {
        type          cyclicAMI;
    }

    internal
    {
        type          zeroGradient;
    }

    front
    {
        type          empty;
    }

    back
    {
        type          empty;
    }
}

```

We observe that there are 3 principal entries in field data files:

- **Dimensions:**  
specifies the dimensions of the field, here *kinematic* pressure.
- **internalField:**  
the internal field data which can be uniform, described by a single value; or nonuniform, where all the values of the field must be specified.
- **boundaryField:**  
the boundary field data that includes boundary conditions and data for all the boundary patches.

Here, we have 4 different entry conditions for each side as explained below:

- **cyclicAMI:** enables two patched whose faces are non-matching to be treated as they are physically connected. This boundary condition is usually used for sliding interface in rotating geometry cases.
- **zeroGradient:** This boundary condition extrapolates the pressure (generally every quantity) to the boundary patch from the nearest cell value. The meaning is that the pressure is developed and its gradient is equal to zero in direction perpendicular to the boundary ( $\partial P/\partial x=0$ ).
- **fixedValue:** value of  $p$  is specified by a value ( In our case at left boundary field  $p=1$  and at right  $p=0$  [ $m^2/s^2$ ])
- **empty:** This condition characterizes the front and rear planes of the two-dimensional geometry, so they are posed as voids

### Physical properties

The physical properties for the case are stored in dictionaries whose names contains the word "Properties". For a SimpleFoam case, the only property that must be specified is the kinematic viscosity which is stored in transportProperties. The user

can check that the kinematic viscosity is set correctly by opening the `transportProperties` dictionary to view/edit its entries. The keyword for kinematic viscosity is `nu`, the phonetic label for the Greek symbol,  $\nu$ , by which it is represented in equations. Initially this case will be run with a Reynolds number of  $10^{-3}$ , where the Reynolds number is defined as:

$$Re = \frac{L|U|}{\nu}$$

Where

$L$  is the characteristic length [m]

$|U|$  is the characteristic velocity

$\nu$  is the kinematic viscosity.

Here  $L=1$  [mm],  $|U|=1$  [m/s], so that for  $Re=10^{-3}$ ,  $\nu=1$  [  $m^2/s$  ] (for  $\mu=10^3$ [Pa·s=kg/(s·m)] and  $\rho=10^3$ [kg/m<sup>3</sup>]).

The correct file entry for kinematic viscosity is thus specified below:

```
transportModel Newtonian;
```

```
nu      [0 2 -1 0 0 0 0] 1e-00;
```

### Control

Input data relating to the control of time and reading and writing of the solution data are read in from the `controlDict` dictionary. The user should view this file as a case control file, it is located in the `system` directory.

The start/stop times and the time step for the run must be set. OpenFOAM offers great flexibility with time control. In our case we wish to start the run at time  $t=0$ s which means that OpenFOAM needs to read field data from a directory named `0` for more information of the case file structure. Therefore we set

the startFrom keyword to startTime and then specify the startTime keyword to be zero. Also we set as endTime 2000 steps because our case we are studying does not converge. Below are shown the entries in the controlDict [6]:

```
application      simpleFoam;
startFrom        startTime;
startTime        0;
stopAt           endTime;
endTime          2000;
deltaT           1;
writeControl     timeStep;
writeInterval    1;
purgeWrite       2;
writeFormat      binary;
writePrecision   6;
writeCompression off;
timeFormat       general;
timePrecision    6;
runTimeModifiable true;
```

### 2.2.3 Running application

We choose to run OpenFOAM applications in the foreground, as a Linux executable. On this occasion we run simpleFoam solver, which is executed by entering the case directory and typing to the terminal window:

```
simpleFoam
```

### 2.2.4 Post-processing

We type the following commands in order to be executed by the OpenFoam. For the OpenFoam these are functions and return to the user the values of various variables

of the case. These values correspond to the latest iteration where convergence is achieved.

```
postProcess -func 'flowRatePatch(name=left)' -latestTime  
postProcess -func 'flowRatePatch(name=right)' -latestTime  
postProcess -func 'minMaxComponents(p)' -latestTime
```

The function of “flowRatePatch” returns the values of the flowrate (by integrating the profile of velocity) at the inlet:  $Q_{in}$  (name=left, for the left side of the unit cell) and at the outlet:  $Q_{out}$  (name= right) as shown respectively in the following Figures (8 and 9).

```
Executing functionObjects  
surfaceRegion flowRatePatch(name=left) write:  
sum(left) of phi = -0.000512613
```

*Figure 8: Flow rate for the left side of the unit cell ( $Q_{in}$ )*

```
Executing functionObjects  
surfaceRegion flowRatePatch(name=right) write:  
sum(right) of phi = 0.000469613
```

*Figure 9: Flow rate for the right side of the unit cell ( $Q_{out}$ )*

The function of “minMaxComponents(p)” returns the values of the minimum and maximum pressure and the exact location these pressures are encountered in our geometry, as shown in the Figure 10.

```
Executing functionObjects  
fieldMinMax minMaxComponents(p) write:  
min(p) = -2.60544 at location (0.554603 0.501099 0.05)  
max(p) = 1.37202 at location (0.418536 0.846212 0.05)
```

*Figure 10: Minimum and maximum pressure for an exact location*

By reaching convergence the results are saved to time directories and via a post-processing open-source tool, named ParaView, they can be viewed. This tool can be used by typing at the command line paraFoam. At this case we are interested in extracting conclusions by the contour plots of velocity and pressure which show us the magnitudes of these values and by using the application of glyph in the paraView we get the vectors of velocity.

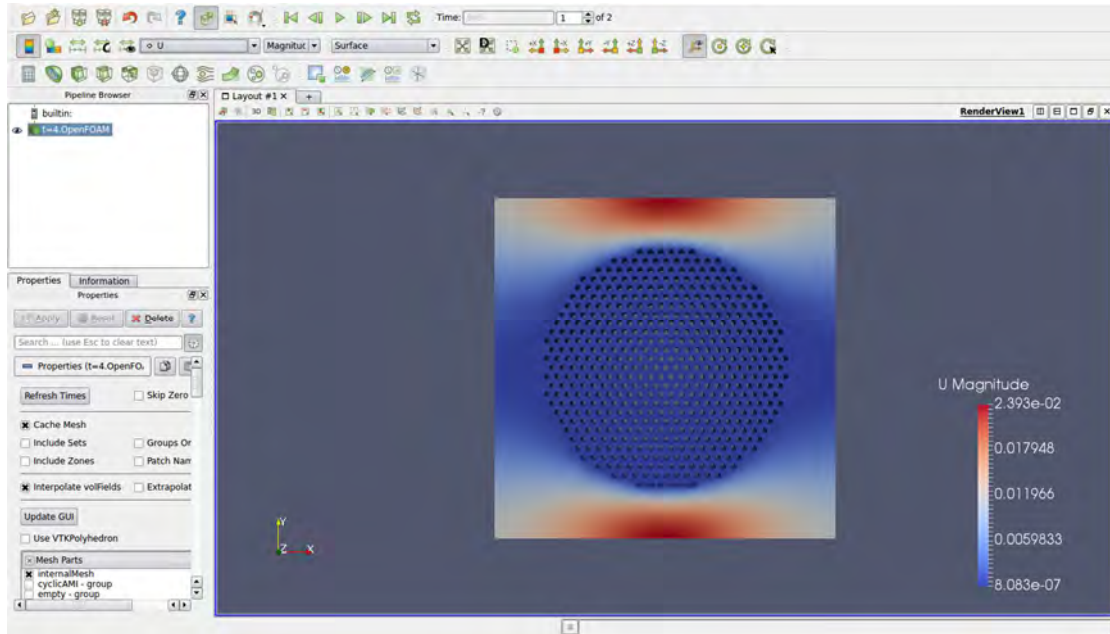


Figure 11: paraView environment - velocity profile of a unit cell

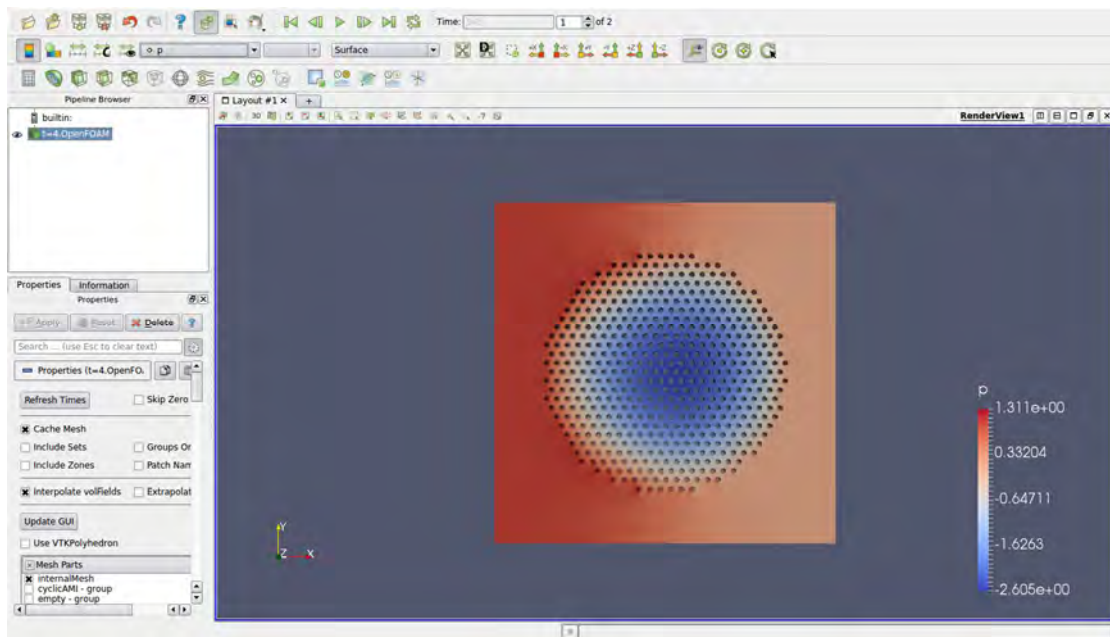


Figure 12: paraView environment - pressure profile of a unit cell

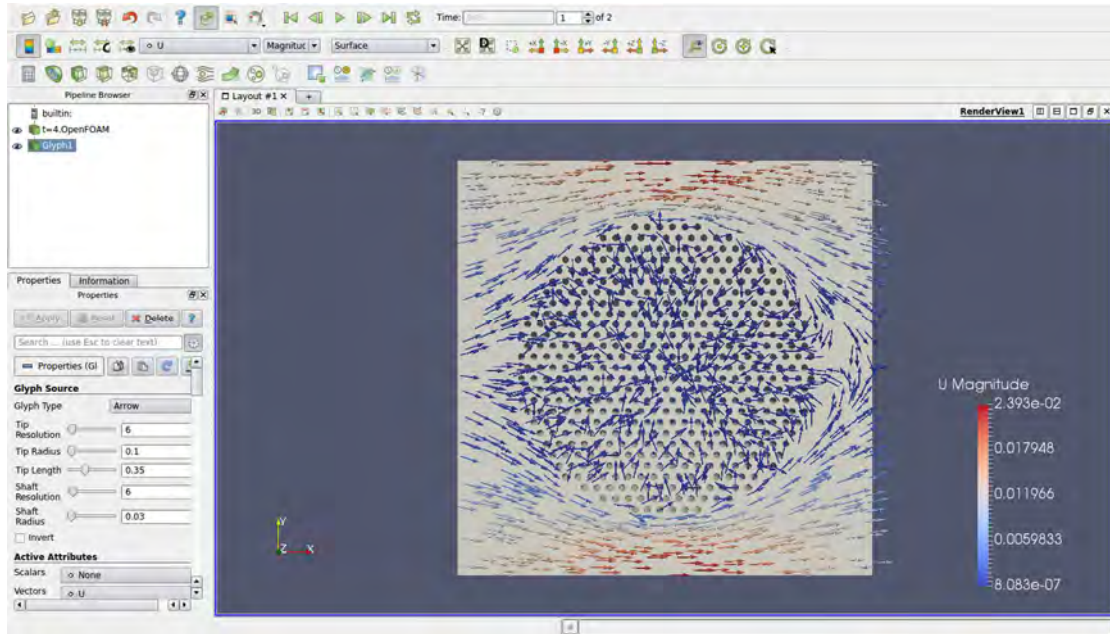


Figure 13: paraView environment – velocity vectors in the unit cell



## Chapter 3 Non-linear behavior of absorption rate

### 3.1 Geometry generation

The case consists of long cylindrical bundles, arranged in a square packing. Within each bundle are located a number of  $N_f = 500$  rigid individual cylindrical filaments, arranged in hexagonal packing, of radius  $R_f$ . Our study is focused on one of these square packaged bundles, which forms a unit cell. We assume that the dimensions of the cell are  $L=H=1$  [mm], where  $L$  and  $H$  represent the length and height respectively. To continue we must first determine the volume fraction of the bundle ( $\Phi_i$ ) and of the filaments that compose the bundle ( $\Phi_t$ ). The volume fraction of the bundle in a two dimensional unit cell (Figure 4) is defined as:

$$\Phi_i = \frac{\pi R_t^2}{L H} = \frac{\pi R_t^2}{H^2} \quad (3.1)$$

Where  $R_t$  is the radius of the bundle. The volume fraction of the filaments is defined as:

$$\Phi_t = N_f \left[ \frac{R_f}{R_t} \right]^2 \quad (3.2)$$

Where  $N_f$  is the number and  $R_f$  the radius of the cylindrical filaments in each bundle and  $R_t$  is the radius of the bundle.

In order to solve the problem we will create a program that will accept the number of filaments and the volume fractions of the bundle and filaments as data. It will be able to create the cell containing the bundle and the filaments. Furthermore the program will be capable of placing the filaments inside the bundle in hexagonal array. Follows an analysis of how the program places the filaments.

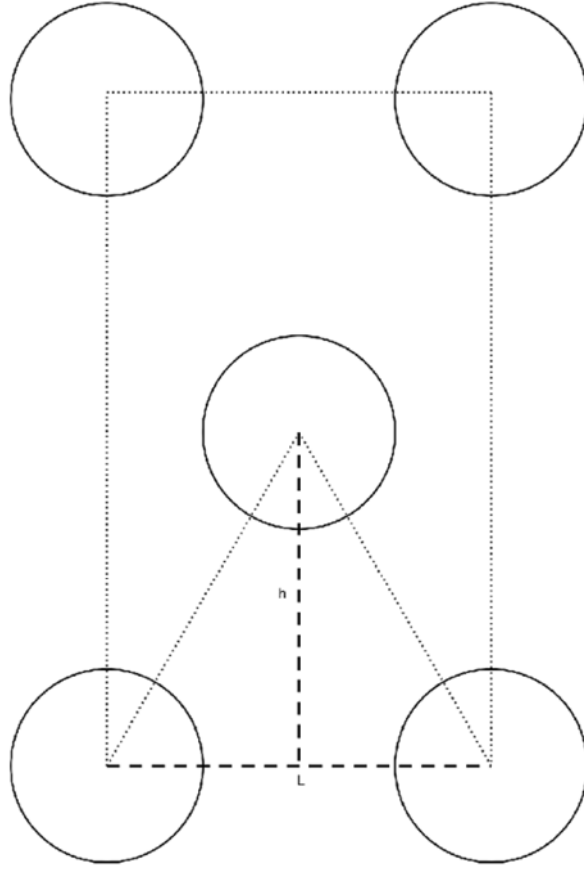


Figure 14: 2D structure for hexagonal arrays of filaments

In Figure 14 appears a lattice of the filaments that are packed in hexagonal array. The horizontal distance between their centers is called  $L$ , while the vertical  $h$ . To develop a relationship between these two dimensions, we need to deepen the geometry of the image. It is observed that between the two circles of the lower layer and the circle on the middle layer are created two isosceles right triangles, which allows us to apply the Pythagoras theorem to one of them and as a result we get:

$$h = L \frac{\sqrt{3}}{2} \quad (3.3)$$

In addition, we are calculating the area of the square created by joining the outer centers results:

$$4 \frac{\pi R_f^2}{4} + \pi R_f^2 = \Phi_t \cdot L \cdot 2h \rightarrow L = \left( \frac{2\pi R_f^2}{\Phi_t \sqrt{3}} \right)^{\frac{1}{2}} \quad (3.4)$$

The program works with coordinates, so starting from the point opposite the center of the big circle begins to place the filaments along the horizontal axis at a distance  $L$  between them. Just before the filaments get out of the bundle, the process of horizontal placement stops. Then we move at a height  $h$  in the next up and down levels and start the horizontal placement process on the new levels. With the only difference that the first point at which the positioning begins, shifts horizontally by  $L/2$  relative to the first point from the previous layer. This happens only at the first point of each layer, so the distance between every filament in each plane remains  $L$ . These calculations are made by a program which is written on visual basic and the output of the program is a .geo format file, so a mesh can be subsequently generated and be processed by OpenFOAM. Even though we work in two dimensions, the program produces a three-dimensional cell ( $L=H=W=1\text{mm}$ ) in order to be able to run on the OpenFOAM (Chapter 2.2)

Ultimately, the user only needs to give the values in the volume fractions and the number of the filaments and will get a visual result of the case we are studying as it appears in the Figure 15. A part of the code is placed on Appendix A.

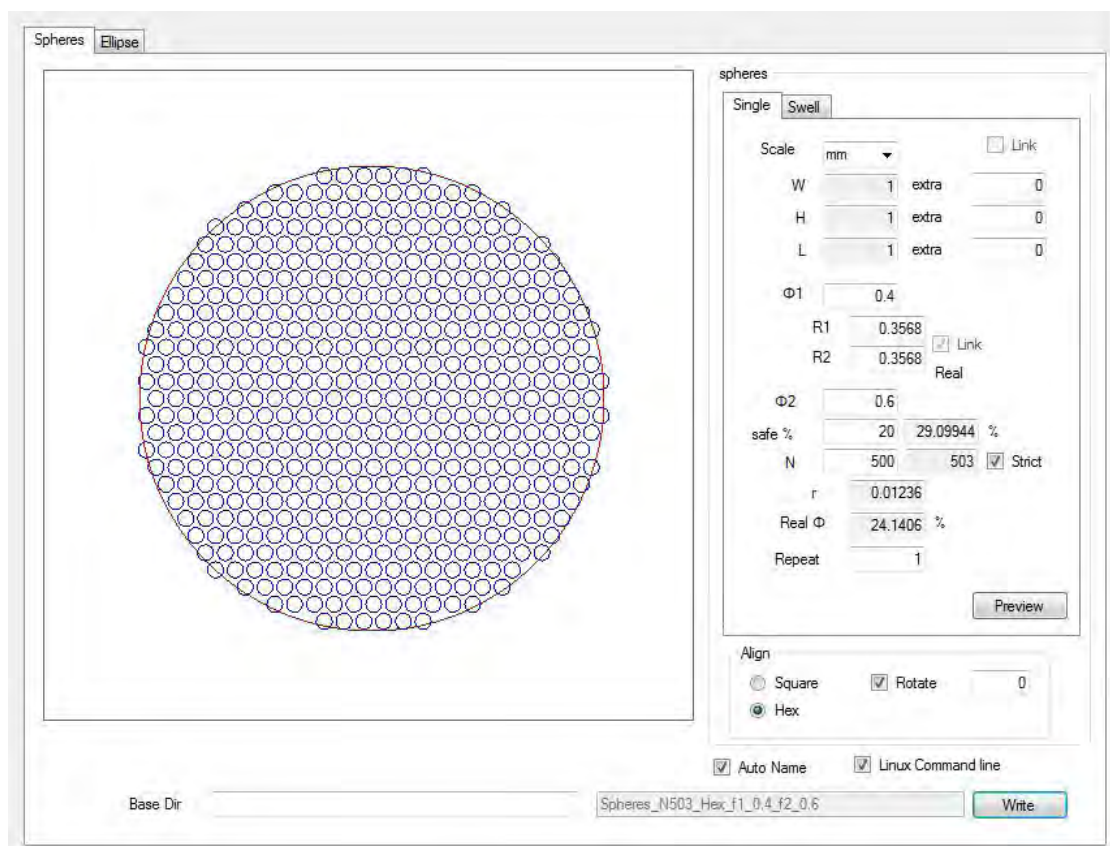
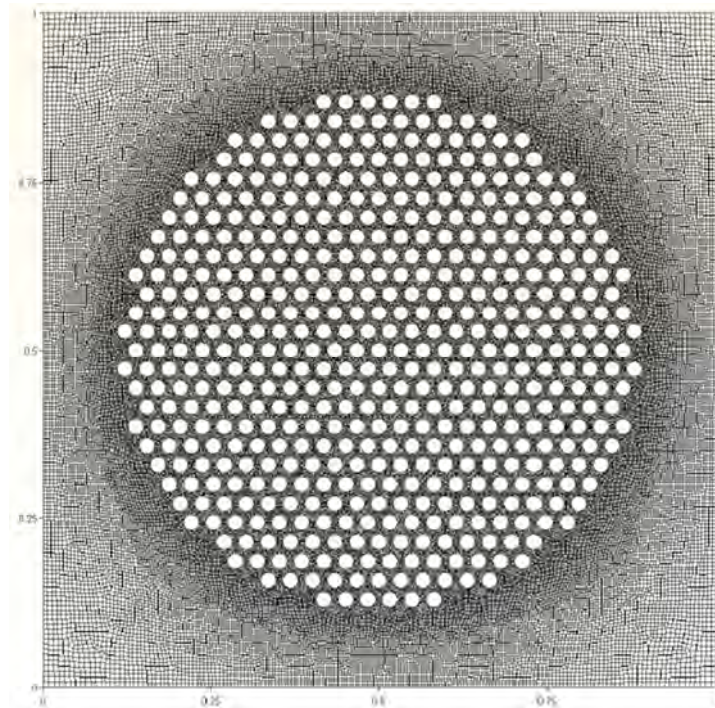


Figure 15: Visual result of the program that creates the unit cell

The user will notice that the number of filaments in the bundle, at fixed  $R_t$ , may vary a bit along with  $\Phi_i$  and  $\Phi_t$  because of the way the bundle is filled.

### 3.2 Mesh

By creating the geometry, as described above, we can now generate our mesh, on which we are going to solve numerically the governing equations described in the previous section. A mesh results in the discretization of the inter-filament space into finite volumes, it is on these finite volumes that the conservation equations are subsequently solved by OpenFoam. A boundary zone defines inlet or outlet boundaries within the geometry. A computational mesh is generated by utilizing the mesh generator provided with OpenFOAM. This command runs the Gmsh, an implement that converts the .geo file format geometries, which have been created with the visual basic program, into .msh file format. Numerical results may vary depending on the number of elements we are using. The more elements exist in our mesh the less is the grid spacing. We can determine the grid spacing, by changing a value on the .geo file format which is called 'characteristic length factor'. The finest grid solution is considered to be one with zero grid spacing.



*Figure 16: Mesh of a unit cell*

### 3.3 Boundary conditions

#### Pressure

In order to make the fluid flow we have to apply pressure difference on the inlet (left border) and outlet (right border). With OpenFoam it is possible to determine the kinematic pressure as fixed values in the boundary layers. The kinematic pressure is given by the following relationship:

$$p = \frac{P}{\rho} \quad (3.5)$$

Where:

$p$  = Kinematic Pressure [ $\text{m}^2/\text{s}^2$ ]

$\rho = 10^3$  [ $\text{kg}/\text{m}^3$ ] (density)

We choose to set:

$$p = 1 \text{ at left boundary}$$

And

$$p = 0 \text{ at right boundary}$$

That means the pressure difference  $\Delta p = -1$  [ $\text{m}^2/\text{s}^2$ ] or  $\Delta P = -1000$  [Pa]

#### Velocity

The case we study has single phase flow across x direction as identifying trait. That means that setting the velocity in such direction perpendicular to the boundary, is a priority. That requirement is satisfied by setting the gradient of velocity equal to zero in x direction.

$$\frac{\partial U}{\partial x} = 0 \quad (3.6)$$

And because we study a plane cross-sectional that also means:

$$\frac{\partial Q}{\partial x} = 0 \quad (3.7)$$

This is succeeded with the “zeroGradient” condition (chapter 2.2.2)

In the case where the fluid is absorbed in the interior of the geometry by the filaments, so the liquid does not just flow through the porous space, we need to add an extra internal condition of the velocity field on the filament surfaces. Specifically we give a fixed value to the flowrate absorbed by the porous medium. At the field of pressure there are no changes. At the OpenFoam file this is translated to the following commands:

```
internal
{
    type flowRateInletVelocity;
    volumetricFlowRate -0.000043;
    value uniform (0 0 0); // placeholder
```

### 3.4 Absorption

At the case of absorption, with which we are dealing at this thesis, the fluid is absorbed by the filaments of the porous medium. As a result the diameter of the filaments increases and during the process of absorption some of the perimetric filaments exceed the boundary of the bundle by the length of  $dr$ . The bundle stops absorbing fluid only when the radius of each filament begins to osculate each other. At this state the bundle is also considered as an impermeable entity (for values of  $\Phi_t$  higher than 70%). Consequently the volume fraction of the filaments changes through time, which of course has an impact on the flow rate and the permeability (conclusions that will be made by our computational analysis). It should also be mentioned that the flow rate is divided and absorbed equally by the filaments.

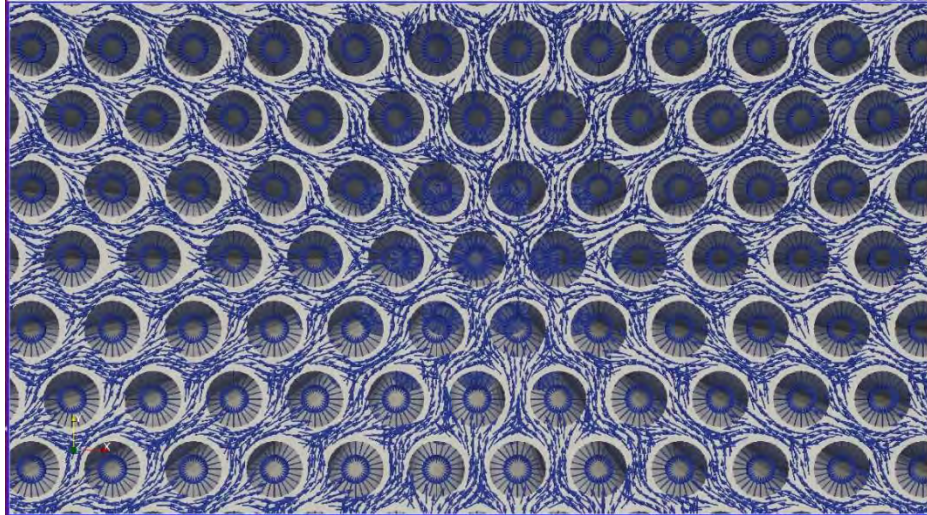


Figure 17: Vertical flow of liquid into the porous medium due to absorption

At this point we need to explain the way we calculate the initial quantity of fluid absorbed by the filaments. We assume that this quantity is equal to a small percentage of the flow rate passing through one rigid filament ( $Q_{base}$ ) equal to the area that is occupied by the bundle of filaments in our case. The problem is solved as explained at chapter 1.4.1 and by applying the boundary conditions for a flow without absorption as seen previously (chapter 3.3). So it is true that:

$$Q_{inlet}=Q_{outlet}=Q_{base} \quad (3.8)$$

And the result of the flow rate per unit width we get by solving this case with OpenFoam is:  $Q_{base}=0.0043 \text{ [m}^2\text{/s]}$

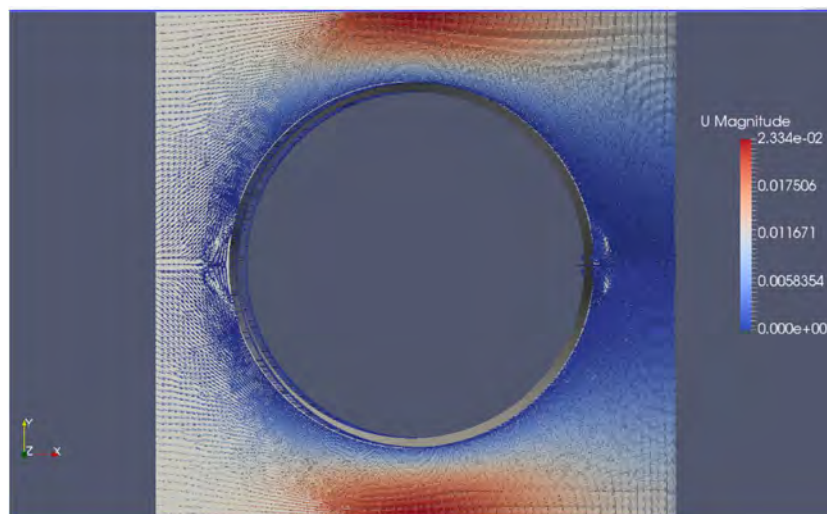


Figure 18: Velocity vectors of a single impermeable filament, used for the calculation of  $Q_{base}$

The final value of flow rate per unit width absorbed, for a steady flow, is calculated by the following equation:

$$Q_{absorbed} = \alpha \cdot Q_{base} \quad (3.9)$$

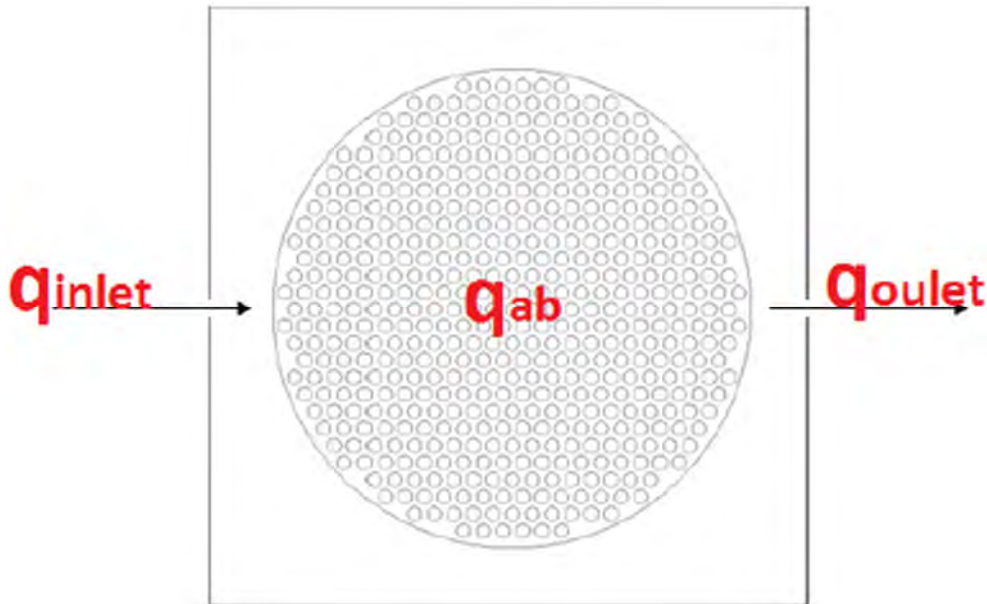


Figure 19: Appears where flow rate is present

In our case we are investigating the results of five different values of the absorption coefficient ( $\alpha$ : 0.01-0.03-0.05-0.07-0.1) and for each one obviously the rate of growth changes differently (which means radius and volume fraction change with different way). By applying Eq. 3.9 we get the values of  $Q_{ab}$ :

absorption coefficient (a)	1%	3%	5%	7%	10%
$Q_{ab}$ [m <sup>2</sup> /s]	0.000043	0.000129	0.000215	0.000301	0.00043

Table 3.1: Amount of the flowrate absorbed for each different value of the absorption coefficient (a)

These values of  $Q_{ab}$  for each occasion change through the process of absorption and it is correlated to the way the radius of the filaments changes through time. This leads also to the fact, that the  $Q_{inlet}$  changes through time so that the mass balance can be satisfied ( $Q_{in} - Q_{out} - Q_{ab}=0$ ). This equation is verified, according to the results shown on Appendix D, as the residuals are considered really small.



The relationship between the radius of the filaments and the flow rate absorbed by them is expressed by the following equation which represents the rate of growth of the filaments:

$$2\pi r dr = \frac{Q_{ab}}{N_f} \frac{R_{max} - r}{r} dt \quad (3.10)$$

This equation states that the rate of growth of the size of each filament (left side of Eq. (3.10)) equals the absorption rate (right side). The latter is not considered constant in this case, but decreases as the filament size increases. When the filament size becomes equal to  $R_{max}$ , the absorption rate becomes zero.

By integrating we get:

$$\int_B^r \frac{X^2}{A - X} dX = \int_0^t \frac{Q_{ab}}{2\pi N_f} dt \quad (3.11)$$

And the result is:

$$\frac{1}{2} \left[ 2A^2 \ln \left| \frac{A - B}{A - r} \right| + 2(B - r)A + B^2 - r^2 \right] = \frac{Q_{ab}t}{2\pi N_f} \quad (3.12)$$

Where (X) is the integration variable and:

A →  $R_{max}$ : the maximum radius achieved [m]

B →  $R_0$ : initial radius [m]

$Q_{ab}$ : amount of fluid absorbed by the filaments [ $m^2/s$ ]

t= time [sec]

Equation 3.12 is a non-linear equation that gives the change of filament size with time.

Our case is additionally described by the following parameters:

$$\Phi_i = 0.4$$

$$N_f = 500$$

$$R_0 = 0.0036 \text{ [mm]} \rightarrow \Phi_t = 5\%$$

$$R_{\max} = 0.0133 \text{ [mm]} \rightarrow \Phi_t = 69.44\%$$

The above non-linear equation (3.12) is solved with the aid of the computational tool Wolfram Mathematica, for each individual rate of absorption. The way that is solved is by finding the root of the above equation while specifying the numerical method, the initial time, the latest time and the time step within a loop. As a result the values of the radius are printed for each time step.

```

A = 0.0133
0.0133

B = 0.0036
0.0036

Qb = 0.0043
0.0043

a = 0.1
0.1

q = Qb * a
0.00043

v[r_] := 1 / 2 * (2 * A^2 * Log[Abs[A - B]] + 2 * (B - r) * A + B^2 - r^2) - (q / (2 * n)) * t

v[r]
-0.0000684366 t +
1/2 (0.00001296 + 0.0266 (0.0036 - r) - r^2 + 0.00035378 Log[0.0097 / Abs[0.0133 - r]])

f = Module[{s = 0, e = 0},
  {FindRoot[v[r] == 0, {r, 0.003, 0.01330001}, Method -> "Brent", StepMonitor -> s++,
    EvaluationMonitor -> e++], "Steps" -> s, "Evaluations" -> e}
Do[Print[f, t], {t, 0, 30, 0.1}]
{FindRoot[v[r] = 0, {r, 0.003, 0.0133}, Method -> Brent, StepMonitor -> s$66395++,
  EvaluationMonitor -> e$66395++], Steps -> 0, Evaluations -> 0}

{{r -> 0.0036}, Steps -> 0, Evaluations -> 0}0.
{{r -> 0.00600049}, Steps -> 0, Evaluations -> 0}0.1
{{r -> 0.00707409}, Steps -> 0, Evaluations -> 0}0.2

```

Figure 20: Mathematica code used for solving Eq. 3.12

The values of the  $Q_{ab}$  during the absorption process can be now calculated by equation (3.13) since we know the radius at each time step.

$$Q_{ab}(t) = Q_{ab} \frac{[R_{\max} - r(t)]}{r(t)} dt \quad (3.13)$$

Since we have solved the above problems now we can plot the functions  $r(t)$  and  $Q(t)$  and the results are shown at the following graphs (numerical results of how the values of  $r$  and  $Q_{ab}$  change through time are shown on Appendix F):

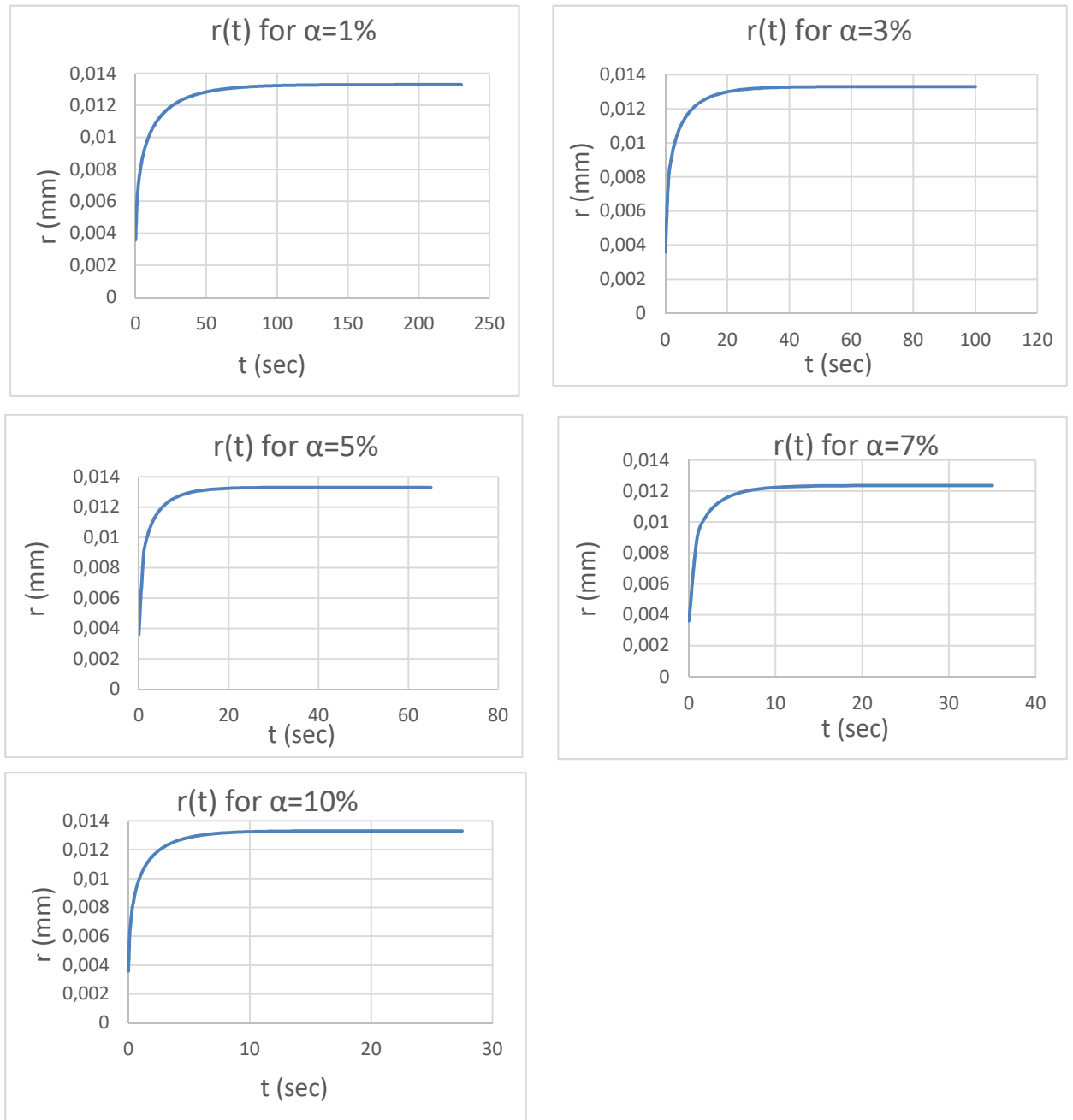


Figure 21: Graphs of the radius of the filaments versus time for various values of the absorption coefficient ( $\alpha$ )

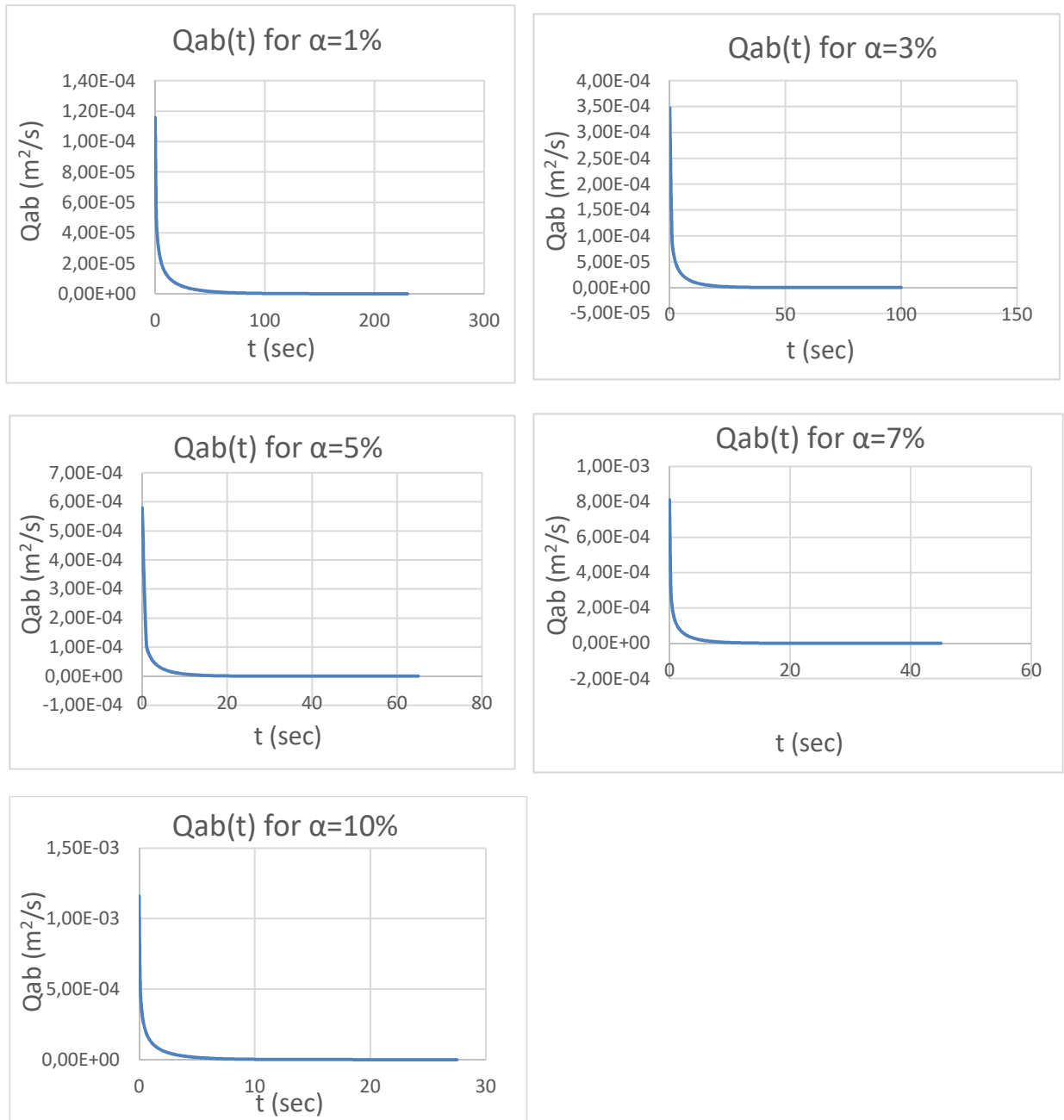


Figure 22: Graphs of the fluid absorbed versus time for various values of the absorption coefficient ( $a$ )

### 3.5 Computational results

The purpose of our simulations is to calculate the permeability and the minimum pressure that develops inside a bundle as a result of fluid absorption. The permeability is calculated from the numerical data from OpenFoam's solver which gives the flow rate on the outlet by integrating the velocity profile. The values of the

flow rate are inserted in the Darcy's law (eq. 1.17) and so the permeability is calculated. The other values needed have also been explained earlier ( $L=H=10^{-3}m$ ,  $\mu=10^3 Pa\cdot s$ ,  $\Delta P=-10^{-3} Pa$ ).

Numerical results are compared to earlier empirical models which have the form of a dimensionless correlation. The overall permeability ( $K_p$ ) of a dual porosity system is affected by the flow through the inter- and intra- tow spaces. The latter is related to the permeability of the tow itself ( $K_{tow}$ ) while the former will be related to permeability of a system with the same inter-tow porosity but made up of impermeable tows ( $K_s$ ). Consequently the overall permeability can be expressed in a general form:

$$K_p = f(K_{tow}, K_s)$$

The work of Papathanasiou [11] suggests an empirical model with two adjustable parameters ( $\alpha, n$ ) to calculate the permeability,  $K_p$ , of the unit cell.

$$K_p = K_s \left[ 1 + \alpha \left( \frac{K_s}{K_{tow}} \right)^{n-1.5} \right] \quad (3.14)$$

Or in terms of the dimensionless quantity  $Y = K_p K_s^{1/2} (K_{tow}^{3/2})$

$$Y \equiv \frac{K_p K_s^{0.5}}{K_{tow}^{1.5}} = a \left( \frac{K_p}{K_{tow}} \right)^n \left[ 1 + \frac{1}{a} \left( \frac{K_s}{K_{tow}} \right)^{1.5-n} \right] \quad (3.15)$$

$$K = C \left( \sqrt{\frac{V_{fmax}}{1-\phi}} - 1 \right)^{2.5} R^2 \quad (3.16)$$

The values of the permeability's parameters according to the filament arrangement, are shown on the following table:

Fiber arrangement	C	$V_{fmax}$
Quadratic	$\frac{16}{9\pi\sqrt{2}}$	$\frac{\pi}{4}$
Hexagonal	$\frac{16}{9\pi\sqrt{6}}$	$\frac{\pi}{2\sqrt{3}}$

To calculate  $K_s$  we set  $\varphi=\varphi_i$ ,  $R=R_{tow}$  and  $V_{fmax}=\pi/4$  depending on the square packing. To calculate  $K_{tow}$  we use  $\varphi=\varphi_t$ ,  $R=R_f$  and  $V_{fmax} = \frac{\pi}{2\sqrt{3}}$  because of having hexagonal arrangement.

$K_s$  and  $K_{tow}$  are calculated through eq. 3.16 [10] and the overall permeability  $K_p$  from eq. 3.14, with parameters  $\alpha=3$  and  $n=0.56$  and the results are:

$$K_s = 0.005195$$

$$K_{tow} = 2.903 \cdot 10^{-7}$$

$$K_p = 0.005311$$

Our numerical results are shown together with the value of the overall permeability, as calculated above, on the following Figure (23):

### Permeability

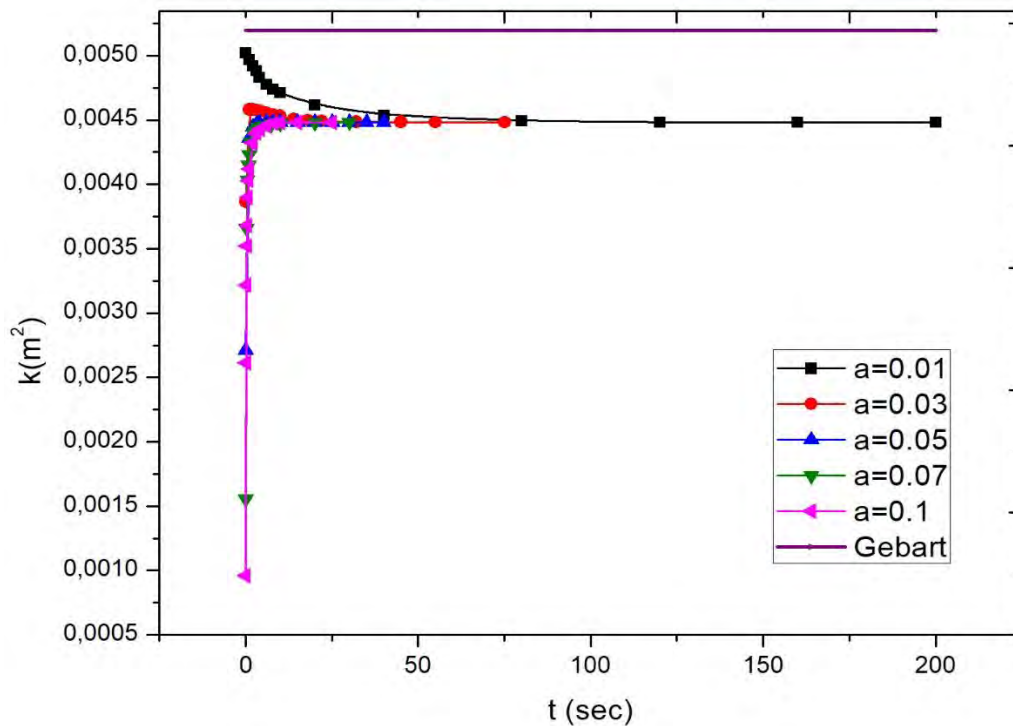


Figure 23: Graph of the permeability versus time for various values of absorption coefficient ( $a$ ), compared with Gebart's model

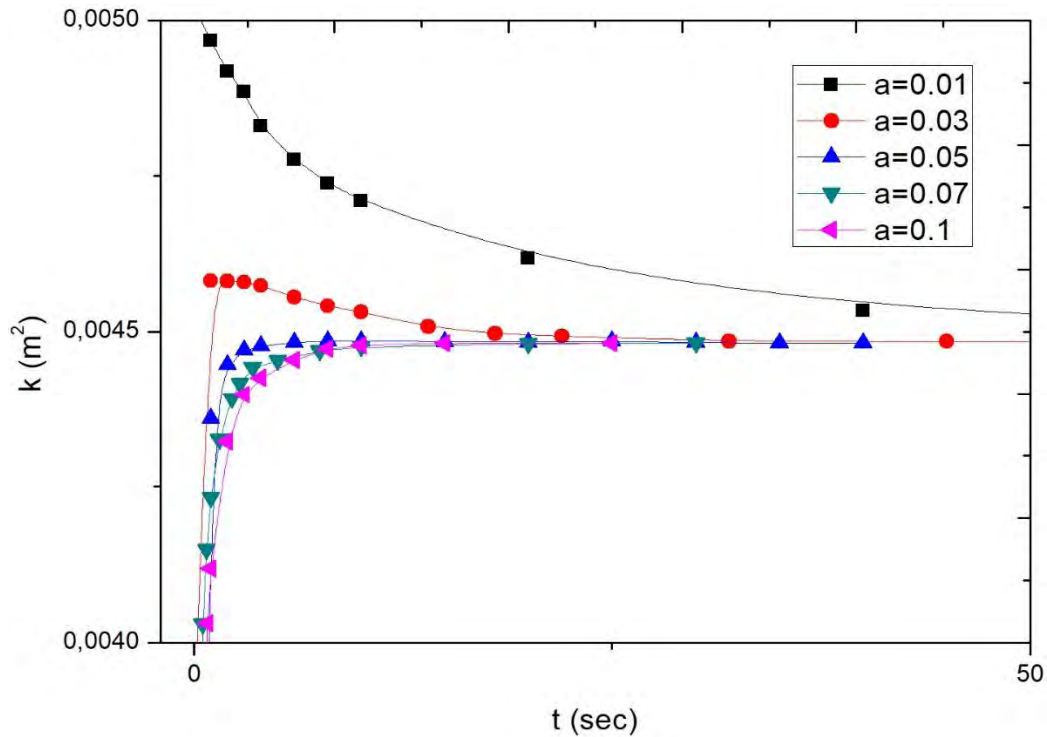


Figure 24: Zoom in a certain area of Figure 23

The overall permeability is compared to the final value reached from all the five different values of the absorption coefficient ( $a$ ). The fact that our numerical result ( $K=0,00448 \text{ [m}^2\text{]}$ ) is a bit different than Gebart's ( $K_p$ ) is perfectly reasonable, since the Gebart model assumes a bundle of perfectly circular perimeter, while our bundle has an irregular outline. But our purpose of this comparison is to see that the solution of Gebart's model lies in the same "order of magnitude".

Furthermore, by our numerical results we can observe that for low values of the absorption coefficient ( $a=0.01-0.03$ ) the values of permeability are realistic and as expected. For higher values, at the early stages of the process of absorption the values of permeability are very low, which means that most of the quantity that enters our unit cell from the left boundary is absorbed by the filaments and also fluid is absorbed by the right side of the bundle, as shown on the figures of velocity vectors (Figure 29), which is not acceptable as it does not represent the physical experiment we are trying to model, namely the absorption of fluid by a bundle of filaments at steady state. In the final stage, when all filaments inside the bundle have absorbed all they could and have almost touched each other, the flow through the bundle is essentially zero and permeability is dictated by Gebart's model. Therefore all resistance to flow is due to the gap outside the bundle (or, as we say the larger-

scale porosity, in our case  $\Phi_i=0.4$ ), and therefore the permeability corresponding to all cases, irrespective of  $a$ , is the same ( $K=0,00448 \text{ m}^2$ ).

### Minimum pressure

One interesting finding of this study is the fact that the process by which fluid is absorbed by all the filaments inside the bundle is only possible by the generation of a negative pressure inside the filament bundle. We are interested in the minimum values of pressure in every case as this difference in pressure is the force that makes the liquid flow inside our bundle of filaments during the absorption process. As we can see on the following Figure (24), pressure reaches a peak for each case of absorption rate at the early stage of the process. Until this point, the increasing minimum pressure is a result of both the increasing volume fraction ( $\Phi_i$ ) and of the amount of fluid that needs to be absorbed. At the final stage of absorption, they all settle at the same value as the fluid flows outside the bundle and not through it anymore.

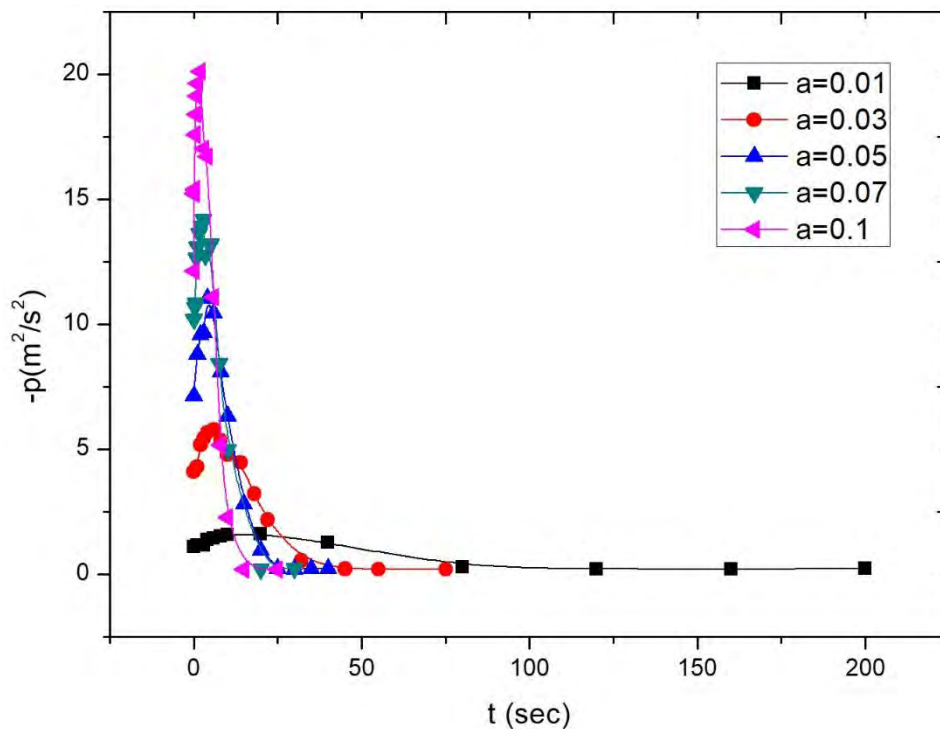


Figure 25: Graph of minimum pressure versus time for various values of absorption coefficient ( $a$ )



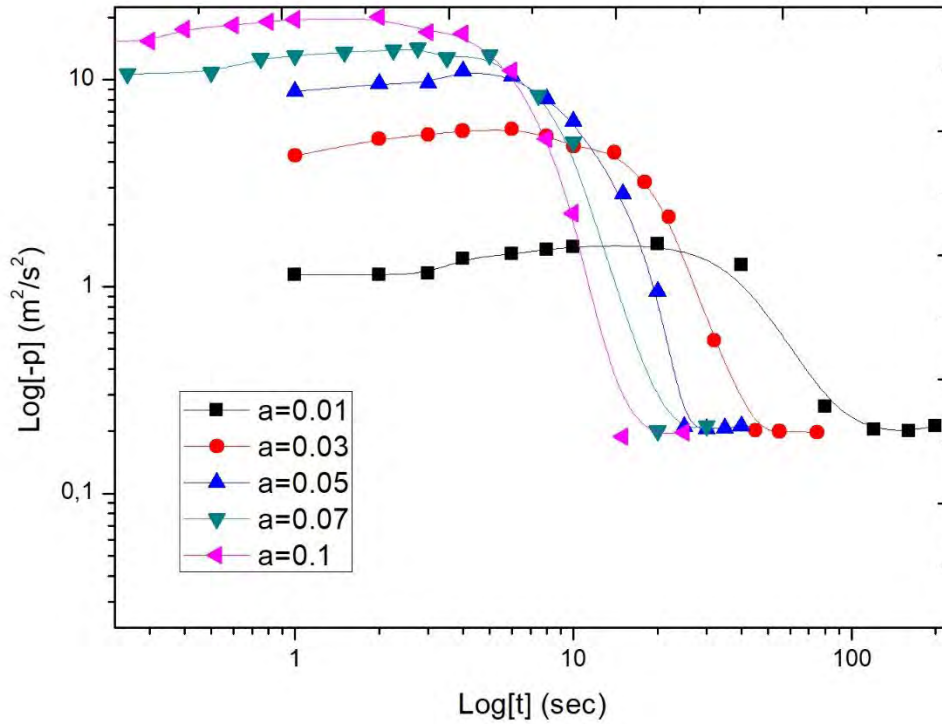


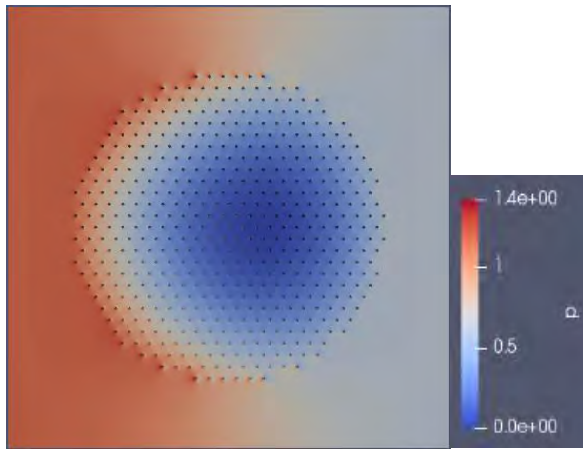
Figure 26: A log-log graph of minimum pressure versus time for various values of absorption coefficient ( $a$ )

### 3.5.1 Post-processing of the results

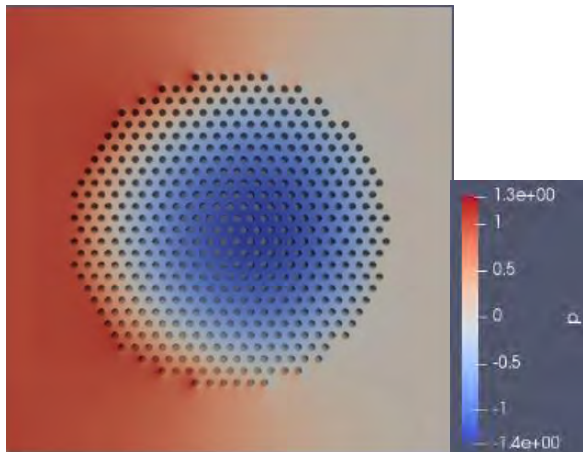
After the numerical experiments are completed, we can graphically represent our numerical results using the design environment paraView (2.2.4). The following figures show how the velocity profile develops as well as the pressure. Furthermore, we add in figures of velocity fields to see how the fluid flows across the unit cell as a function of time.

# Pressure

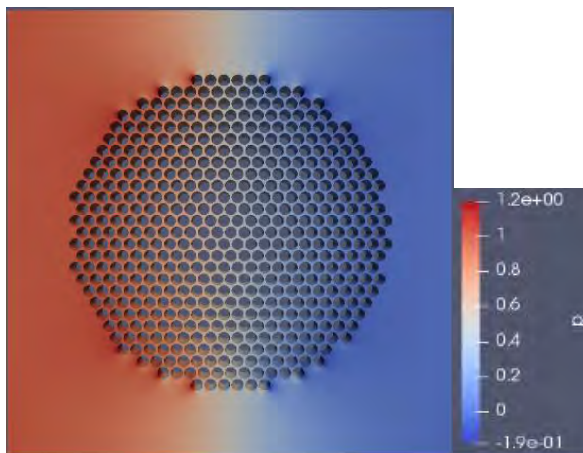
a=1%



$t=0$  s

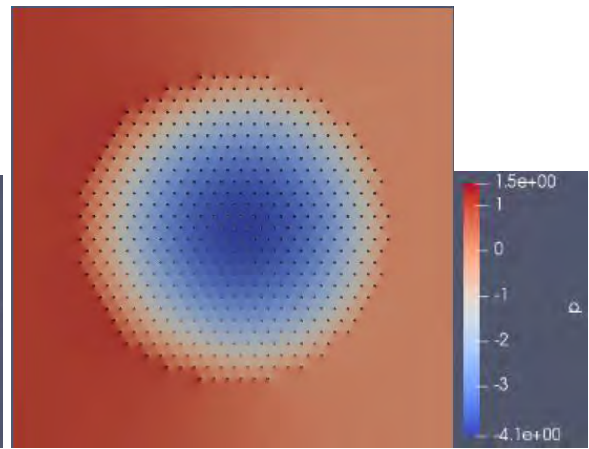


$t=4$  s

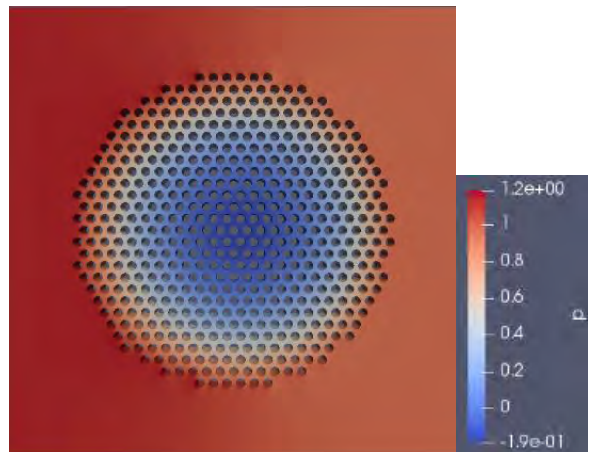


$t=200$  s

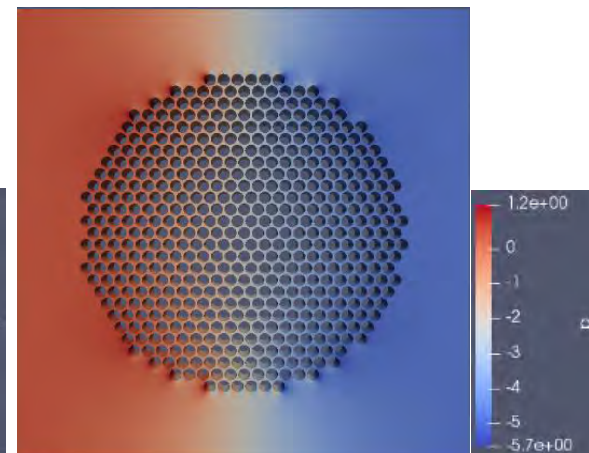
a= 3%



$t=0$  s

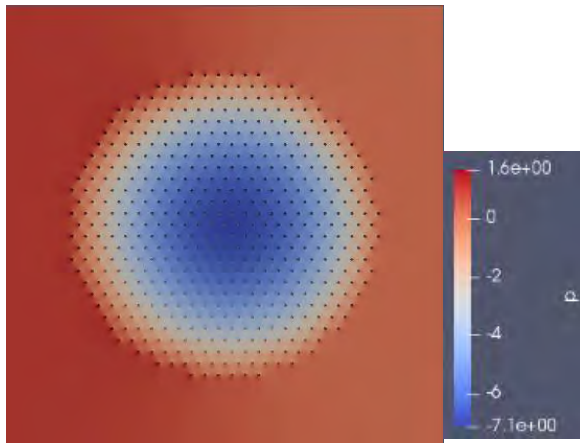


$t=4$  s

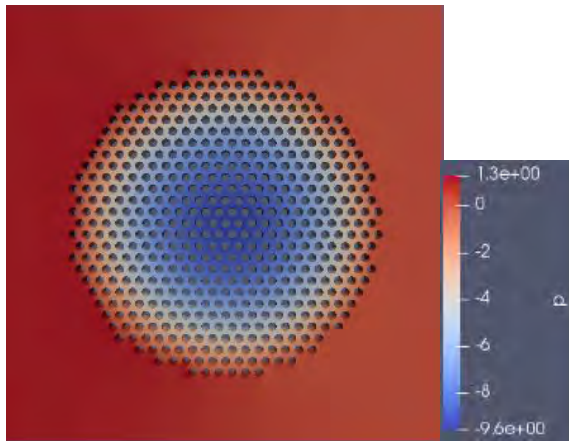


$t=75$  s

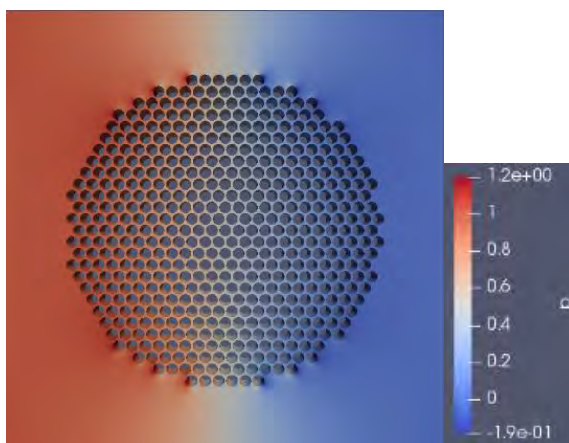
**a = 5%**



*t=0 s*

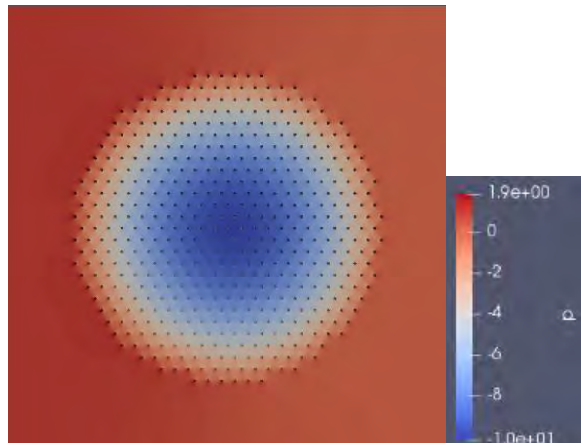


*t=2 s*

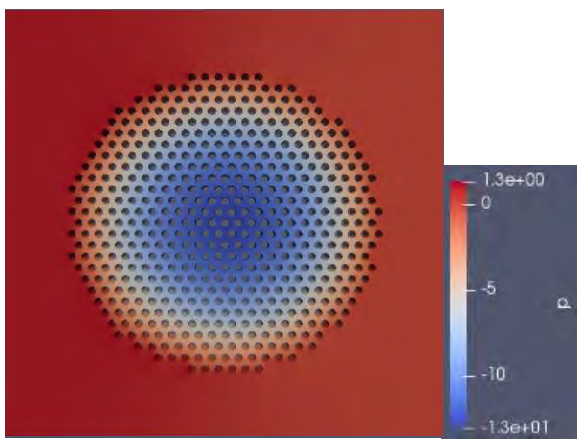


*t=40 s*

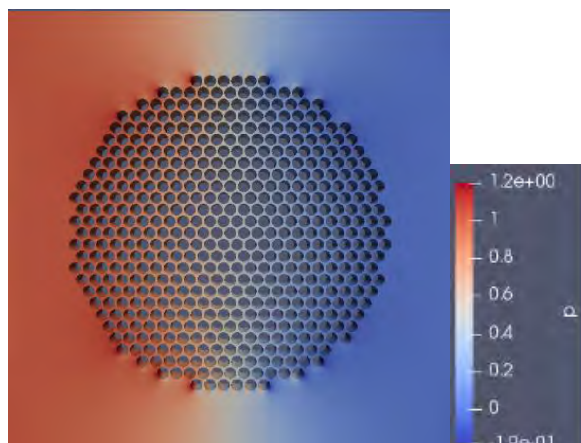
**a = 7%**



*t=0 s*

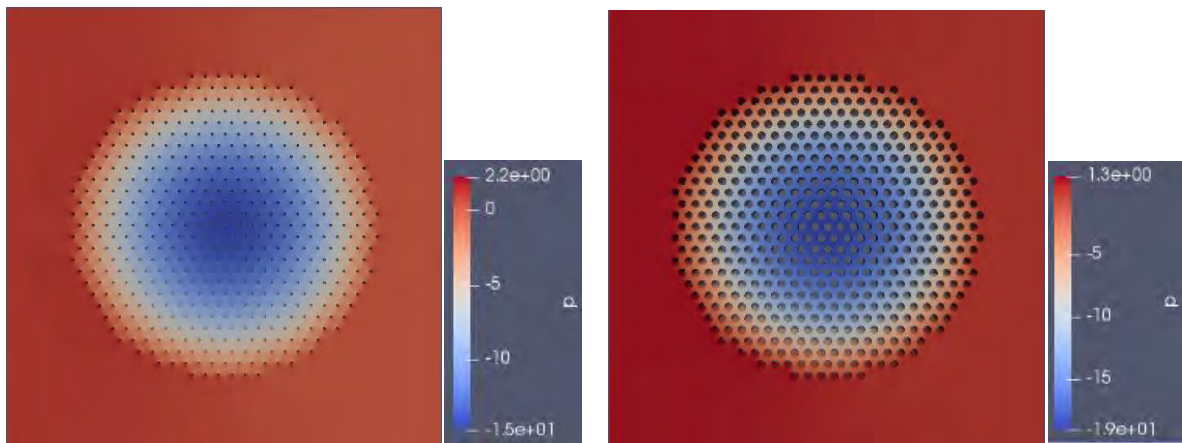


*t=1 s*



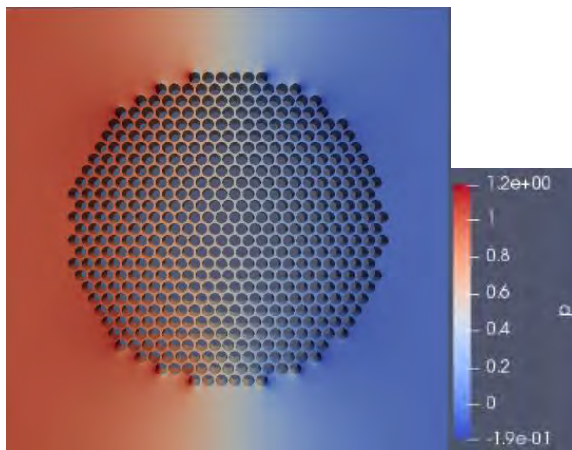
*t=30*

**a= 10%**



$t=0\text{ s}$

$t=0.8\text{ s}$



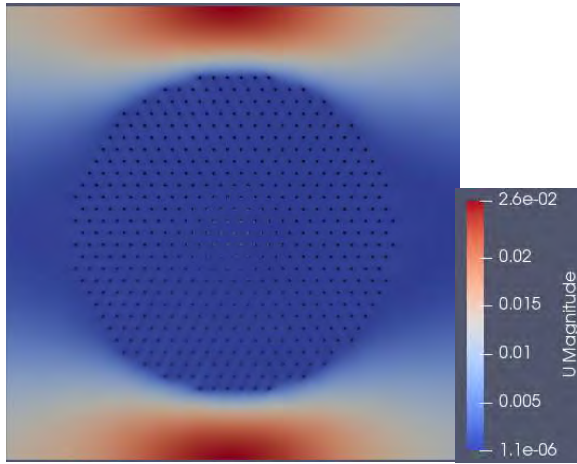
$t=25\text{ s}$

Figure 27: Contour pressure maps through time for all the five values of the absorption coefficient ( $a$ )

Comparing the pressure distributions at various times, it is obvious that for all the different values of the absorption coefficient ( $a$ ), at the final time of the process, the pressure profiles are the same, as at this stage the bundle behaves as an impermeable entity so the difference in pressure is only due to the increased radius of the filaments, since the process of absorption has ended. Furthermore, we can observe that for case of  $a=0.01$  the differences of the pressure at the early stages of the process are not so harsh. On the other hand, for higher values of  $a$ , at the same stage of the process, the values on the internal of the geometry get so low that we cannot distinguish the difference of pressure that we have set on the boundaries.

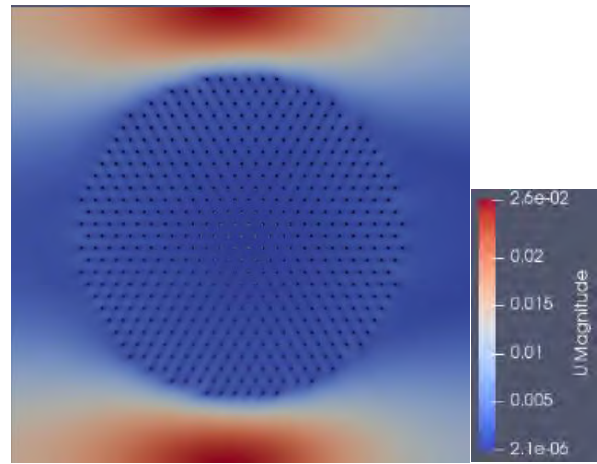
## Velocity

**a= 1%**

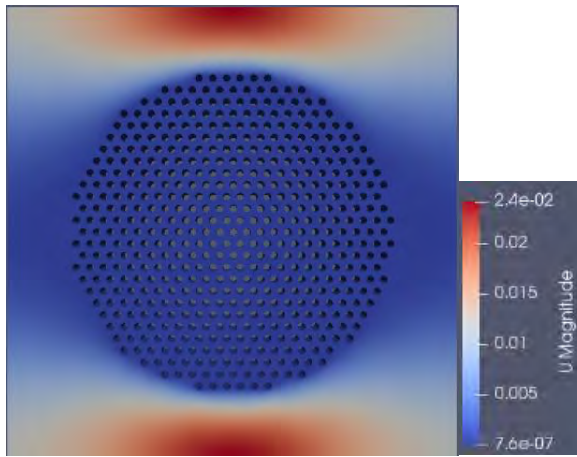


*t=0 s*

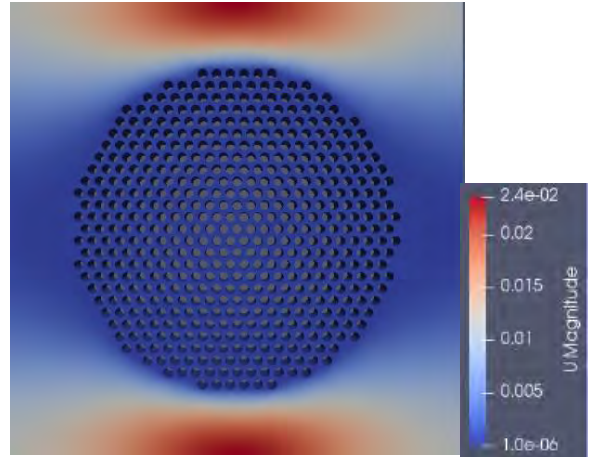
**a= 3%**



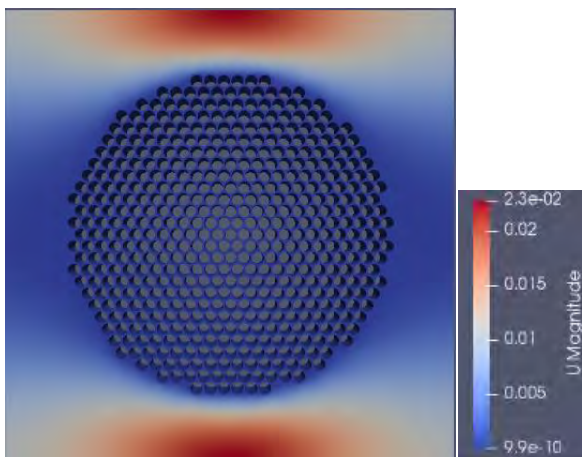
*t=0 s*



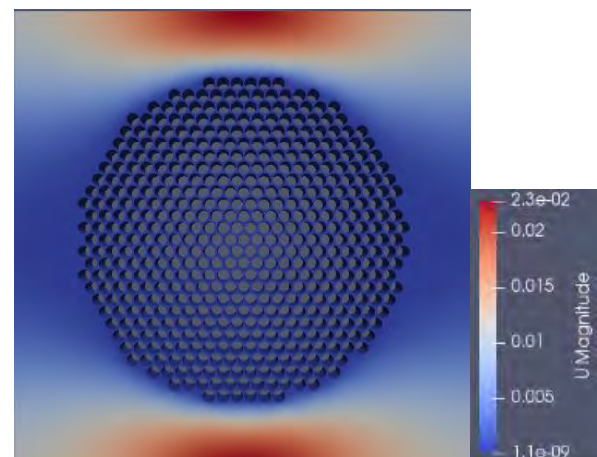
*t=4 s*



*t=4 s*

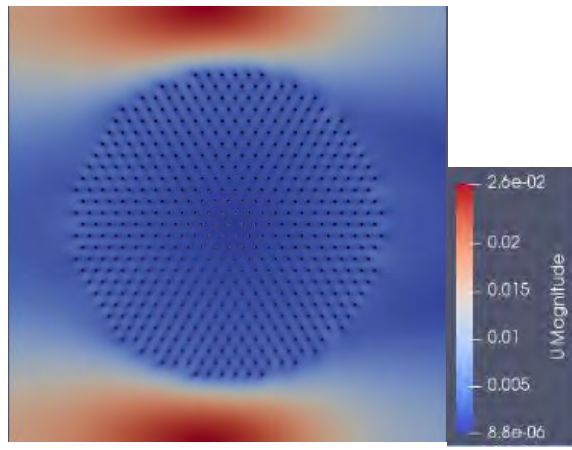


*t=200 s*

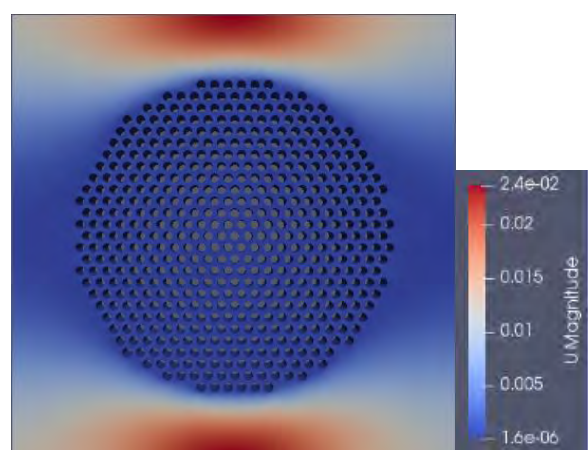


*t=75 s*

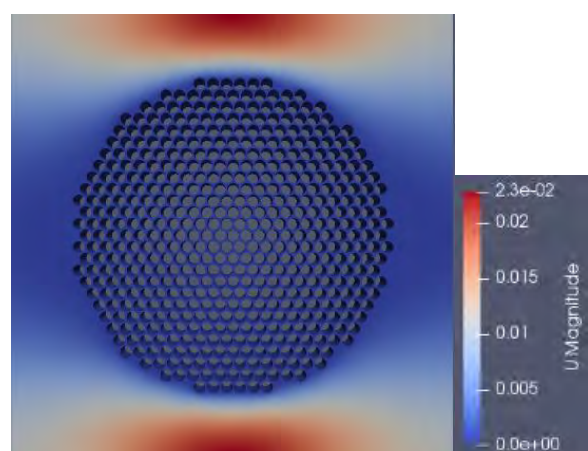
**a = 5%**



t=0 s

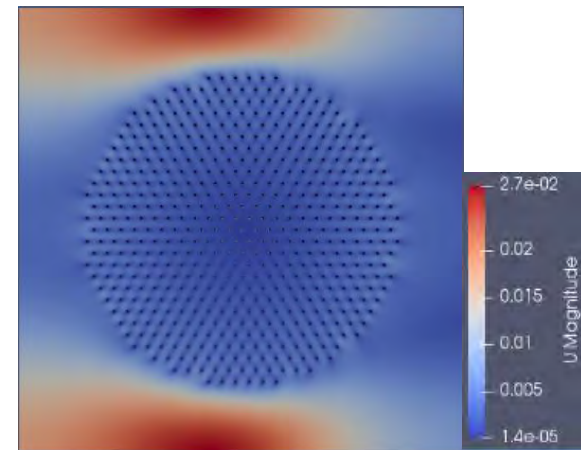


t=2 s

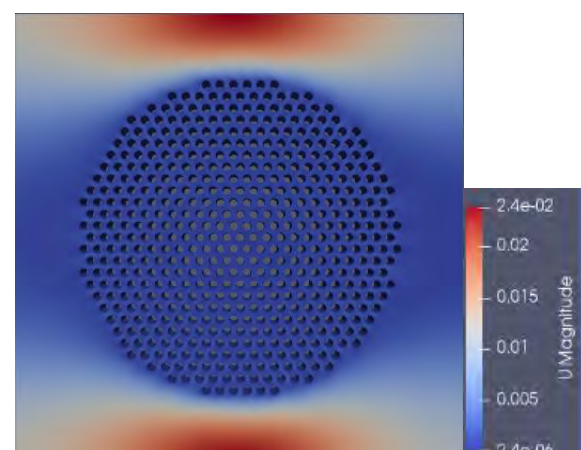


t=40 s

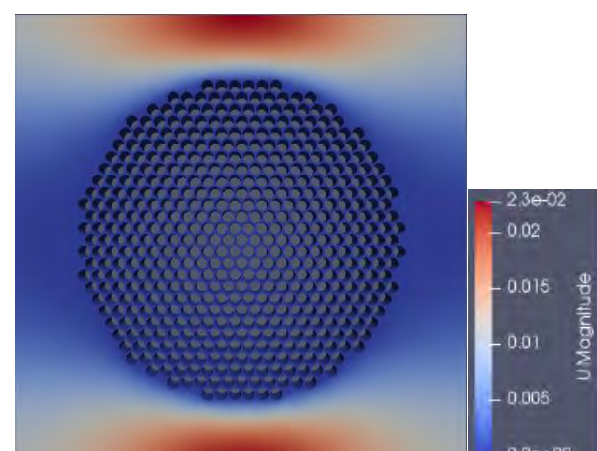
**a = 7%**



t=0 s

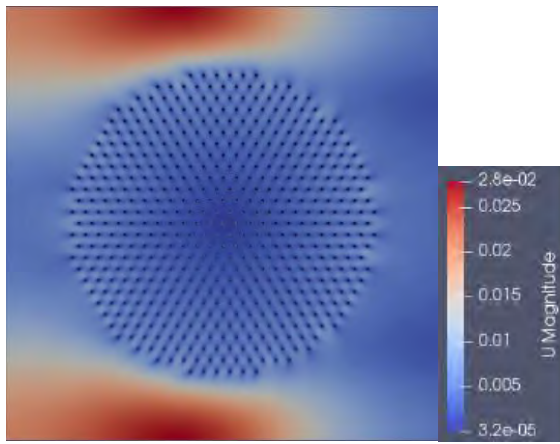


t=1 s

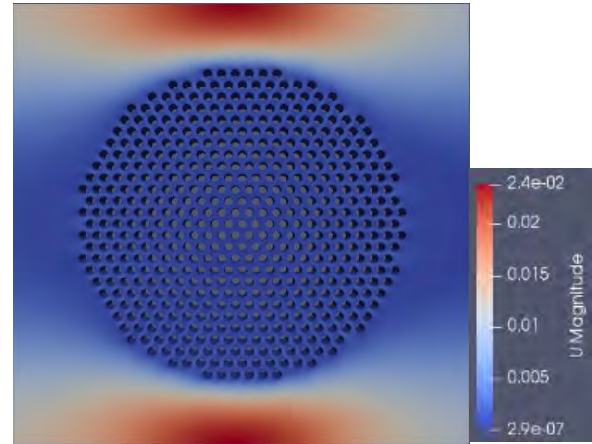


t=30 s

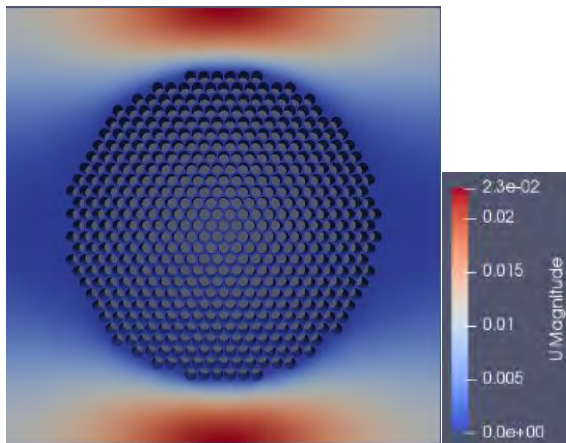
**a= 10%**



$t=0$  s



$t=0.8$  s



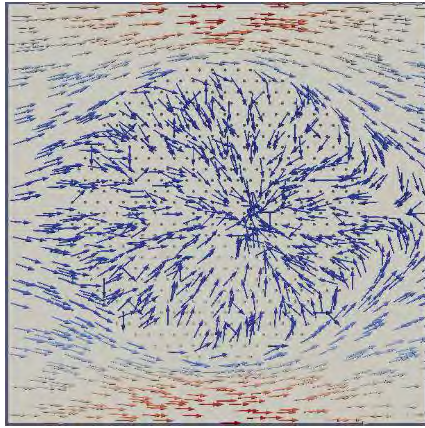
$t=25$

Figure 28: Contour velocity maps through time for all the five values of the absorption coefficient ( $a$ )

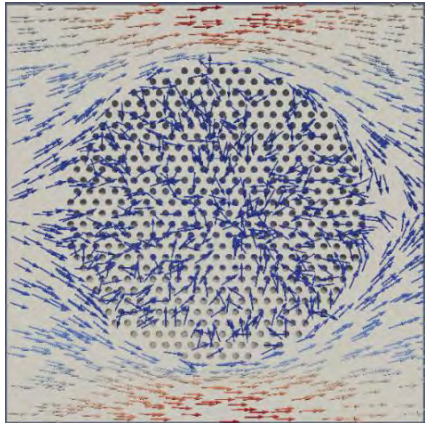
It is noted that the velocity profile remains virtually unchanged, at the right boundary. The major differences on the velocity profile occur for  $t=0$  s for each different rate of absorption, where the inflow absorbed by the filaments gets its maximum value. Generally, the factor that determines the velocity, primarily, is the percentage occupied by the bundle within the unit cell ( $\Phi_i$ ), which remains stable during the course of the study.

## Velocity vectors

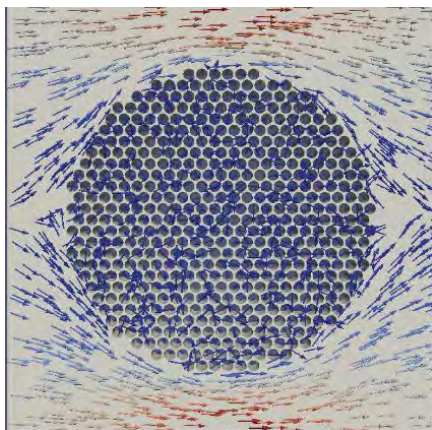
a=1%



t=0 s

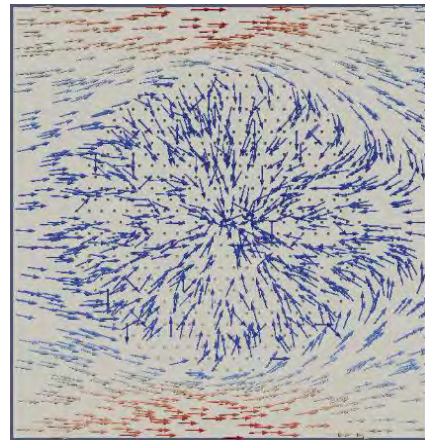


t=4 s

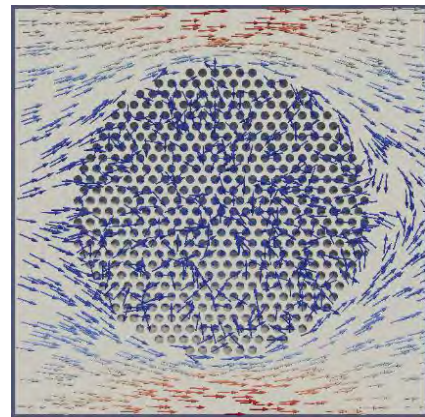


t=200 s

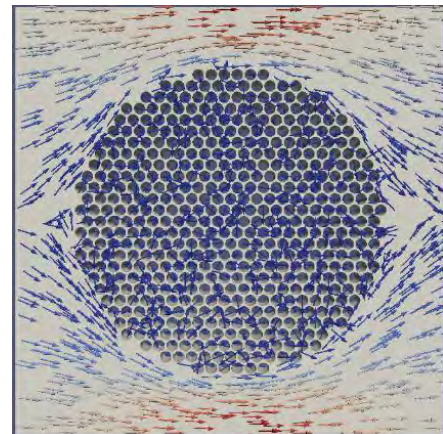
a=3%



t=0 s



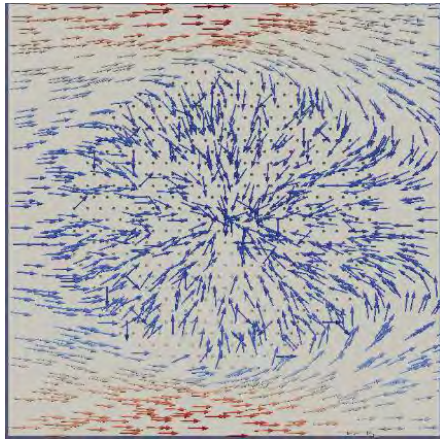
t=4 s



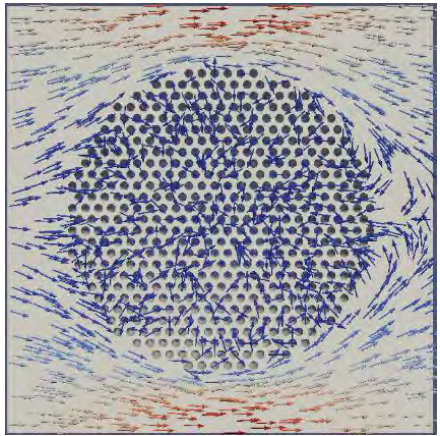
t=75 s



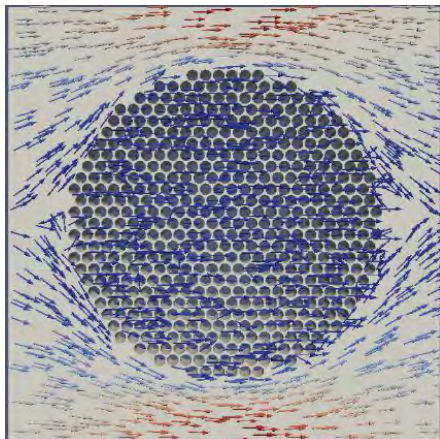
a=5%



t=0 s

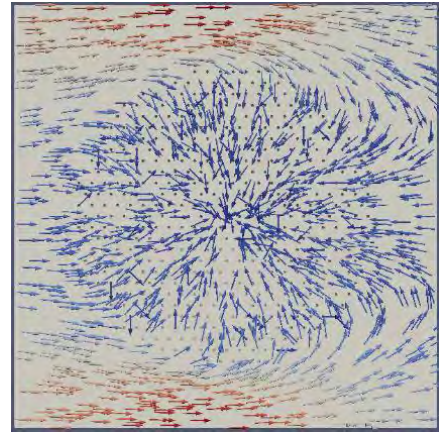


t=2 s

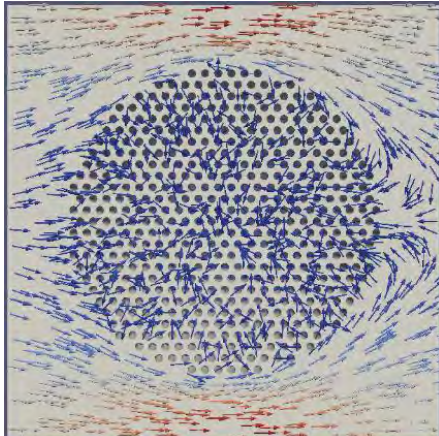


t=40 s

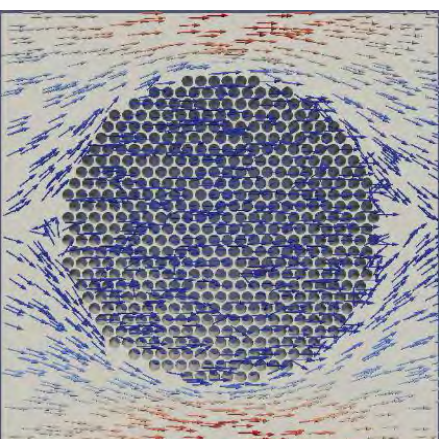
a=7%



t=0 s

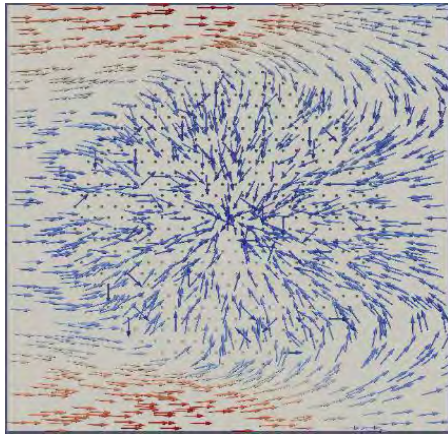


t=1 s

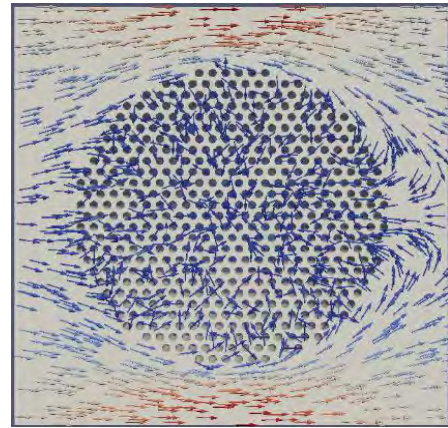


t=30 s

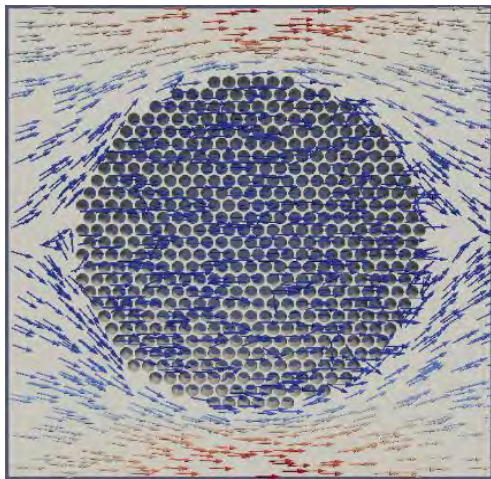
**a=10%**



t=0 s



t=0.8 s



t=25 s

*Figure 29: Velocity vectors of the swelling porous media through time for all the five values of the absorption coefficient ( $a$ )*

## Chapter 4 Linear behavior of absorption rate

### 4.1 Absorption at a constantly decreasing flow rate

In this chapter, as in the previous, we also investigate the flow of a Newtonian fluid through a unit cell where a part of it is absorbed by the filaments. The difference is that at this case the quantity of fluid absorbed decreases at a constant rate through time ( $dQ_{ab}/dt=\text{constant}$ ). So the goal of this chapter is to compare the results of the computational analysis of the previous chapter with the ones of this chapter. The main parameters remain the same, so that the two cases can be compared, which means that,  $N_f=500$ , the volume fraction of the bundle  $\Phi_i = 40\%$ , which means that the  $Q_{base}$  calculated previously (3.4) is the same and the initial and final values of volume fraction within the bundle are  $\Phi_t=5\%$  and  $\Phi_t=69.44\%$ . They are also studied the same values of the absorption coefficient ( $a=0.01-0.03-0.05-0.07-0.1$ ) and the amount of fluid absorbed is calculated as previously, so the initial values of  $Q_{ab}$  are these shown on Table [3.1] for each coefficient respectively.

We must mention that the flow at the input varies through time until the process of absorption is complete. As a consequence there is a limitation on the generalization of the results. To make it more conspicuous, the fluid supply at the inlet for a stack of staggered dimensions is not stable, but varies within a small range that changes along with the filament geometry. This is a consequence of the conservation of the mass ( $Q_{in} = Q_{ab} + Q_{out}$ ).

With the assumption that the absorption at each filament decreases through time until complete blockage of the flow path by the expanding filaments occurs, the rate of the increase of the radius of each filament is given by the following equation:

$$\frac{dr}{dt} = \frac{Q_{ab}(t)}{2\pi r N_f} \quad (4.1)$$

Where  $dr/dt$  is the rate of the increase of the radius measured in m/s and  $Q_{ab}$  is a linear function of time (Figure 32). Here it is also assumed that the density of the absorbed fluid is the same as the density of the flowing fluid [9].

At each time step the radius value is defined by:

$$r_t = dt \cdot \Delta r + r_o \quad (4.2)$$

Where

$r_0$  is the initial radius of the filament [m]

$dt$  is the time step [sec]

$r_t$  is the radius of the filament after  $dt$  time steps

The time needed to reach  $r_{\max}$  can be found by eq. 4.2 and  $r_{\max}$  is acquired by eq. (3.2) for  $\Phi_{\max}=0.6944$ . So we can calculate  $r_t$  for each time step, which is succeeded with this simple code of Mathematica.

```
c = (0.01332 - 0.00362) * n * 500
0.257501

qb = qab * 10
0.00043

tmax =  $\frac{2 * c}{qb}$ 
1197.68

dq = -  $\frac{qb}{tmax}$ 
-3.59028 * 10-7

r0 = 0.0036
0.0036

qab = 0.000043
0.000043

nf = 500
500

For [t = 0; r = 0, t < 1199, t = t + 9, r =  $\sqrt{r0^2 + \frac{dq * \frac{t^2}{2} + qb * t}{n * nf}}$ ; Print[r]]
0.0036
0.00392613
0.00422497
0.00450198
0.00476096
0.00500471
0.00523537
0.00545458
0.00566368
0.00586376
0.0060557
```

Figure 30: Mathematica code for calculating the values of the radius of the filaments at each time step, for  $Q_{ab}$  that decreases at a constant rate

We can get a taste of how radius grows through time, with  $Q_{ab}$  decreasing on a constant rate, by observing the following graph:

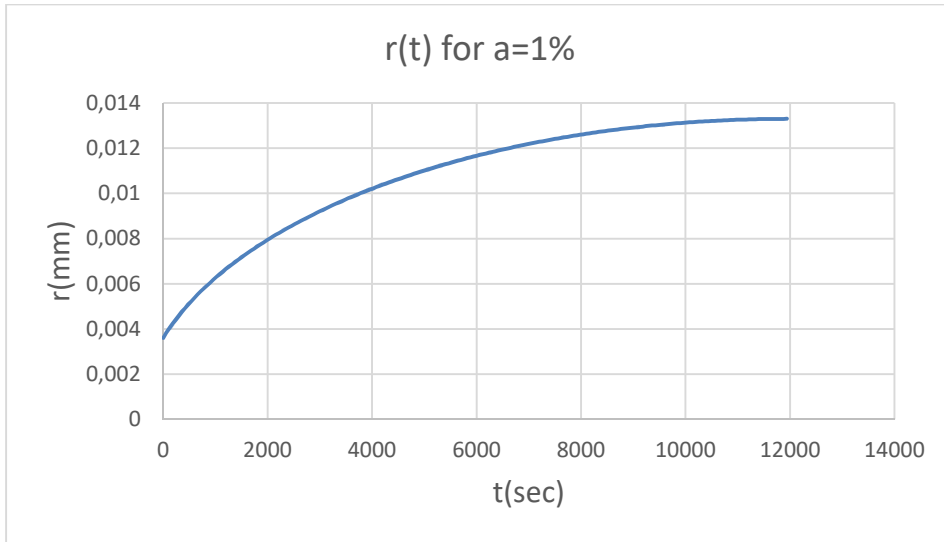


Figure 31: Graph of the radius of the filaments versus time for  $Q_{ab}$  that decreases at a constant rate

At this case, it is obvious that the function of  $r(t)$  has a different behavior, in contrast to the graphs of Figure 22 where the  $Q_{ab}$  varies significantly through time.

The values of  $Q_{ab}$  start from the initial value of  $Q_{ab}$  for each different value of absorption coefficient and all settle at the value of zero obviously at a different time. The following graph shows the behavior of  $Q_{ab}$  for  $a=1\%$  through time. (The graphs showing  $r(t)$  and  $Q_{ab}(t)$  of the other values of absorption coefficients are placed on Appendix G)

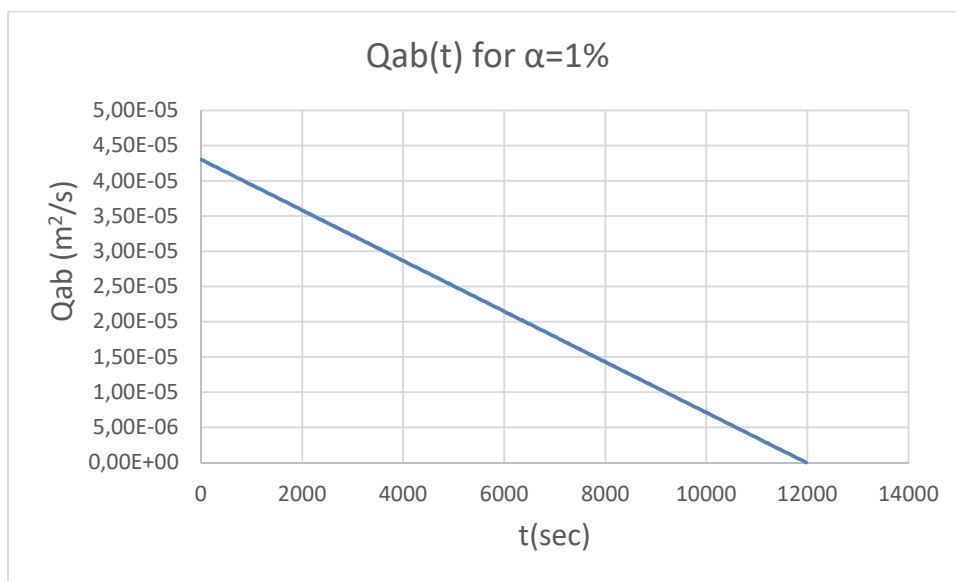


Figure 32: Graph of the fluid absorbed that decreases at a constant rate versus time, for  $a=1\%$

## 4.2 Computational results

After the simulations have been completed for each  $r_t$ , which corresponds to a particular time and geometry that is produced using the visual basic program, through OpenFOAM's process, we get the computational results which can be plotted versus time.

The results of the permeability are placed on Appendix E and the resulting graph is the following:

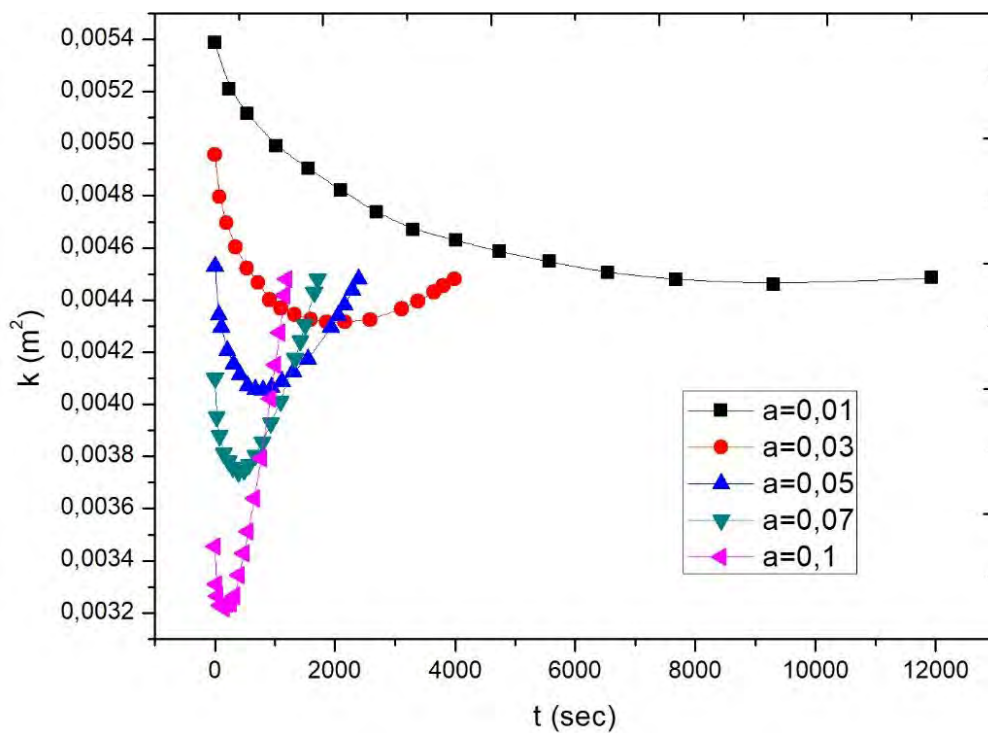


Figure 33: Graph of the permeability versus time for various values of absorption coefficient ( $a$ ), at a constantly decreasing amount of fluid absorbed

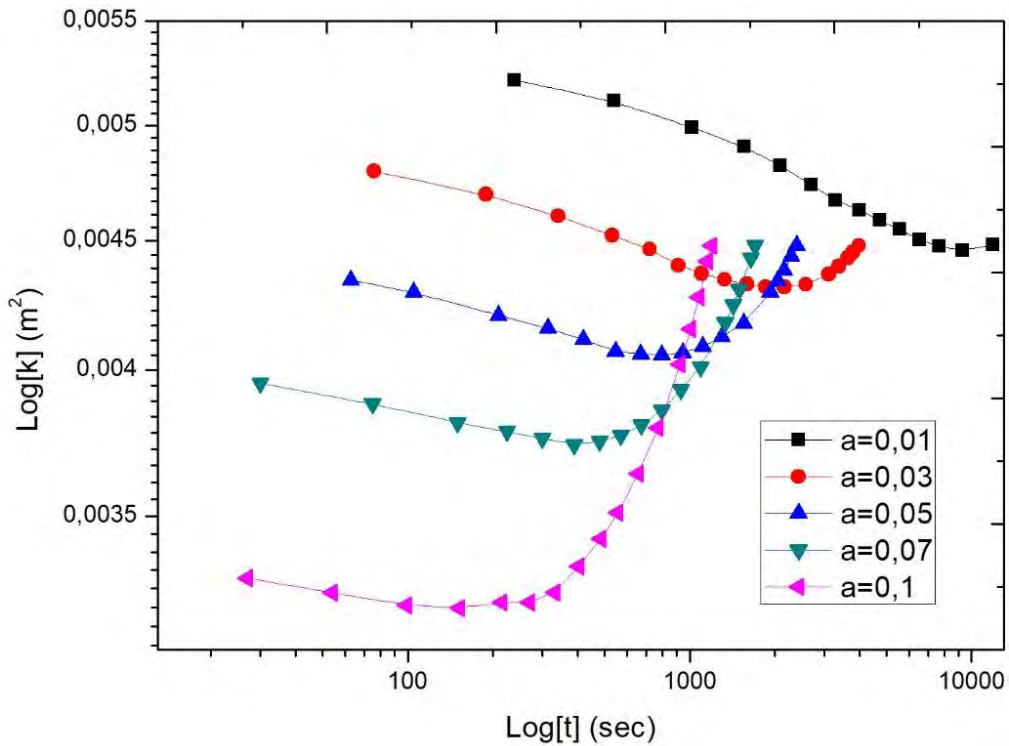


Figure 34: A log-log graph of the permeability versus time for various values of absorption coefficient ( $a$ ), at a constantly decreasing amount of fluid absorbed

It is obvious on the above figures, that as the value of coefficient ( $a$ ) increases the initial value of permeability (for  $t=0$  (sec)) is getting lower as the amounts of liquid absorbed get bigger and of course the state of maximum volume fraction, where the filaments of our bundle start to touch each other, is reached at shorter spaces of time. Permeability reduces constantly through time only for the value of  $a=1\%$ . For the other values of coefficient ( $a$ ) this is observed for a large part of the process of absorption and at the end they reach the same value of permeability. The difference is that by increasing the value of ( $a$ ), the the way this value is approached is getting steeper.

Results of the minimum pressure are also placed on Appendix E, and a taste of how the minimum pressure advances through time is given on the following graphs:

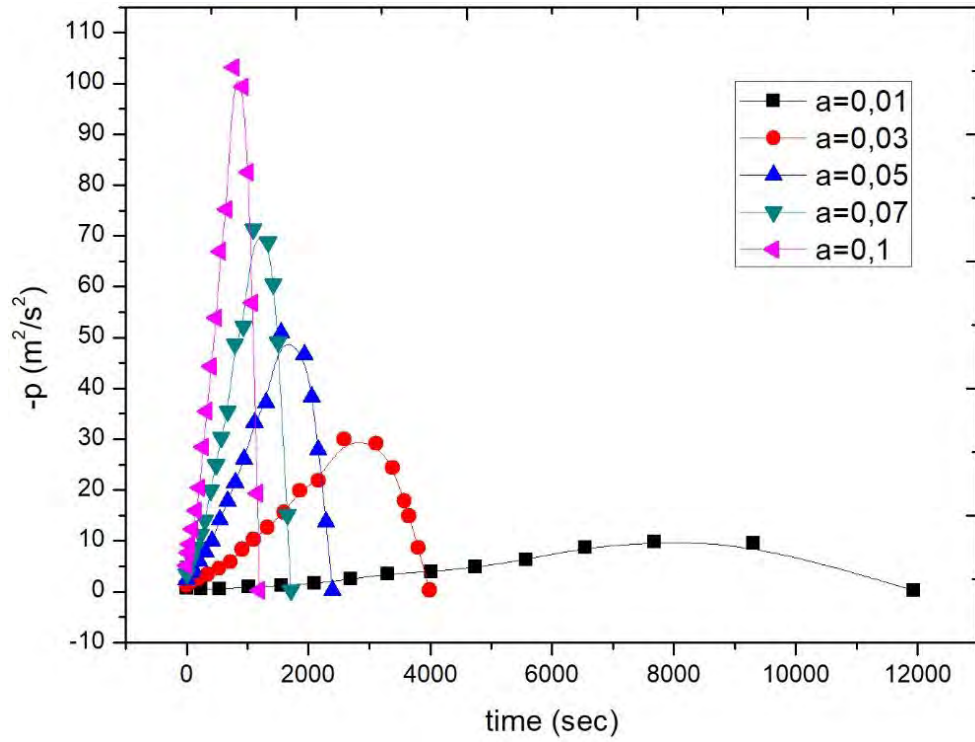


Figure 35: Graph of the minimum pressure versus time for various values of absorption coefficient ( $a$ ), at a constantly decreasing amount of fluid absorbed

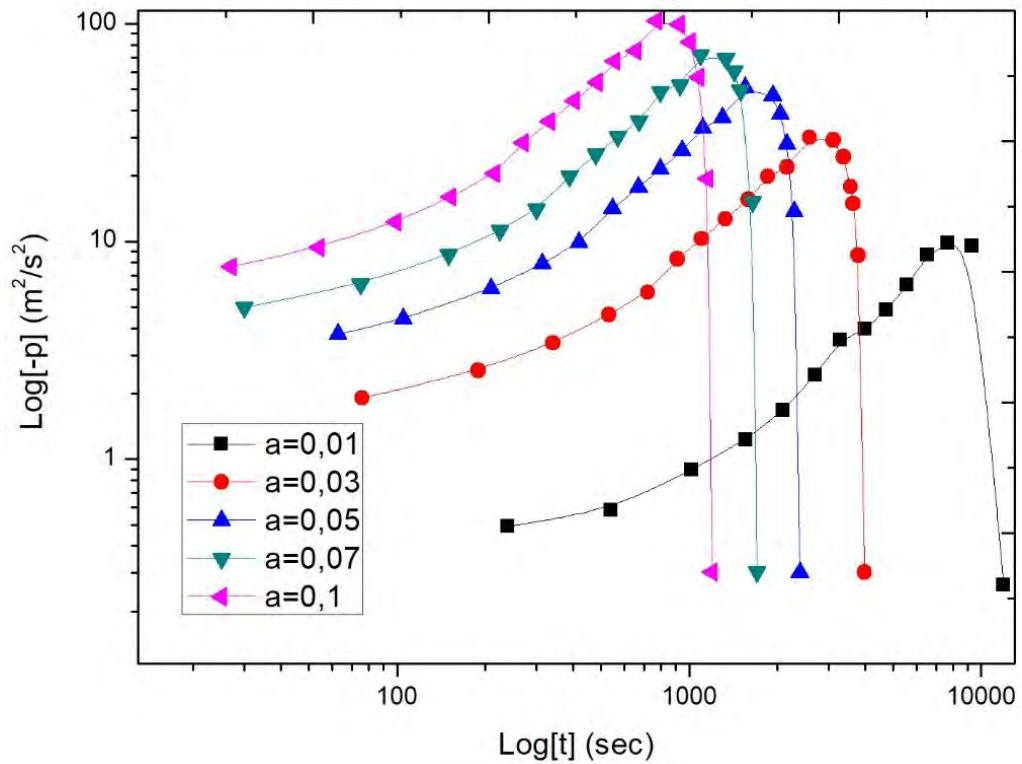


Figure 36: A log-log graph of the minimum pressure versus time for various values of absorption coefficient ( $a$ ), at a constantly decreasing amount of fluid absorbed



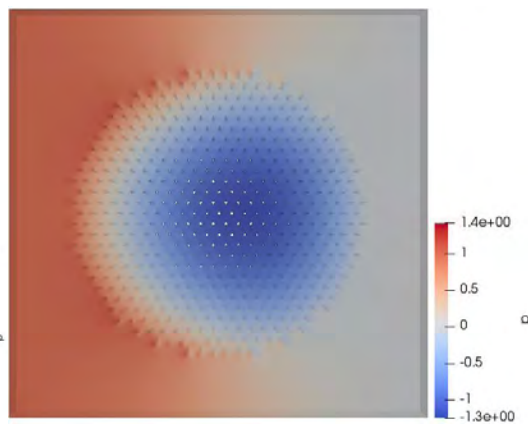
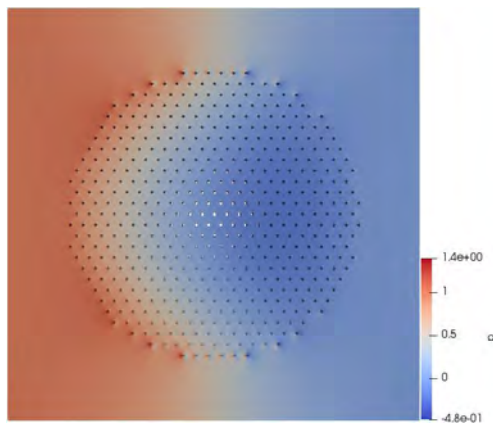
By observing the above graph of minimum pressure we can see that for all the different values of absorption coefficient ( $\alpha$ ) it increases through time until a maximum value is reached and then drops. This is reasonable, as by increasing the radius of the fibers, it is more difficult for the fluid to flow between them. For this reason, the minimum pressure that is met inside the bundle of fibers grows as the fiber radius increases. However, the amount to be absorbed decreases through time and at the latest time of the process of absorption is equal to zero. This is the reason of this reduction at the end of the process. At the latest time the minimum pressure depends only on the intra-tow volume fraction, which is 40%, and that's why the last value is the same for all the values of coefficient ( $\alpha$ ).

After the simulations have been completed, variations in the pressure distribution due to the absorption over time are observed. Below we cite the contour maps for pressure, at four particular time steps, for all the values of coefficient ( $\alpha$ ). Similar behavior of pressure distribution is observed and at Figure 27.

**Pressure**

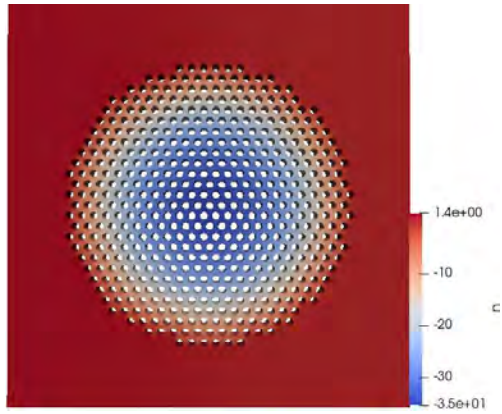
**$\alpha=1\%$**

**$\alpha=3\%$**

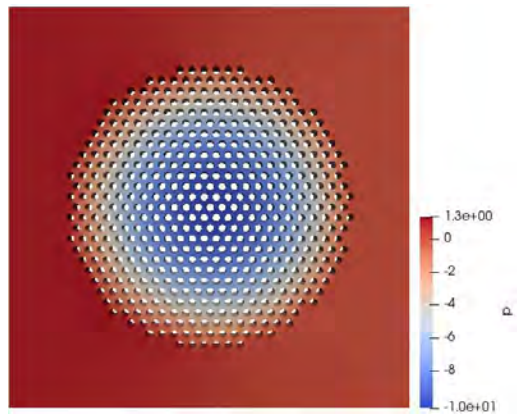


$t=0\text{ s}$

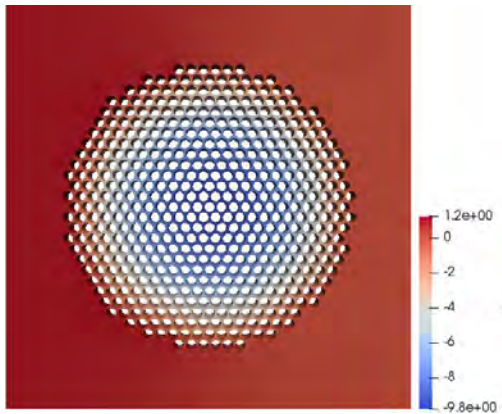
$t=0\text{ s}$



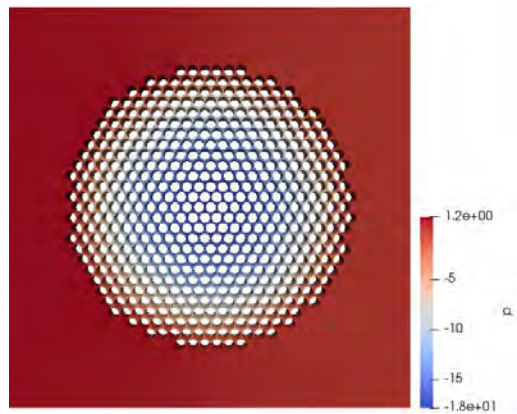
$t=3300\text{ s}$



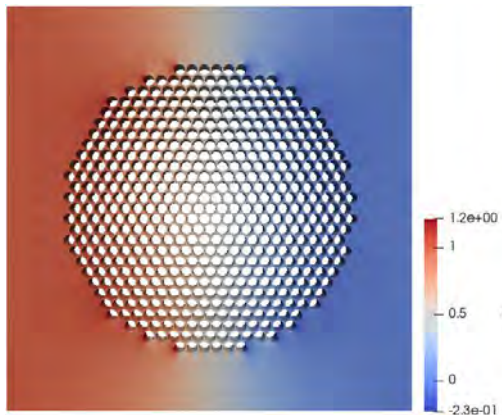
$t=1102\text{ s}$



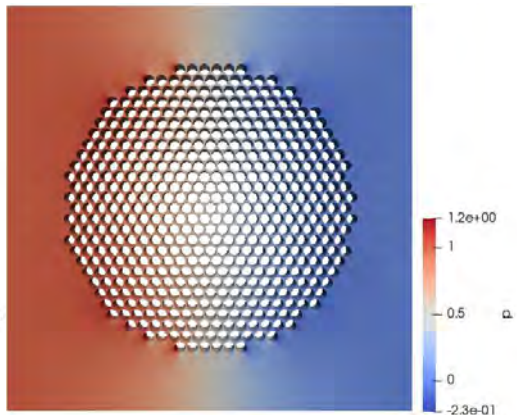
$t=7680\text{ s}$



$t=3572\text{ s}$



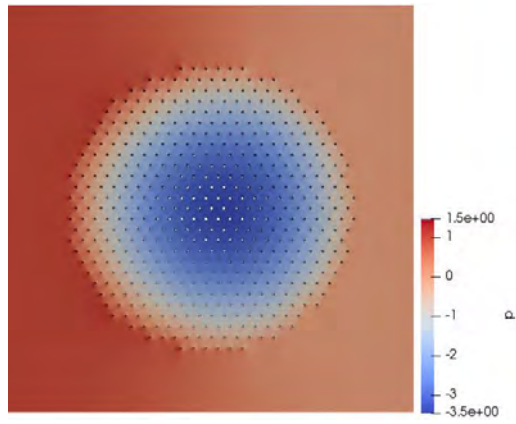
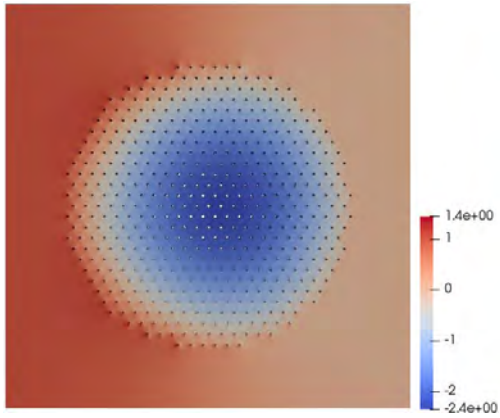
$t=11940\text{ s}$



$t=3990\text{ s}$

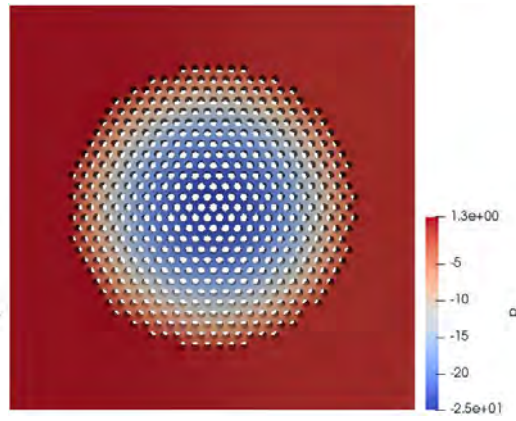
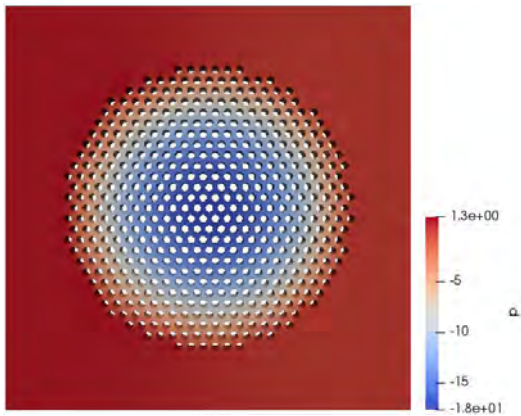
**a=5%**

**a=7%**



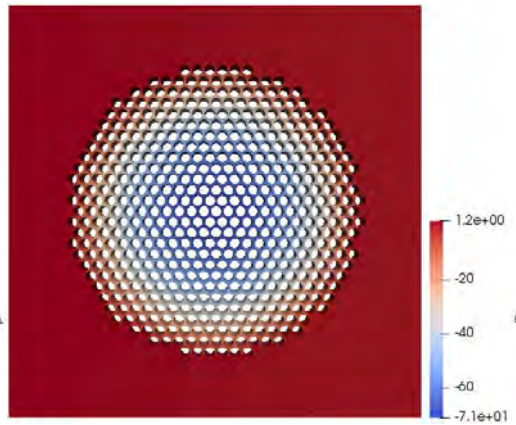
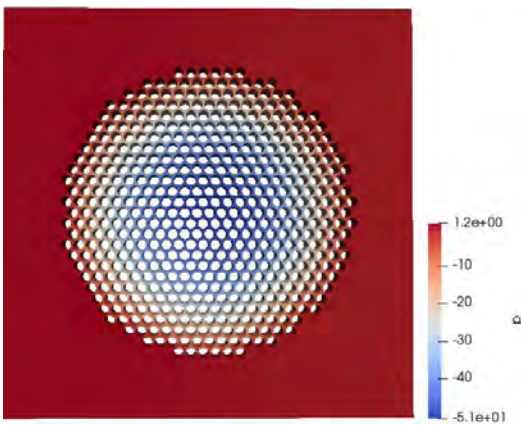
*t=0 s*

*t=0 s*



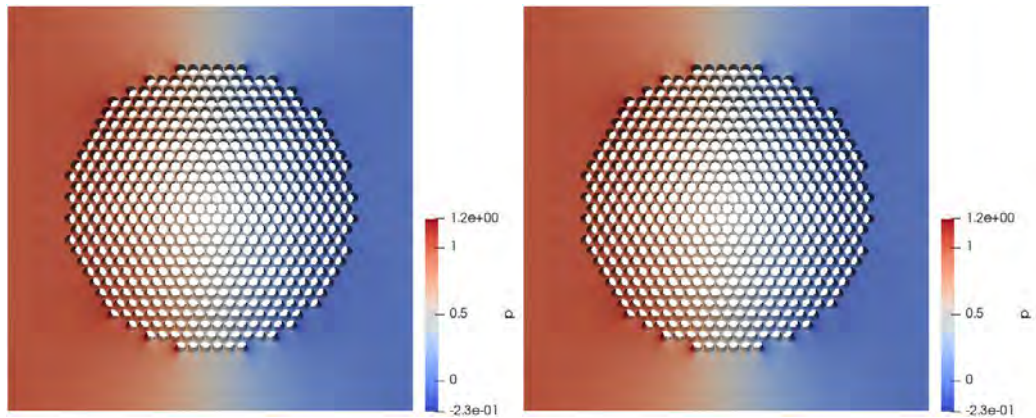
*t=672 s*

*t=480 s*



*t=1554 s*

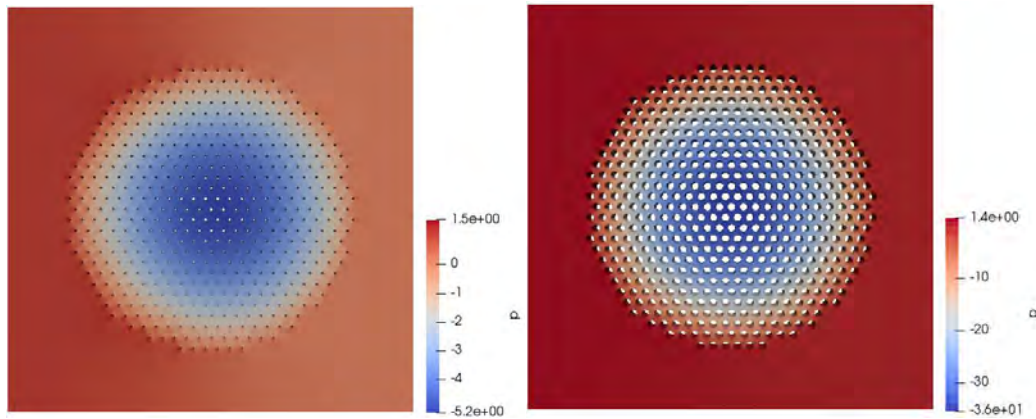
*t=1095 s*



$t=2394s$

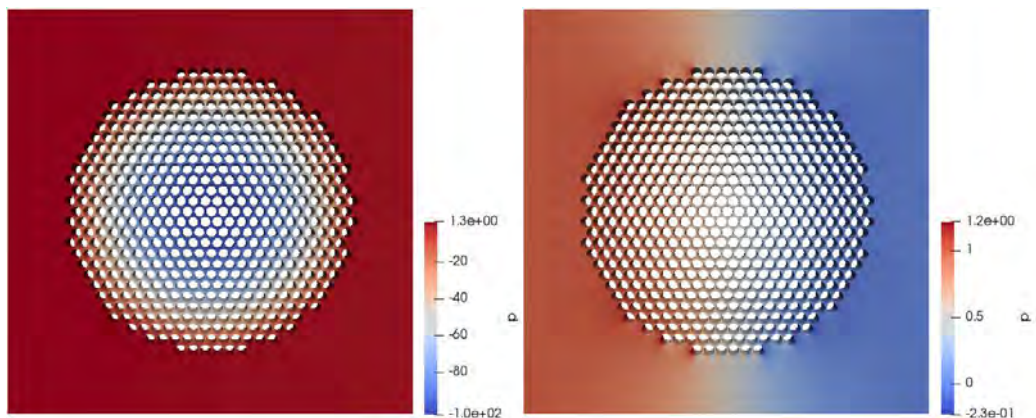
$t=1710s$

**a=10%**



$t=0s$

$t=333s$



$t=774s$

$t=1197s$

Figure 37: Contour pressure maps through time for all the five values of the absorption coefficient ( $a$ ) for  $Q_{ab}$  that decreases at a constant rate

### 4.3 Comparison and conclusions

The reason of this chapter is to compare the two different cases that we examined so that conclusions can be made.

A main difference is at the rate of growth of the fibers inside the bundle as the value of  $\Phi_{\max}$  is reached faster in the case of absorption of Chapter 3, where the amount of liquid absorbed decreases through time and at the end converges to the value of zero.

Moreover, as we can see, the graphs that result from our numerical data for these two different types of continuous absorption (shown on chapters 3.5 and 4.2), differ qualitatively, as far as permeability is concerned (as shown on Figure 38).

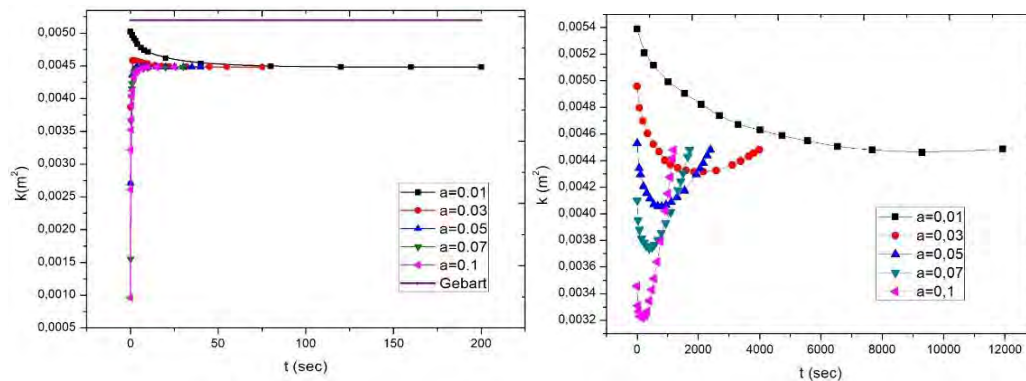


Figure 38: Comparison between Figures 23 and 33

It is a fact, that at both cases the permeability reaches the same final value for all the different values of absorption coefficient ( $a$ ) which is  $K=0.00448$  ( $m^2$ ). This happens because, as we said, all resistance to flow is due to the gap outside the bundle and therefore the permeability corresponding to all cases, irrespective of  $a$ , is the same. The difference is detected on the behavior of these curves and at the way this final value is approached. At the first case the curves converge to this value asymptotically, while at the second case we observe a steep approach. Also the initial values of permeability on the first case for values of the absorption coefficient ( $a$ ) greater than 1% are significantly lower compared to these of the case of the constant reduction of  $Q_{ab}$ .

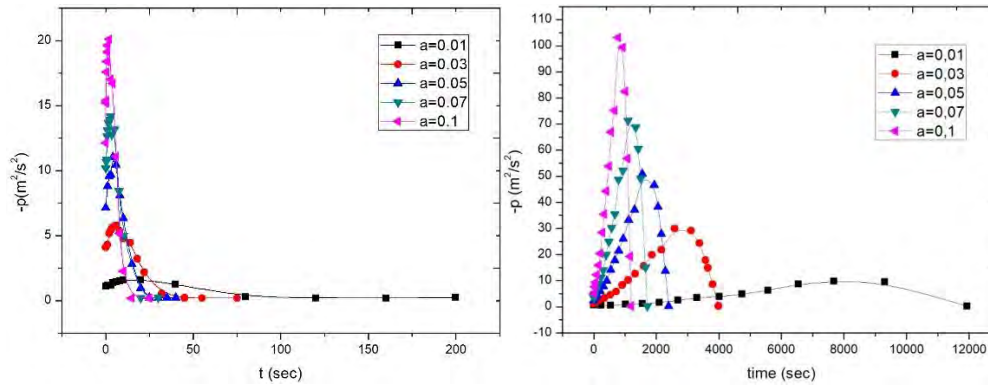


Figure 39: Comparison between Figures 25 and 35

From the above Figure (39), where the graphs of minimum pressure are compared, we can see that at both cases for every value of the absorption coefficient ( $a$ ), maximum value is reached and then drops at the same value, which corresponds to the stage of the complete blockage of the flow through the bundle of filaments, as they have almost touched each other. The differences that are observed is that at the case at which the amount absorbed decreases at a constant rate, higher values of minimum pressure are reached and again as at the case of permeability are observed the same differences in the way this final value is approached through time. Also another difference observed is that the initial values of minimum pressure, for the case discussed on Chapter 3.5, are higher. This is due to the fact that  $Q_{ab}$  gets higher values for  $t=0$  (sec) at this case.

In conclusion, we can tell for both cases that low values of coefficient ( $a$ ) correspond to reality. On the other hand, this cannot be claimed for the higher values (5%,7% ,10%) of coefficient ( $a$ ), which is proved by the figures of velocity vectors (Figure 29), where in order to be satisfied the amount of liquid absorbed, the solver provides fluid from the right border of our unit cell.

#### 4.4 Proposals for further study

For further study, we could recommend that should be investigated the case where the density of the liquid that has already been absorbed by the fibers is different to the density of the liquid that flows between the gaps.

Another issue for discussion is the random distribution of filaments in the unit cell. This will radically affect the flow of fluid as well as the permeability and the drop in pressure. Also in this scenario, the number of fibers will be different as they will be randomly inserted into the bundle and the fibers between them will not follow any specific arrays. By this way is succeeded that the geometry will be closer to the real structure of a material.

# Appendix

## Appendix A

Part of the Visual Basic program that results in the geometry of the cell. (The part that fills the bundle)

```
Private Sub Fill_Spheres(ByVal write As Boolean, ByVal nm As String)
    Dim i As Integer, j As Integer
    Dim x As Single, y As Single
    Dim pen As New Pen(Color.Blue, 1)
    Dim e As Graphics
    Dim vol As Single = H.Text() * H.Text()
    Dim Rc As Single, Veff As Single, Rc2 As Single
    Dim Ac As Single
    Dim Lh As Single, Hh As Single
    Dim iRf As Integer
    Dim check As Single
    Dim cList As New List(Of PointF)
    Dim r_x1 As Single, r_x2 As Single, r_y1 As Single, r_y2 As Single
    Dim r_step As Single, caount As Single
    Dim cp As PointF, cp2 As PointF
    Dim k As Integer

    vol = Math.PI * R1.Text() * R1.Text()
    Veff = vol * F2.Text()
    Ac = Veff / CSng(N.Text())

    Rc2 = Math.Sqrt(Ac / Math.PI)

    Veff = vol
    Ac = Veff / N.Text()
    Rc = Math.Sqrt(Ac / Math.PI)

    check = 500 * Math.PI * Rc2 * Rc2
    If Rc2 = 0 Then Exit Sub

    safe_r.Text() = (100 * (Rc - Rc2) / Rc2).ToString("0.000")
    safe_r.BackColor = safe_r.BackColor
    safe_r.ForeColor = Color.Black
    If CSng(safe_r.Text()) < CSng(safe_limit.Text()) Then
safe_r.ForeColor = Color.Red

    e = pb.CreateGraphics
    i = 1
    iRf = 0

    If align_hex.Checked() = True Then
        r_x1 = -(0.5 / Rc) : r_x2 = -r_x1
        r_y1 = -(0.7 / Rc) : r_y2 = -r_y1
        r_step = 0.5

    If strict.Checked() = False Then
        r_x1 = 0 : r_x2 = 1 / Rc
        r_y1 = 0 : r_y2 = 1.4 / Rc
        r_step = 1.5
    End If

    Lh = 0
    Hh = 0
    cp.Y = 0.5
    cp.X = 0.5
```



```

caount = 0
For i = r_y1 To r_y2

    cp.Y = cp.Y + Hh
    cp.X = -0.5 + (Lh / 2) * caount
    For j = r_x1 To r_x2

        If Rot_check.Checked() = True Then
            cp = RotatePoint(cp)
        End If

        If Math.Sqrt((cp.X - 0.5) ^ 2 + (cp.Y - 0.5) ^ 2) <
(CSng(R1.Text())) Then
            iRf += 1
            If Math.Sqrt((cp.X - 0.5) ^ 2 + (cp.Y - 0.5) ^ 2) <
(CSng(R1.Text() + 0.1)) Then
                e.DrawEllipse(pen, 500 * (cp.X - Rc2) + 1, 500 *
(cp.Y - Rc2) + 1, Rc2 * 1000, Rc2 * 1000)
            End If
            For k = 0 To Repeat.Text() - 1
                cp2 = cp
                cp2.X += k
                cList.Add(cp2)
            Next

        End If
        Lh = Math.Sqrt((2 * Math.PI * (Rc2 ^ 2)) / (F2.Text() *
Math.Sqrt(3)))
        cp.X = cp.X + Lh
    Next
    caount = caount - 1
    Hh = (Lh * Math.Sqrt(3)) / 2
Next
Lh = Math.Sqrt((2 * Math.PI * (Rc2 ^ 2)) / (F2.Text() *
Math.Sqrt(3)))
Hh = (Lh * Math.Sqrt(3)) / 2
cp.Y = 0.5
cp.X = -0.5
caount = -1
For i = r_y1 To r_y2

    cp.Y = cp.Y - Hh
    cp.X = -0.5 + (Lh / 2) * caount
    For j = r_x1 To r_x2

        If Rot_check.Checked() = True Then
            cp = RotatePoint(cp)
        End If

        If Math.Sqrt((cp.X - 0.5) ^ 2 + (cp.Y - 0.5) ^ 2) <
(CSng(R1.Text())) Then
            iRf += 1
            If Math.Sqrt((cp.X - 0.5) ^ 2 + (cp.Y - 0.5) ^ 2) <
(CSng(R1.Text() + 0.1)) Then
                e.DrawEllipse(pen, 500 * (cp.X - Rc2) + 1, 500 *
(cp.Y - Rc2) + 1, Rc2 * 1000, Rc2 * 1000)
            End If
            For k = 0 To Repeat.Text() - 1
                cp2 = cp
                cp2.X += k
                cList.Add(cp2)
            Next

        End If
    End If
End If

```

```

        Lh = Math.Sqrt((2 * Math.PI * (Rc2 ^ 2)) / (F2.Text() *
Math.Sqrt(3)))
        cp.X = cp.X + Lh
    Next
    caount = caount - 1
    Hh = (Lh * Math.Sqrt(3)) / 2
Next
End If

If align_square.Checked() = True Then
    r_x1 = -(0.5 / Rc) : r_x2 = -r_x1
    r_y1 = -(0.7 / Rc) : r_y2 = -r_y1
    r_step = 0.5

    If strict.Checked() = False Then
        r_x1 = 0 : r_x2 = 1 / Rc
        r_y1 = 0 : r_y2 = 1.4 / Rc
        r_step = 1.5
    End If

    For i = r_x1 To r_x2

        For j = r_y1 To r_y2

            cp.X = r_step - Rc * (2 * i)
            cp.Y = r_step - Rc * (2 * j)
            If Rot_check.Checked() = True Then
                cp = RotatePoint(cp)
            End If

            If Math.Sqrt((cp.X - 0.5) ^ 2 + (cp.Y - 0.5) ^ 2) <
(CSng(R1.Text())) Then
                iRf += 1
                If Math.Sqrt((cp.X - 0.5) ^ 2 + (cp.Y - 0.5) ^ 2) <
(CSng(R1.Text() + 0.1)) Then
                    e.DrawEllipse(pen, 500 * (cp.X - Rc2) + 1, 500 *
(cp.Y - Rc2) + 1, Rc2 * 1000, Rc2 * 1000)
                End If
                For k = 0 To Repeat.Text() - 1
                    cp2 = cp
                    cp2.X += k
                    cList.Add(cp2)
                Next
            End If
        Next
    Next
End If

Real_f.Text() = (100 * (iRf * Rc2 * Rc2 * Math.PI) / (H.Text() *
H.Text())).ToString("0.0000")
Real_N.Text() = iRf.ToString()
r.Text() = Rc2.ToString("0.0000")
If write = True Then WriteMesh(cList, Rc2, nm)
End Sub

```

## Appendix B

OpenFoam's boundary condition for pressure and velocity for flow through porous media are listed:

### Velocity:

```
/*----- C++ -----*/
| \ \ \ \ \ \ | Field      | OpenFOAM: The Open Source CFD Toolbox
| \ \ \ \ \ \ | Operation | Version: 4.0
| \ \ \ \ \ \ | And      | Web: www.OpenFOAM.org
| \ \ \ \ \ \ | Manipulation |
|-----|

FoamFile
{
  version      2.0;
  format       ascii;
  class        volVectorField;
  object       U;
}

// ..... //

dimensions    [0 1 -1 0 0 0 0];

internalField uniform (0 0 0);

boundaryField
{
  left
  {
    type      zeroGradient;
  }
  right
  {
    type      zeroGradient;
  }
  top
  {
    type      cyclicAMI;
  }
  bottom
  {
    type      cyclicAMI;
  }
  internal
  {
    type      flowRateInletVelocity;
    volumetricFlowRate -0.000129;
    value     uniform (0 0 0); // placeholder
  }
  front
  {
    type      empty;
  }
  back
  {
    type      empty;
  }
}

// ..... //
```



## Appendix C

Numerical results of permeability and minimum pressure for flow rate absorbed that varies through time.

t	-p(a=0.01)	k(a=0.01)	-p(a=0.03)	k(a=0.03)
sec	m <sup>2</sup> /s <sup>2</sup>	m <sup>2</sup>	m <sup>2</sup> /s <sup>2</sup>	m <sup>2</sup>
0	1,09253	0,0050228	4,10252	0,003864
1	1,13871	0,0049673	4,29651	0,004582
2	1,14123	0,0049173	5,1795	0,004582
3	1,15511	0,0048849	5,43589	0,00458
4	1,36563	0,0048299	5,66114	0,004574
6	1,44008	0,0047766	5,78957	0,004556
8	1,51333	0,0047384	5,35203	0,004541
10	1,55926	0,0047097	4,77176	0,004532
14	--	--	4,46436	0,004508
18	--	--	3,20907	0,004497
20	1,60951	0,0046174	--	--
22	--	--	2,17275	0,004493
32	--	--	0,549634	0,004485
35	--	--	--	--
40	1,27401	0,0045332	--	--
45	--	--	0,202268	0,004485
55	--	--	0,19953	0,004483
75	--	--	0,197601	0,004482
80	0,263785	0,0044932		
120	0,203305	0,0044828		
160	0,201236	0,0044805		
200	0,212023	0,0044806		

t	-p(a=0.05)	k(a=0.05)	-p(a=0.07)	k(a=0.07)	-p(a=0.1)	k(a=0.01)
sec	m <sup>2</sup> /s <sup>2</sup>	m <sup>2</sup>	m <sup>2</sup> /s <sup>2</sup>	m <sup>2</sup>	m <sup>2</sup> /s <sup>2</sup>	m <sup>2</sup>
0	7,12731	0,0027121	10,1833	0,001555	12,1352	9,59E-04
0,1	--	--	--	--	15,2344	0,00261208
0,2	--	--	--	--	15,2513	0,00321669
0,25	--	--	10,677	0,0036608	--	--
0,3	--	--	--	--	15,3979	0,0035234
0,4	--	--	--	--	17,5921	0,00368162
0,5	--	--	10,84	0,0040306	--	--
0,6	--	--	--	--	18,3928	0,00389791
0,75	--	--	12,6437	0,0041495	--	--
0,8	--	--	--	--	19,1137	0,00403089
1	8,78505	0,0043594	13,0892	0,0042326	19,6219	0,00411846
1,5	--	--	13,6072	0,0043257	--	--
2	9,56179	0,0044472	--	--	20,0957	0,00432274
2,25	--	--	13,9139	0,0043916	--	--
2,75	--	--	14,1887	0,0044171	--	--
3	9,65965	0,0044708	--	--	17,0117	0,00439842
3,5	--	--	12,7578	0,0044421	--	--
4	11,0459	0,0044769	--	--	16,7068	0,00442626
5	--	--	13,1865	0,0044533	--	--
6	10,4452	0,0044828	--	--	11,0853	0,00445481
7,5	--	--	8,41681	0,0044698	--	--
8	8,08154	0,0044855	--	--	5,17195	0,004473
10	6,3034	0,004485	4,97382	0,0044759	2,26503	0,00447826
14	--	--	--	--		
15	2,81585	0,0044845	--	--	0,188039	0,00448198
18	--	--	--	--	--	--
20	0,943994	0,0044833	0,200171	0,0044811	--	--
22	--	--	--	--	--	--
25	0,209717	0,0044849	--	--	0,197603	0,00448161
30	0,205202	0,0044827	0,212025	0,0044824		
32	--	--				
35	0,207289	0,0044826				
40	0,212025	0,0044824				

## Appendix D

Results showing that the mass balance is satisfied.

a=0.01				
t(sec)	Qout (m <sup>2</sup> /sec)	Qin (m <sup>2</sup> /sec)	Qab (m <sup>2</sup> /sec)	Qin-Qout-Qab (m <sup>2</sup> /sec)
0	0,00502	0,006181	0,00115861	2,5423E-06
1	0,004967	0,00549	0,00052309	0
2	0,004917	0,005296	0,000378443	7E-09
3	0,004888	0,005188	0,000303482	-3,583E-06
4	0,004829	0,005084	0,000255317	3E-09
6	0,004777	0,004971	0,000194772	-2E-09
8	0,004738	0,004895	0,000157038	2E-09
10	0,00471	0,00484	0,00013073	0
20	0,004617	0,004683	6,52073E-05	2,7E-09
40	0,004533	0,004557	2,36765E-05	3,5E-09
80	0,004493	0,004498	4,44242E-06	-2,42E-09
120	0,004486	0,004486	9,23407E-07	6,593E-09
160	0,004481	0,004481	1,94073E-07	-4,073E-09
200	0,004482	0,004482	0	4E-08

a=0.03				
t(sec)	Qout (m <sup>2</sup> /sec)	Qin (m <sup>2</sup> /sec)	Qab (m <sup>2</sup> /sec)	Qin-Qout-Qab (m <sup>2</sup> /sec)
0	0,003864	0,007344	0,00348	0
1	0,004582	0,005492	0,00091	0
2	0,004582	0,005166	0,000584	0
3	0,00458	0,005008	0,000428	-4,33681E-19
4	0,004574	0,004907	0,000333	0
6	0,004556	0,004777	0,000221	0
8	0,004541	0,004697	0,000156	0
10	0,004531	0,004646	0,000114	4,5E-07
14	0,004508	0,004573	0,0000649	-3,25261E-19
18	0,004497	0,004535	0,0000385	-5,28549E-19
22	0,004493	0,004516	0,0000234	-1,89735E-19
32	0,004485	0,004492	0,00000707	5,13302E-19
45	0,004485	0,004486	0,00000154	3,95141E-19
55	0,004483	0,004484	4,85E-07	-5E-09
75	0,004482	0,004482	0	5E-08

a=0.05				
t(sec)	Qout (m <sup>2</sup> /sec)	Qin (m <sup>2</sup> /sec)	Qab (m <sup>2</sup> /sec)	Qin-Qout-Qab (m <sup>2</sup> /sec)
0	0,002712	0,008502	0,00579	0
1	0,004359	0,005459	0,0011	0
2	0,004447	0,005101	0,000654	0
3	0,004471	0,004918	0,000447	0
4	0,004486	0,004812	0,000326	0
6	0,004494	0,004684	0,00019	0
8	0,004486	0,004604	0,000118	0
10	0,004485	0,004561	0,0000762	-6,36969E-19
15	0,004484	0,004512	0,0000271	3,86247E-19
20	0,004483	0,004493	0,0000101	-1,33831E-19
25	0,004485	0,004489	0,00000379	4,31987E-20
30	0,004483	0,004484	0,00000144	1,21761E-19
35	0,004482	0,004483	0,00000055	2,03076E-19
40	0,004482	0,004482	0	0

a=0.07				
t(sec)	Qout (m <sup>2</sup> /sec)	Qin (m <sup>2</sup> /sec)	Qab (m <sup>2</sup> /sec)	Qin-Qout-Qab (m <sup>2</sup> /sec)
0	0,001555	0,009665	0,00811	0
0,25	0,00406	0,00609	0,00283	-0,0008
0,5	0,004031	0,005971	0,00194	0
0,75	0,00415	0,00565	0,0015	0
1	0,004233	0,005453	0,00122	0
1,5	0,004326	0,005203	0,000877	0
2,25	0,004392	0,004987	0,000595	0
2,75	0,004417	0,004894	0,000477	0
3,5	0,004442	0,004796	0,000354	0
5	0,004453	0,004662	0,000209	0
7,5	0,00447	0,004566	0,0000959	3,25261E-19
10	0,004476	0,004522	0,0000465	5,35325E-19
20	0,004481	0,004484	0,00000297	-2,90956E-19
30	0,004484	0,004482	0	-1,69E-06



a=0.1				
t(sec)	Qout (m <sup>2</sup> /sec)	Qin (m <sup>2</sup> /sec)	Qab (m <sup>2</sup> /sec)	Qin-Qout-Qab (m <sup>2</sup> /sec)
0	9,59E-04	0,001101	0,00911	-8,97E-06
0,1	0,002612	0,007842	0,00523	0,00E+00
0,2	0,003217	0,006997	0,00378	0,00E+00
0,3	0,003523	0,006553	0,00303	0,00E+00
0,4	0,003682	0,006232	0,00255	-1,00E-08
0,6	0,003898	0,005848	0,00195	0,00E+00
0,8	0,004031	0,005609	0,00157	8,01E-06
1	0,004118	0,005428	0,00131	0,00E+00
2	0,004323	0,004975	6,52E-04	0,00E+00
3	0,004398	0,004778	0,00038	0,00E+00
4	0,004426	0,004663	2,37E-04	2,44E-19
6	0,004455	0,004565	1,00E-04	1,00E-05
8	0,004473	0,004517	4,44E-05	0,00E+00
10	0,004478	0,004498	2,01E-05	-5,42E-19
15	0,004482	0,004485	2,88E-06	2,44E-19
25	0,004482	0,004482	0	0,00E+00

## Appendix E

Numerical results of permeability and minimum pressure for a linearly decreasing absorption rate, as a function of time.

### Permeability

t	K[m <sup>2</sup> ]				
	(a=0.01)	sec	(a=0.01)	sec	(a=0.01)
0	0,005386	0,004957	0,004528	0,004099	0,003455
27	--	--	--	--	0,003309
30	--	--	--	0,003952	--
54	--	--	--	--	0,003265
63	--	--	0,004342	--	--
75	--	--	--	0,003879	--
76	--	0,004796	--	--	--
99	--	--	--	--	0,003228
105	--	--	0,004296	--	--
150	--	--	--	0,003813	--
153	--	--	--	--	0,00322
190	--	0,004696	--	--	--
210	--	--	0,004205	--	--
216	--	--	--	--	0,003236
225	--	--	--	0,003781	--
240	0,005209	--	--	--	--
270	--	--	--	--	0,003237
300	--	--	--	0,003758	--
315	--	--	0,004155	--	--
333	--	--	--	--	0,003265
342	--	0,004603	--	--	--
390	--	--	--	0,003737	--
405	--	--	--	--	0,003345
420	--	--	0,004113	--	--
480	--	--	--	0,003748	--
486	--	--	--	--	0,003429
532	--	0,004522	--	--	--
540	0,005114	--	--	--	--
546	--	--	0,004069	--	--
558	--	--	--	--	0,003513
570	--	--	--	0,003768	--
657	--	--	--	--	0,003638
672	--	--	0,004058	--	--
675	--	--	--	0,003803	--
722	--	0,004466	--	--	--
774	--	--	--	--	0,003794

782	--	--	--	--	--
795	--	--	--	0,003856	--
798	--	--	0,004055	--	--
912	--	0,004401	--	--	--
927	--	--	--	--	0,004022
930	--	--	--	0,003928	--
945	--	--	0,004064	--	--
1008	--	--	--	--	0,004152
1020	0,00499	--	--	--	--
1080	--	--	--	--	0,004276
1095	--	--	--	0,004011	--
1102	--	0,004368	--	--	--
1113	--	--	0,004086	--	--
1161	--	--	--	--	0,004417
1197	--	--	--	--	0,004481
1302	--	--	0,004125	--	--
1330	--	0,004344	--	--	--
1335	--	--	--	0,004176	--
1425	--	--	--	0,004244	--
1500	--	--	--	0,004305	--
1554	--	--	0,004174	--	--
1560	0,004904	--	--	--	--
1596	--	0,004326	--	--	--
1650	--	--	--	0,004428	--
1710	--	--	--	0,004481	--
1862	--	0,004316	--	--	--
1932	--	--	0,004294	--	--
2058	--	--	0,004339	--	--
2100	0,00482	--	--	--	--
2163	--	--	0,004382	--	--
2166	--	0,004316	--	--	--
2289	--	--	0,004436	--	--
2394	--	--	0,00448	--	--
2584	--	0,004324	--	--	--
2700	0,004735	--	--	--	--
3116	--	0,004366	--	--	--
3300	0,00467	--	--	--	--
3380	--	0,004396	--	--	--
3572	--	--	--	--	--
3648	--	0,004431	--	--	--
3800	--	0,004454	--	--	--
3990	--	0,004481	--	--	--
4020	0,004629	--	--	--	--
4740	0,004585	--	--	--	--
5580	0,004547	--	--	--	--

6540	0,004505				
7680	0,004478				
9300	0,00446				
11940	0,004485				

### Minimum Pressure

t	-p(m <sup>2</sup> /s <sup>2</sup> )				
	a=0.01	sec	a=0.01	sec	a=0.01
0	0,59956	1,26061	2,36506	3,48853	5,17373
27	--	--	--	--	7,66838
30	--	--	--	4,96672	--
54	--	--	--	--	9,37972
63	--	--	3,74353	--	--
75	--	--	--	6,35586	--
76	--	1,90522	--	--	--
99	--	--	--	--	12,245
105	--	--	4,40178	--	--
150	--	--	--	8,67508	--
153	--	--	--	--	15,9761
190	--	2,5483	--	--	--
210	--	--	6,06011	--	--
216	--	--	--	--	20,4692
225	--	--	--	11,2231	--
240	0,49219	--	--	--	--
270	--	--	--	--	28,401
300	--	--	--	14,0038	--
315	--	--	7,88091	--	--
333	--	--	--	--	35,5368
342	--	3,40885	--	--	--
390	--	--	--	19,9504	--
405	--	--	--	--	44,3478
420	--	--	9,86795	--	--
480	--	--	--	25,0186	--
486	--	--	--	--	53,8628
532	--	4,60645	--	--	--
540	0,581697	--	--	--	--
546	--	--	14,1154	--	--
558	--	--	--	--	66,991
570	--	--	--	30,2729	--
657	--	--	--	--	75,1757
672	--	--	17,7359	--	--

675	--	--	--	35,5562	--
722	--	5,82749	--	--	--
774	--	--	--	--	103,125
782	--	--	--	--	--
795	--	--	--	48,6803	--
798	--	--	21,4863	--	--
912	--	8,29222	--	--	--
927	--	--	--	--	99,343
930	--	--	--	52,152	--
945	--	--	26,0113	--	--
1008	--	--	--	--	82,5563
1020	0,891704	--	--	--	--
1080	--	--	--	--	56,8313
1095	--	--	--	71,3022	--
1102	--	10,2636	--	--	--
1113	--	--	33,1984	--	--
1161	--	--	--	--	19,3908
1197	--	--	--	--	0,302269
1302	--	--	37,1085	--	--
1330	--	12,6847	--	--	--
1335	--	--	--	68,8401	--
1425	--	--	--	60,4293	--
1500	--	--	--	49,1801	--
1554	--	--	50,9892	--	--
1560	1,22459	--	--	--	--
1596	--	15,5992	--	--	--
1650	--	--	--	15,1409	--
1710	--	--	--	0,302269	--
1862	--	19,9081	--	--	--
1932	--	--	46,624	--	--
2058	--	--	38,3597	--	--
2100	1,66557	--	--	--	--
2163	--	--	27,9679	--	--
2166	--	21,8694	--	--	--
2289	--	--	13,7033	--	--
2394	--	--	0,30156	--	--
2584	--	30,0402	--	--	--
2700	2,4252	--	--	--	--
3116	--	29,1642	--	--	--
3300	3,5305	--	--	--	--
3380	--	24,4074	--	--	--
3572	--	17,8645	--	--	--
3648	--	14,92096	--	--	--
3800	--	8,64656	--	--	--
3990	--	0,302269	--	--	--

4020	3,94638				
4740	4,82716				
5580	6,28952				
6540	8,678092				
7680	9,80509				
9300	9,52922				
11940	0,263136				

## Appendix F

Values of r and Qab for a=0.01, as a function of time.

t(sec)	r(mm)	Q <sub>ab</sub> (m <sup>2</sup> /s)
0	0,0036	0,000115861
1	0,00600049	0,0000523089
2	0,00707409	0,0000378443
3	0,00779706	0,0000303482
4	0,00834504	0,0000255317
5	0,00878591	0,0000220929
6	0,00915374	0,0000194772
7	0,0094683	0,0000174016
8	0,00974213	0,0000157038
9	0,00998375	0,0000142831
10	0,0101992	0,0000130730
11	0,010393	0,0000120274
12	0,0105686	0,0000111131
13	0,0107285	0,0000103066
14	0,010875	0,0000095885
15	0,0110097	0,0000089451
16	0,011134	0,0000083652
17	0,0112492	0,0000078392
18	0,0113562	0,0000073602
19	0,0114558	0,0000069223
20	0,0115487	0,0000065207
21	0,0116357	0,0000061505
22	0,0117172	0,0000058086
23	0,0117936	0,0000054924
24	0,0118655	0,0000051986
25	0,0119332	0,0000049251
26	0,011997	0,0000046703
27	0,0120572	0,0000044322
28	0,0121141	0,0000042095
29	0,0121679	0,0000040007
30	0,0122188	0,0000038049
31	0,0122671	0,0000036206
32	0,0123128	0,0000034476
33	0,0123563	0,0000032841
34	0,0123975	0,0000031303
35	0,0124367	0,0000029849
36	0,0124739	0,0000028477
37	0,0125094	0,0000027176

38	0,0125431	0,0000025948
39	0,0125752	0,0000024784
40	0,0126059	0,0000023676
41	0,0126351	0,0000022628
42	0,0126629	0,0000021634
43	0,0126895	0,0000020688
44	0,0127148	0,0000019791
45	0,012739	0,0000018936
46	0,0127622	0,0000018120
47	0,0127843	0,0000017346
48	0,0128054	0,0000016608
49	0,0128256	0,0000015905
50	0,0128449	0,0000015235
51	0,0128633	0,0000014598
52	0,012881	0,0000013987
53	0,0128979	0,0000013406
54	0,0129141	0,0000012849
55	0,0129296	0,0000012318
56	0,0129444	0,0000011813
57	0,0129586	0,0000011329
58	0,0129723	0,0000010862
59	0,0129853	0,0000010421
60	0,0129978	0,0000009998
61	0,0130098	0,0000009592
62	0,0130213	0,0000009203
63	0,0130323	0,0000008833
64	0,0130429	0,0000008476
65	0,013053	0,0000008137
66	0,0130627	0,0000007811
67	0,013072	0,0000007500
68	0,013081	0,0000007199
69	0,0130896	0,0000006912
70	0,0130978	0,0000006638
71	0,0131057	0,0000006375
72	0,0131133	0,0000006122
73	0,0131206	0,0000005879
74	0,0131276	0,0000005647
75	0,0131343	0,0000005425
76	0,0131407	0,0000005213
77	0,0131469	0,0000005007
78	0,0131528	0,0000004812
79	0,0131585	0,0000004624
80	0,013164	0,0000004442
81	0,0131693	0,0000004268



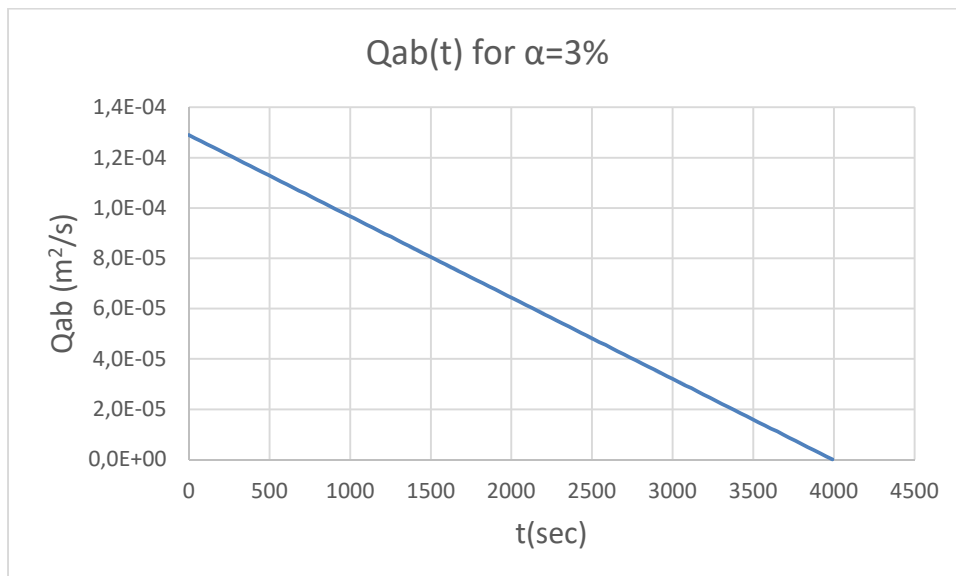
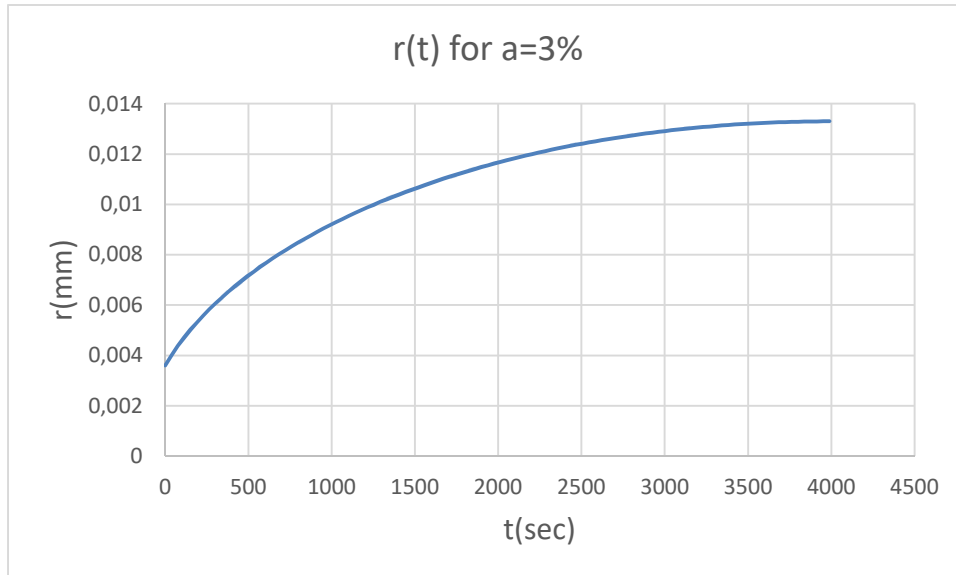
82	0,0131743	0,0000004103
83	0,0131792	0,0000003941
84	0,0131839	0,0000003787
85	0,0131883	0,0000003642
86	0,0131927	0,0000003497
87	0,0131968	0,0000003363
88	0,0132008	0,0000003231
89	0,0132046	0,0000003107
90	0,0132083	0,0000002985
91	0,0132118	0,0000002871
92	0,0132152	0,0000002759
93	0,0132184	0,0000002654
94	0,0132216	0,0000002550
95	0,0132246	0,0000002452
96	0,0132275	0,0000002357
97	0,0132303	0,0000002265
98	0,0132329	0,0000002180
99	0,0132355	0,0000002096
100	0,013238	0,0000002014
101	0,0132403	0,0000001939
102	0,0132426	0,0000001864
103	0,0132448	0,0000001792
104	0,0132469	0,0000001724
105	0,013249	0,0000001655
106	0,0132509	0,0000001593
107	0,0132528	0,0000001531
108	0,0132546	0,0000001473
109	0,0132563	0,0000001418
110	0,013258	0,0000001362
111	0,0132596	0,0000001310
112	0,0132611	0,0000001261
113	0,0132626	0,0000001213
114	0,0132641	0,0000001164
115	0,0132654	0,0000001122
116	0,0132667	0,0000001079
117	0,013268	0,0000001037
118	0,0132692	0,0000000998
119	0,0132704	0,0000000959
120	0,0132715	0,0000000923
121	0,0132726	0,0000000888
122	0,0132737	0,0000000852
123	0,0132747	0,0000000820
124	0,0132756	0,0000000790
125	0,0132766	0,0000000758

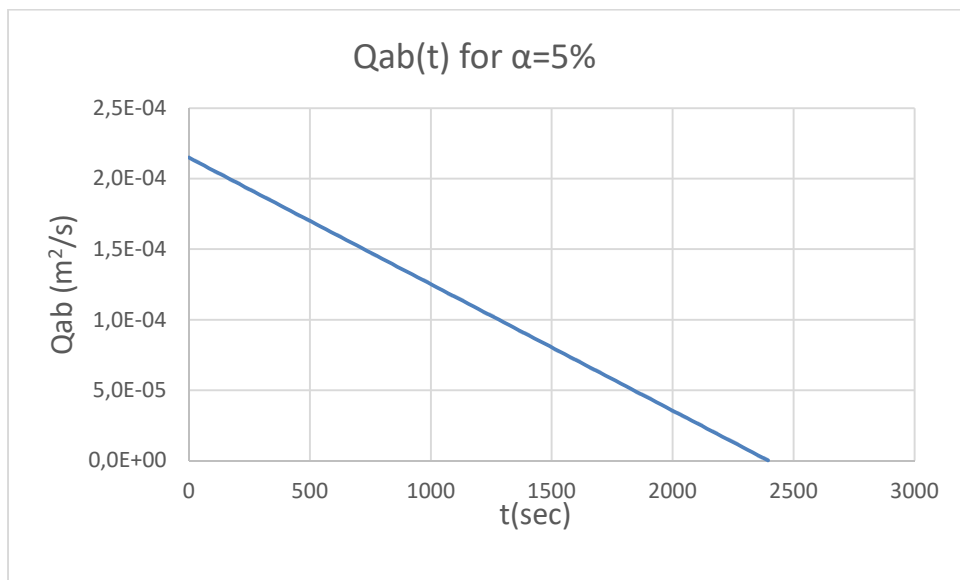
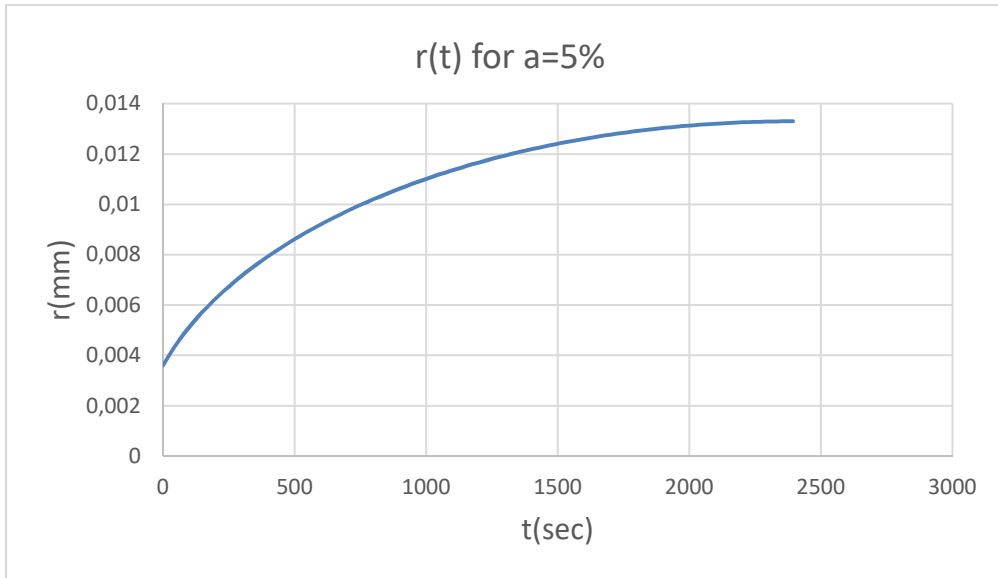
126	0,0132774	0,0000000732
127	0,0132783	0,0000000703
128	0,0132791	0,0000000677
129	0,0132799	0,0000000651
130	0,0132807	0,0000000625
131	0,0132814	0,0000000602
132	0,0132821	0,0000000580
133	0,0132828	0,0000000557
134	0,0132835	0,0000000534
135	0,0132841	0,0000000515
136	0,0132847	0,0000000495
137	0,0132853	0,0000000476
138	0,0132858	0,0000000460
139	0,0132864	0,0000000440
140	0,0132869	0,0000000424
141	0,0132874	0,0000000408
142	0,0132879	0,0000000392
143	0,0132883	0,0000000379
144	0,0132888	0,0000000362
145	0,0132892	0,0000000349
146	0,0132896	0,0000000337
147	0,01329	0,0000000324
148	0,0132904	0,0000000311
149	0,0132908	0,0000000298
150	0,0132911	0,0000000288
151	0,0132914	0,0000000278
152	0,0132918	0,0000000265
153	0,0132921	0,0000000256
154	0,0132924	0,0000000246
155	0,0132927	0,0000000236
156	0,013293	0,0000000226
157	0,0132932	0,0000000220
158	0,0132935	0,0000000210
159	0,0132937	0,0000000204
160	0,013294	0,0000000194
161	0,0132942	0,0000000188
162	0,0132944	0,0000000181
163	0,0132946	0,0000000175
164	0,0132948	0,0000000168
165	0,013295	0,0000000162
166	0,0132952	0,0000000155
167	0,0132954	0,0000000149
168	0,0132956	0,0000000142
169	0,0132957	0,0000000139

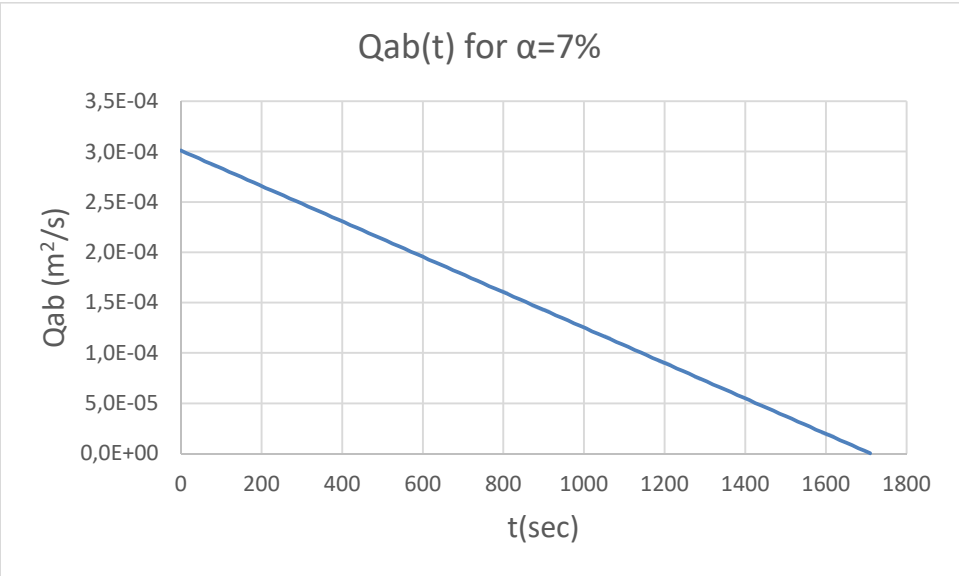
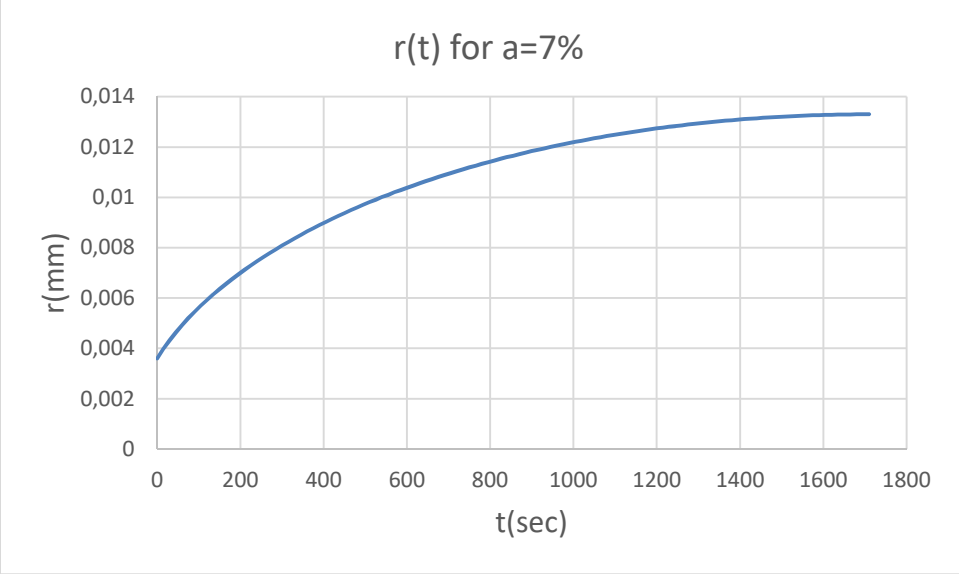
170	0,0132959	0,0000000133
171	0,0132961	0,0000000126
172	0,0132962	0,0000000123
173	0,0132964	0,0000000116
174	0,0132965	0,0000000113
175	0,0132966	0,0000000110
176	0,0132968	0,0000000103
177	0,0132969	0,0000000100
178	0,013297	0,0000000097
179	0,0132971	0,0000000094
180	0,0132972	0,0000000091
181	0,0132973	0,0000000087
182	0,0132974	0,0000000084
183	0,0132975	0,0000000081
184	0,0132976	0,0000000078
185	0,0132977	0,0000000074
186	0,0132978	0,0000000071
187	0,0132979	0,0000000068
188	0,013298	0,0000000065
189	0,013298	0,0000000065
190	0,0132981	0,0000000061
191	0,0132982	0,0000000058
192	0,0132983	0,0000000055
193	0,0132983	0,0000000055
194	0,0132984	0,0000000052
195	0,0132984	0,0000000052
196	0,0132985	0,0000000049
197	0,0132986	0,0000000045
198	0,0132986	0,0000000045
199	0,0132987	0,0000000042
200	0,0132987	0,0000000042

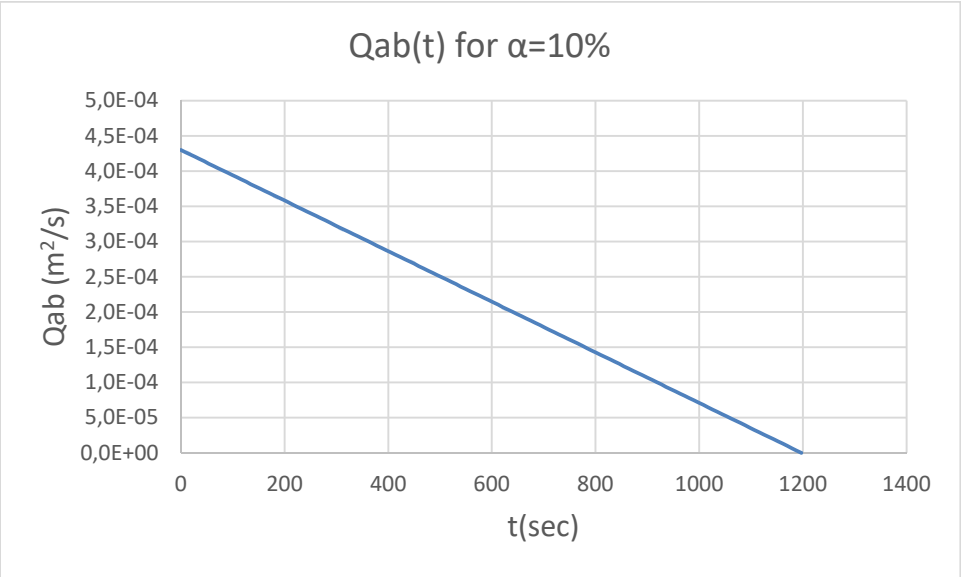
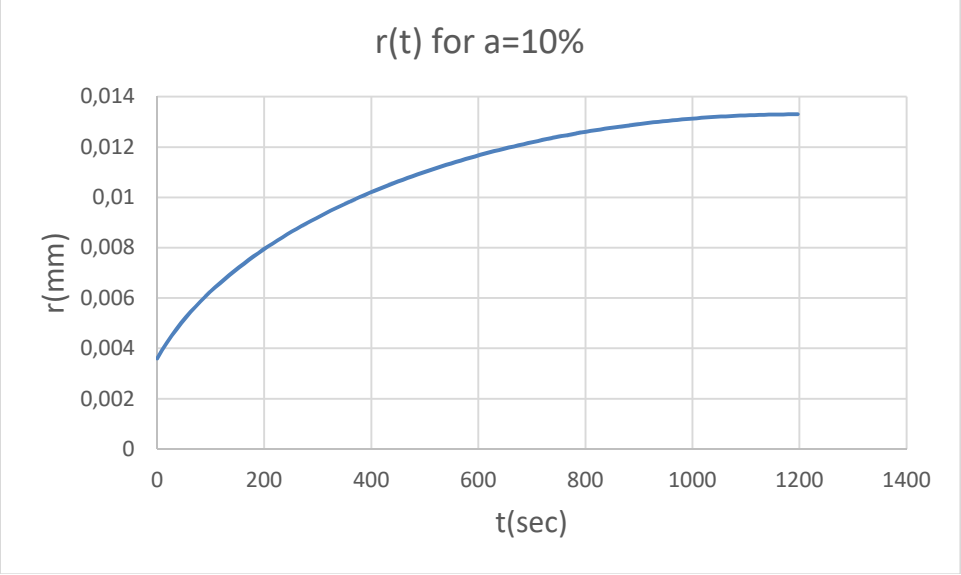
## Appendix G

Graphs of the radius of the filaments and of  $Q_{ab}$  versus time for various values of absorption coefficient ( $\alpha$ ), where  $Q_{ab}$  is a linear function of time









## References

- [1] Anatomy & Physiology , "Skeletal Muscle Structure' , Retrieved from <http://www.karunayoga.in/skeletal-muscle-structure/>
- [2] Ferziger J. H., M. Peric,(2001)., " Computational Methods for Fluid Dynamics", Springer, 3rd Ed.,
- [3] Fetter, C. W. (2000). "Applied hydrogeology", Prentice Hall.
- [4] Greenshields, C. J. (2016). "Openfoam user guide", *OpenFOAM Foundation Ltd, version* , Retrieved 25 January, 2018, from <http://foam.sourceforge.net/docs/Guides-a4/OpenFOAMUserGuide-A4.pdf>
- [5] Kapitola P. (17 August 2006), "Darcy's law". Retrieved from [https://en.wikipedia.org/wiki/Darcy%27s\\_law](https://en.wikipedia.org/wiki/Darcy%27s_law)
- [6] "CFD Direct - The Architects of OpenFOAM".OpenFOAM v5 User Guide, *OpenFOAM Foundation 2011-2017* , version Archived from the original on 22 November 2017.
- [7] Mantanis, G., Young, R., & Rowell, R. (1995). "Swelling of compressed cellulose fiber webs in organic liquids". *Cellulose*, 2(1), 1-22.
- [8] Martins, A. A., Laranjeira, P. E., Braga, C. H., & Mata, T. M. (2009). " Modeling of transport phenomena in porous media using network models", *Progress in Porous Media Research, ISBN, 978-971*.
- [9] Masoodi, R., & Pillai, K. M. (2010). " Darcy's law-based model for wicking in paper-like swelling porous media", *AIChE journal*, 56(9), 2257-2267
- [10] Ngo, N., & Tamma, K. (2004). " Complex three-dimensional microstructural permeability prediction of porous fibrous media with and without compaction", *International journal for numerical methods in engineering*, 60(10), 1741-1757.
- [11] Papathanasiou, T. (2001). " Flow across structured fiber bundles: a dimensionless correlation", *International journal of multiphase flow*, 27(8), 1451-1461.
- [12] Petroleum library , "Well Completion Concepts", Retrieved from <http://www.peldz.com/index.php/well-completion-concepts/>
- [13] Vafai, K. (2015). "Handbook of porous media" Crc Press.
- [14] "What Is Edema", (November 02, 2016). Retrieved from <https://www.webmd.com/heart-disease/heart-failure/edema-overview#1>
- [15] Zhang, C., Simon, T. W., Li, P. Y., & Van de Ven, J. D. (2015). "Numerical modeling of three-dimensional heat transfer and fluid flow through interrupted plates using



unit cell scale”, *Special Topics & Reviews in Porous Media: An International Journal*, 6(2).

[16] Vishal Gawande (2014). “Superabsorbent Polymers”, Retrieved from <https://www.slideshare.net/vishalgawande/superabsorbent-polymers>